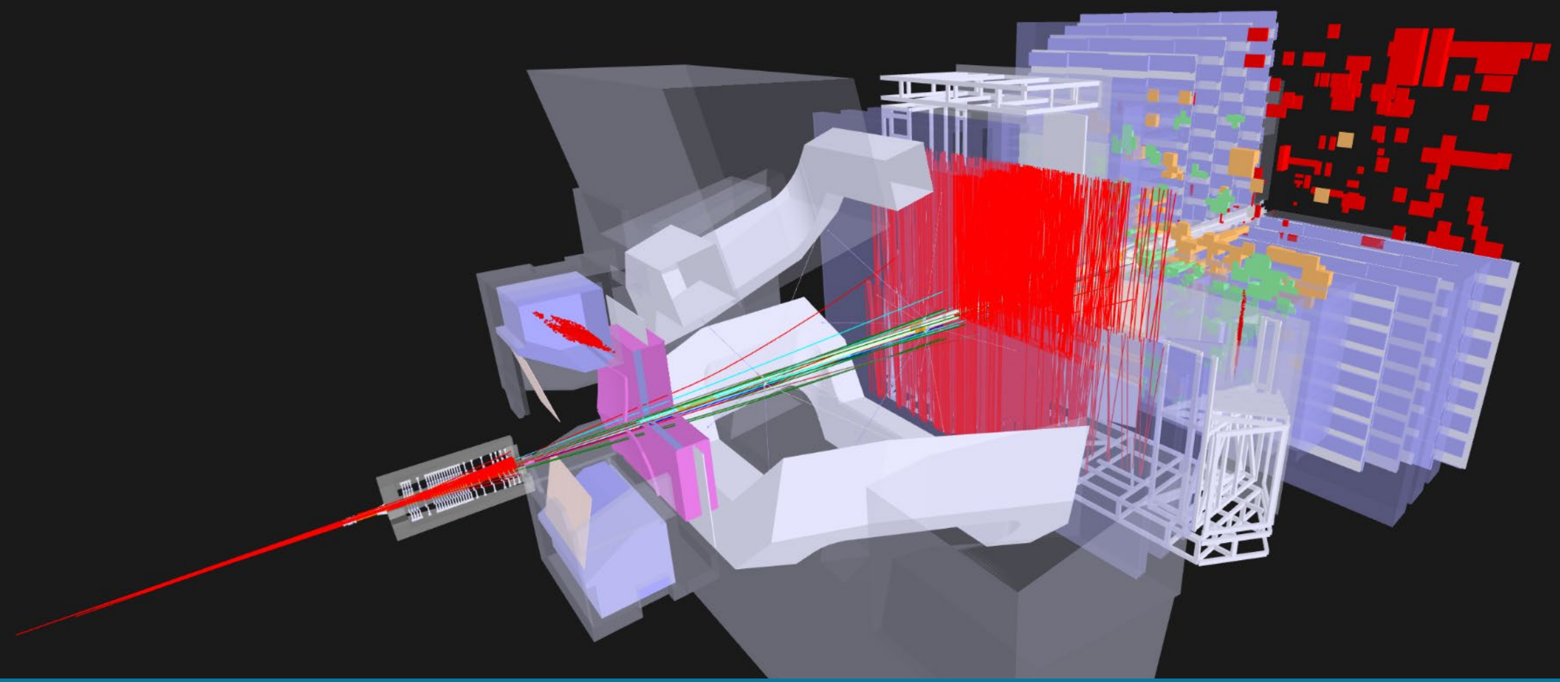

Extending the physics reach of the fixed-target programme at the LHCb experiment

Chiara Lucarelli

Seminar, TU Dortmund
1 October 2024

Introductions

- I was born in Florence, studied and got my Ph.D. there
  → I am now a research fellow at INFN Florence


UNIVERSITÀ DEGLI STUDI FIRENZE

DOTTORATO DI RICERCA IN
Fisica e Astronomia

CICLO XXXVI

Extending the physics reach of the fixed-target programme at the LHCb experiment

Settore Scientifico Disciplinare FIS/04

Dottorando
Lucarelli Chiara

Supervisore
Dott. Graziani Giacomo

Supervisore
Prof. Adriani Oscar

Coordinatore
Prof. Modugno Giovanni

Anni 2020/2023

- First interest for LHCb fixed target physics during my bachelor degree:
  fixed-target luminosity measurement using elastic *pe* collisions.

- A bit of hardware work during my master thesis:
  characterisation of temporal response of 3D diamond pixel sensors.

- Back to my first love (SMOG) since 2020, working mainly on three topics:

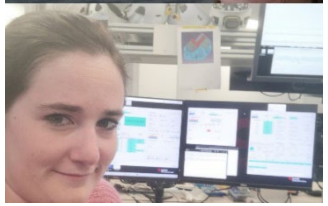

  - **Anti-deuteron searches in *p*He datasample**, relevant for indirect Dark Matter searches.
  - **Gas flow simulations** for injections of non noble gases in upgraded fixed-target apparatus
  - **Operations of fixed-target system**: luminosity measurement, integration in LHCb control system, day-to-day babysitting

I will give you an **overview of the LHCb unique fixed-target programme**,
with a focus on these topics

The LHCb experiment

LHCb is one of the four experiments on the LHC at CERN. It is a general-purpose experiment in the forward direction:

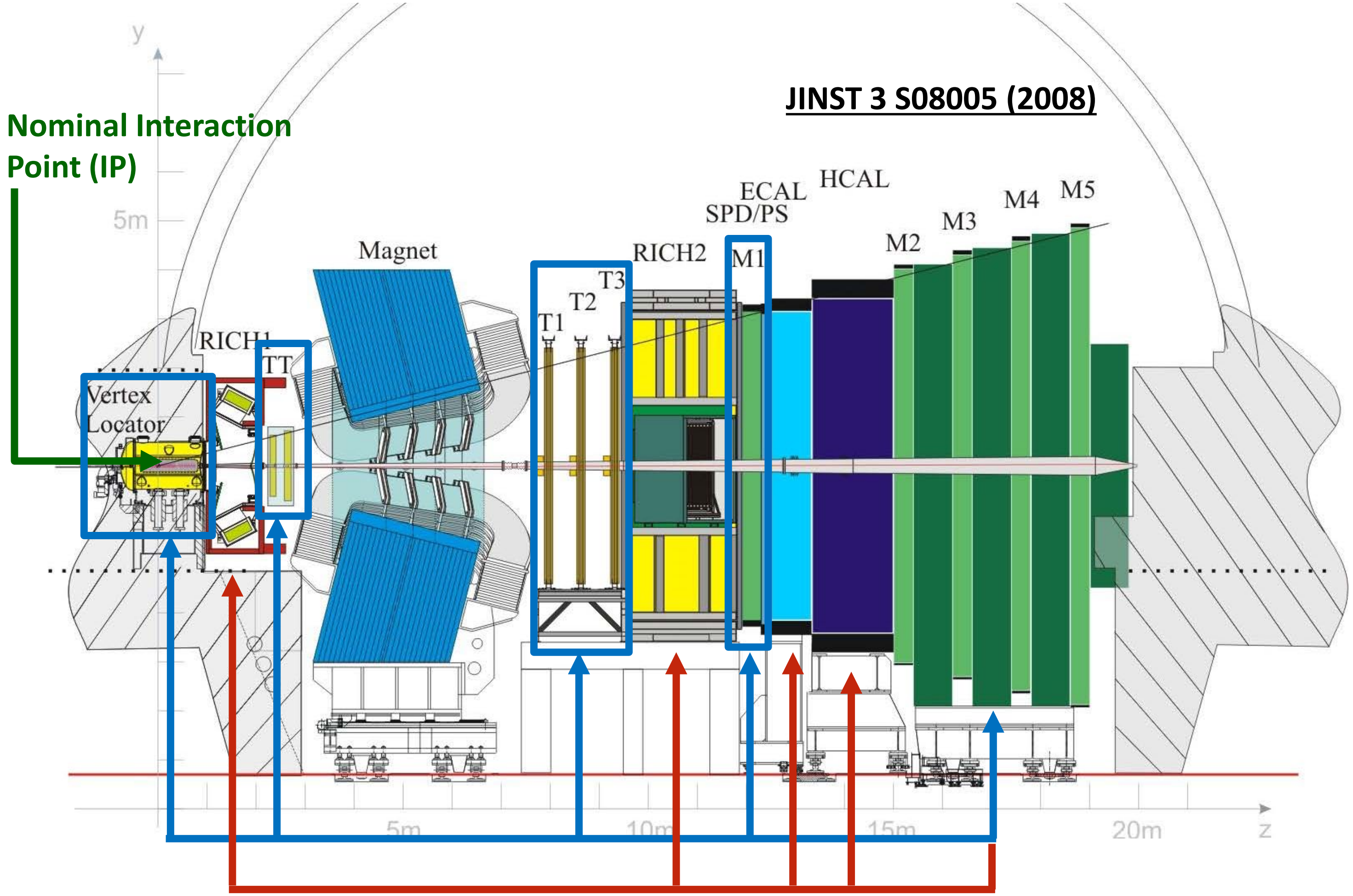

- **Single-arm forward spectrometer**: optimized for $b\bar{b}$ production, $2 < \eta < 5$, $\Theta \in [10, 250]$ mrad.
- **Tracking:** excellent vertexing, momentum resolution: $\Delta p/p = 0.5\% - 1.0\%$.
- **Particle Identification (PID):** excellent separation among K, π and p with momentum in [10, 110] GeV/c range.
- **Trigger:** flexible and versatile, bandwidth up to 15 kHz to disk.
- Its forward geometry is very well suited for **fixed-target physics.**

LHCb fixed-target apparatus

- The *System for Measuring Overlap with Gas* (**SMOG**) can inject gas in LHC beam pipe around (±20 m) the LHCb interaction point
  - → Conceived for luminosity measurements, x100 nominal LHC vacuum
- Since 2015, exploited for LHCb fixed-target physics programme
  - → Different targets and different centre of mass energies.

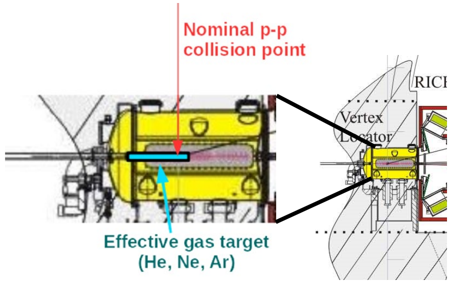

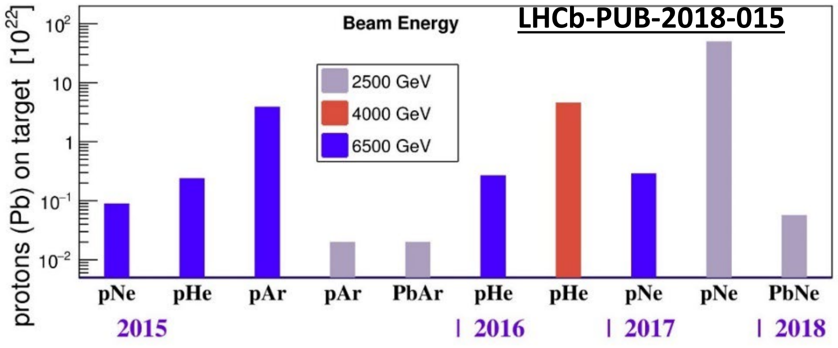

Forward geometry + gas target =
highest-energy ever fixed-target physics experiment

Unique physics opportunities at the LHC

- Unexplored **intermediate energy** to SpS and LHC
- **Large target Bjorken-*x* at low Q^2**
- Collisions with **targets of mass number A intermediate** between *p* and Pb

→

- **Cold nuclear-matter effects** for QGP studies
- **Nuclear PDFs at high-*x*** and nucleon intrinsic charm studies
- **Hadron production** and spectra measurements for Cosmic Rays physics

Antimatter production for Cosmic Rays physics

Dark Matter and antimatter in space

Antimatter fraction in Cosmic Rays (CR) is a sensitive **indirect probe for Dark Matter** (DM):

- Signatures of Dark Matter annihilation and decay processes
- Constrain space of Dark Matter candidates

Space experiments (PAMELA, AMS) measured antimatter fluxes in CR

→ Inconclusive results due to **limited knowledge of production processes**.

E.g. **In 2015, new AMS-02 data for $\bar{p}$ abundance in CRs**:

Excess for T>10 GeV compared to expected $\bar{p}$ from collisions of primary CRs onto interstellar gas (90% H_2, 10% He).

→ **Improved theoretical modelling required** to be conclusive on the nature of this excess

Accelerator experiments can complement Cosmic Rays investigations

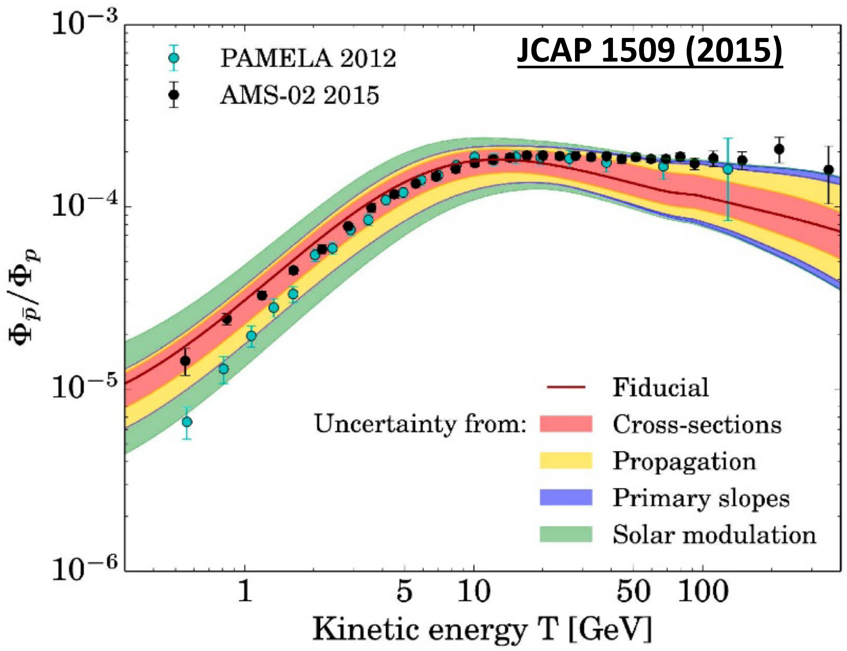

LHCb cosmic programme

During Run2, LHCb with SMOG provided unique results contributing to improve the accuracy of the $\bar{p}$ production models:

PRL 121 (2018) 222001

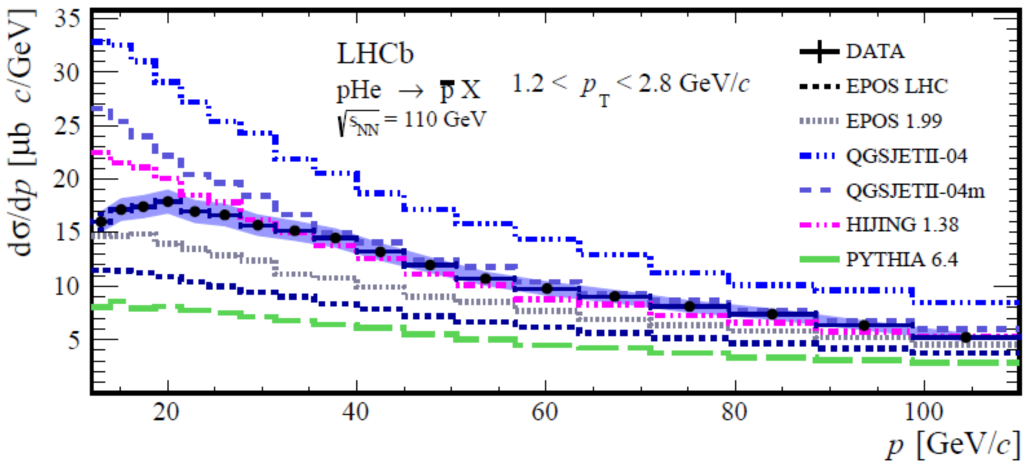

In 2018, first measurement ever of $\sigma(p\mathrm{He} \longrightarrow \bar{p}_{\mathrm{prompt}}\mathrm{X})$ at $\sqrt{s_{\mathrm{NN}}} = 110$ GeV.

- Results uncertainties negligible wrt spread of theoretical models.

In 2022, $\bar{p}$ production from anti-hyperon decays in *p*He collisions at $\sqrt{s_{NN}} = 110$ GeV.

- Larger fraction of detached $\bar{p}$ observed wrt theoretical models.

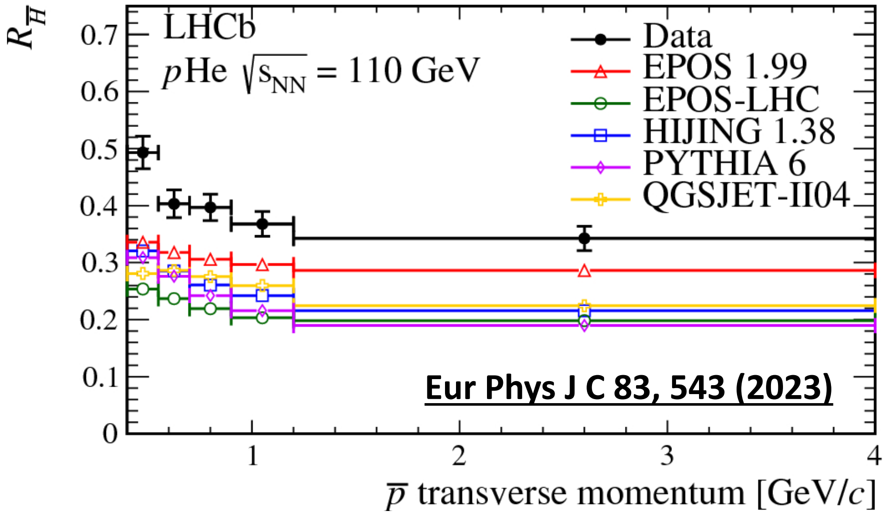

Eur Phys J C 83, 543 (2023)

Impact of the measurements

Important contribution to the improvement of the secondary $\overline{p}$ flux prediction:

→ Room for exotic contribution heavily reduced

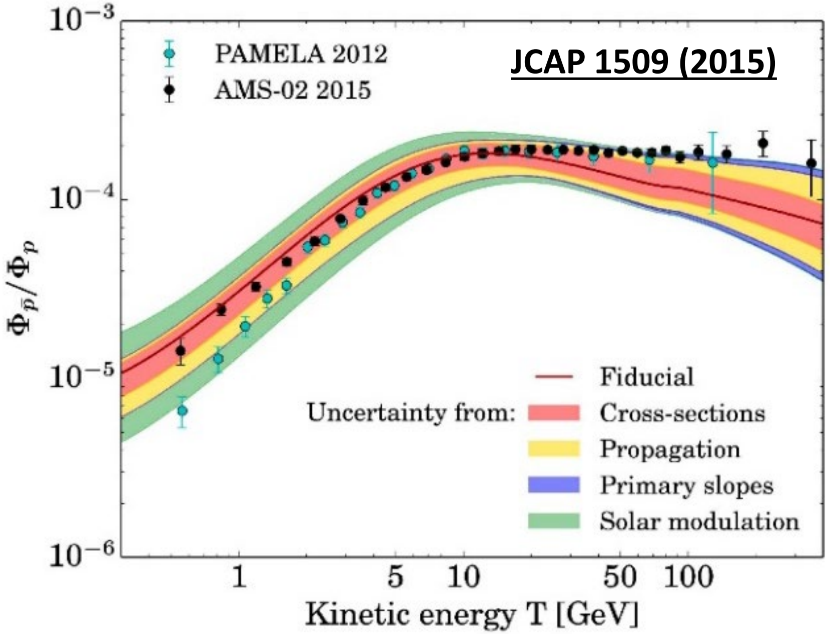

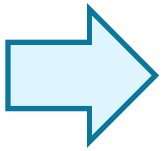

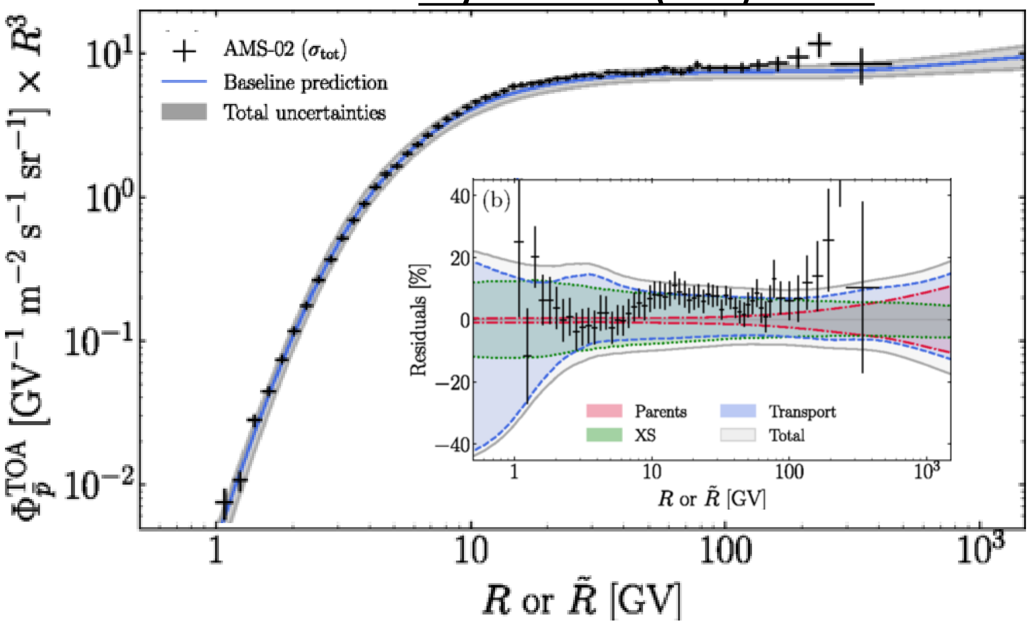

- Knowledge of **cross section still dominates uncertainties.**
- **Heavier probes** (i.e. rarer to produce in known processes) **can be interesting to investigate.**

Light anti-nuclei in space

Light anti-nuclei fraction in Cosmic Rays is a **golden channel** for indirect Dark Matter detection:

- No known primary sources
- Low production cross-section in secondary collisions of Cosmic Rays and interstellar medium

→ **Low background channel**

AMS-02 observed anti-helium and anti-deuteron candidates in Cosmic Rays:

- $\mathcal{O}(10)\ \overline{\mathrm{He}}$ candidates, $\mathcal{O}(1)\ \bar{\mathrm{d}}$ candidates: expected $\bar{\mathrm{d}}/\ {}^{3}\overline{\mathrm{He}}$ around 10^3

→ Needed **knowledge of production processes**

AMS ^{4}He candidate

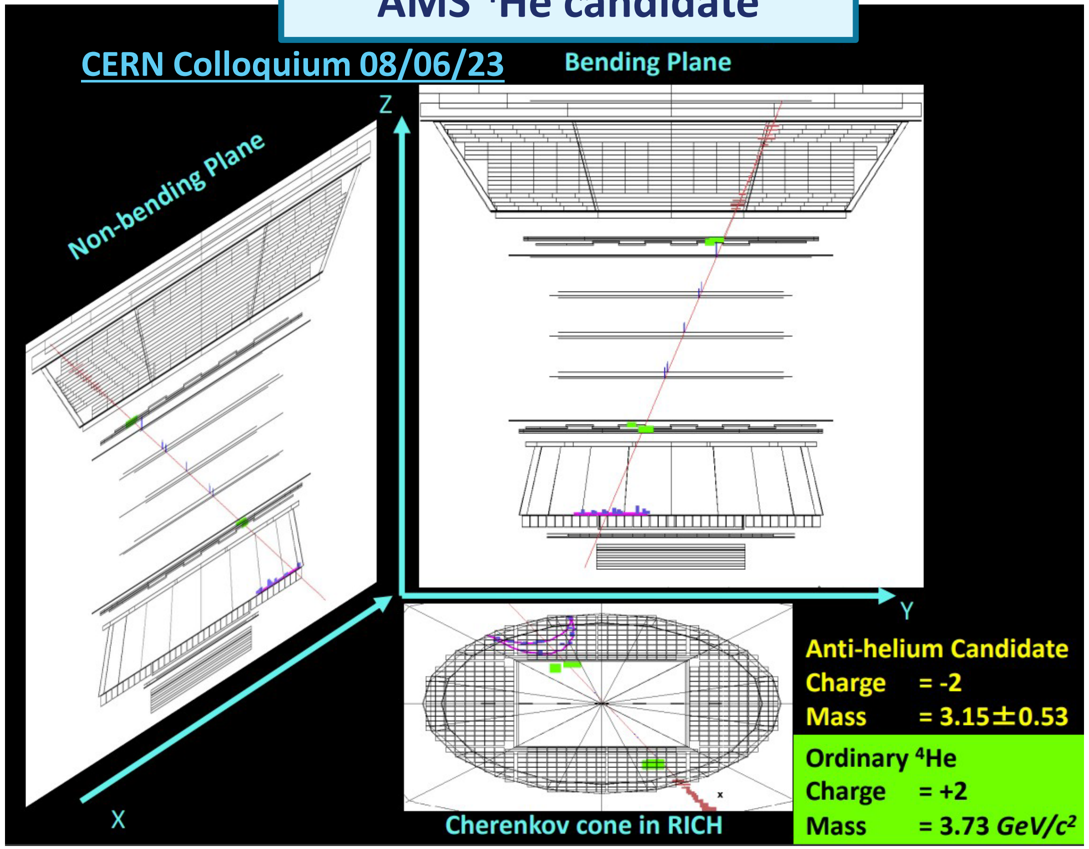

Anti-nuclei production

- **No comprehensive theoretical model** to explain from first principles (anti-)nuclei production in hadronic interactions → **Phenomenological models tuned on data**

Coalescence model:

An anti-nucleus is produced if the nucleons are sufficiently close in phase space: $\boldsymbol{B_A}$ **coalescence probability**.

- Experimental data suggest that B_A depends on the **type of reaction** (*pp*, *p*A or AA) and on the **incident particle momentum** (p_{lab}).

⇩

- ALICE measures d and He production in *pp*, *p*Pb and PbPb interactions at $\sqrt{s} = 13$ TeV and central rapidity
- SpS fixed-target configuration covers $\sqrt{s_{NN}} < 27$ GeV and backward to central rapidity

Large uncertainties on extrapolation models to intermediate energy (E_{cr}~10-100 GeV)

Deuteron identification techniques

Unique opportunities at the LHCb fixed-target:

- Collisions with **targets of mass number A intermediate** between *p* and Pb → **Reproduce Cosmic Rays interactions (pH_2, pHe)**
- **Energy range** $\sqrt{s_{NN}} \in [30, 115]$ GeV for beam energy in $[0.45, 7]$ TeV → **Unexplored gap** between SpS and LHC/RHIC.

PROBLEM: LHCb detector not designed to identify light (anti-)nuclei

⇩

Two possible techniques available with the LHCb detector

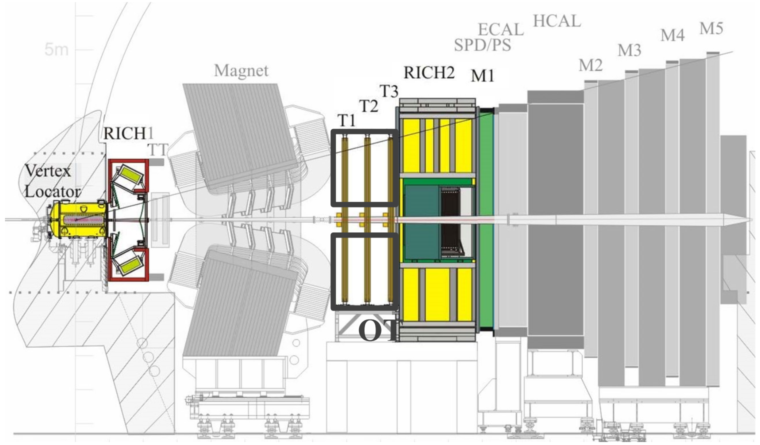

1 Charged particles emits Cherenkov radiation when moving in medium with $\beta > 1/n_{ref}$
→ RICH detector to **identify high momentum d**

OT: 2.4 ns σ_t

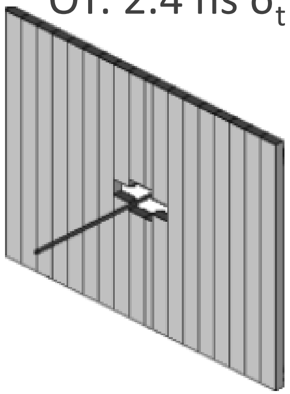

M1: 3-4 ns σ_t

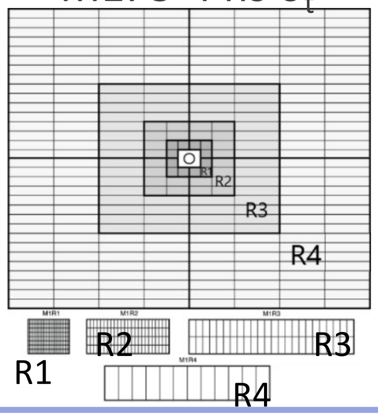

2 Light nuclei significantly slower than c: **M dependence** of particle speed
→ **Time-of-flight** in OT and M1 to **identify d,**

Light anti-nuclei at the LHCb experiment

Search for $\bar{d}$ in Run2 SMOG *p*He ($\sqrt{s_{NN}}$= 110 GeV) dataset.

RICH PID: high *p* region (*p*>30 GeV/c)

Limited discrimination power

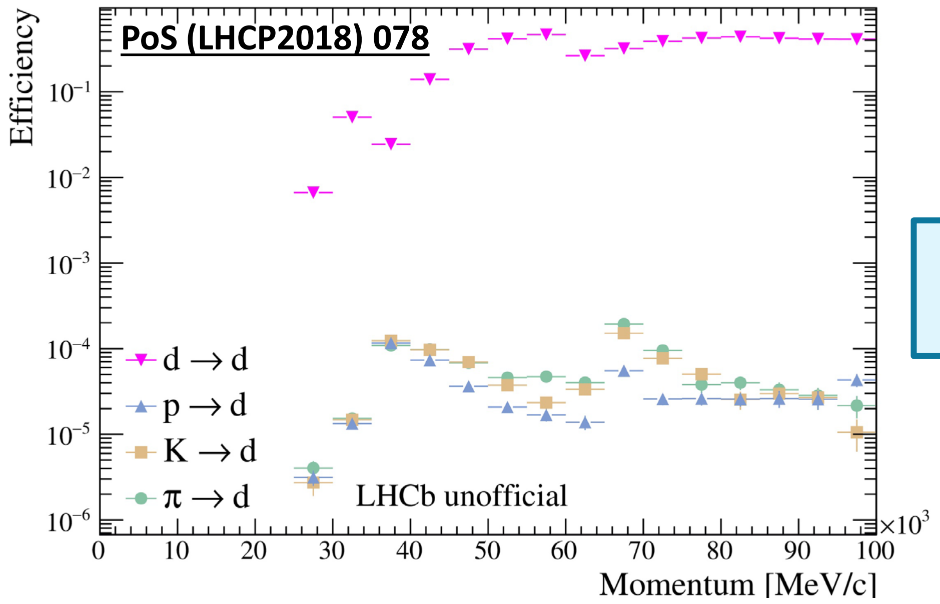

π→d misidentification same level as expected signal

Time of flight between interaction point and Outer Tracker: low *p* region (*p*<10 GeV/c)

Conceived and developed in my PhD thesis!

Time-of-flight measurement at LHCb

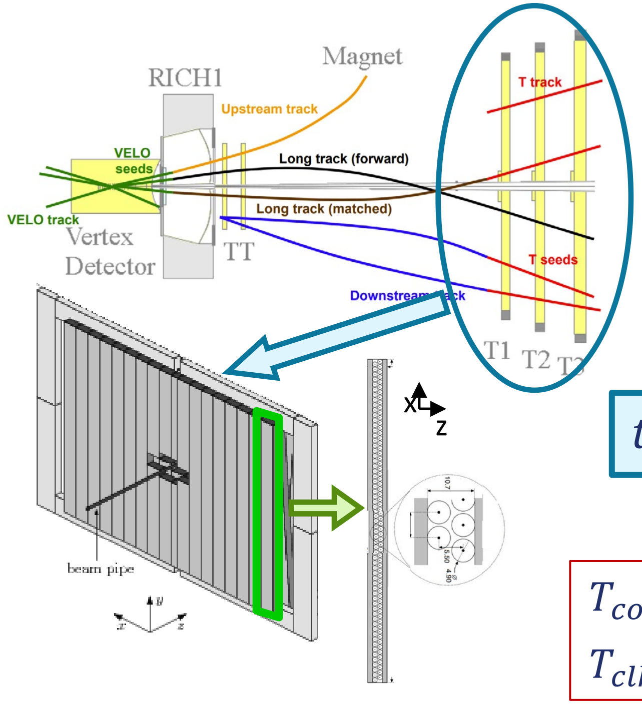

OT (Outer Tracker): largest area, straw-tube drift chambers

OT measures the arrival time t_{TDC} of the ionization cluster with respect to the beam crossing time

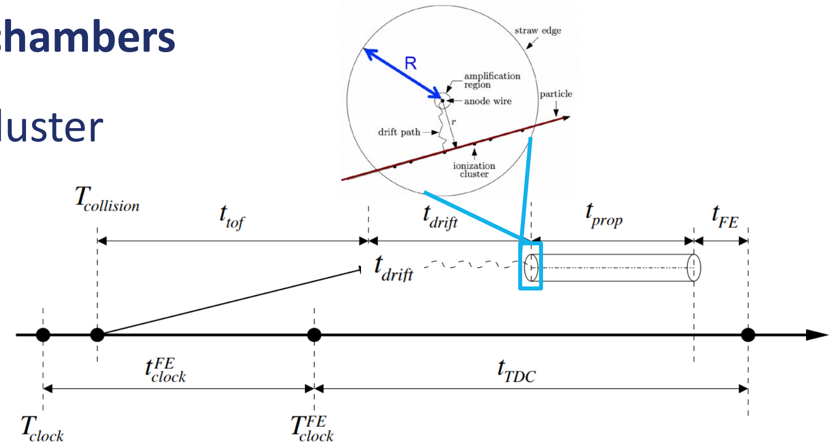

$$t_{TDC} = (T_{coll} - T_{clk}) + t_{TOF} + t_{drift} + t_{prop} + t_0$$

T_{coll} = bunch crossing time of collision

T_{clk} = LHC clock

t_0 = offset from T_{clk} drift and FE delay drift

- Hit position from ionization cluster t_{drift}– r relation

$$t_{drift} = t_{TDC} - t_{TOF} - t_{prop}$$

JINST 12 (2017) P11016

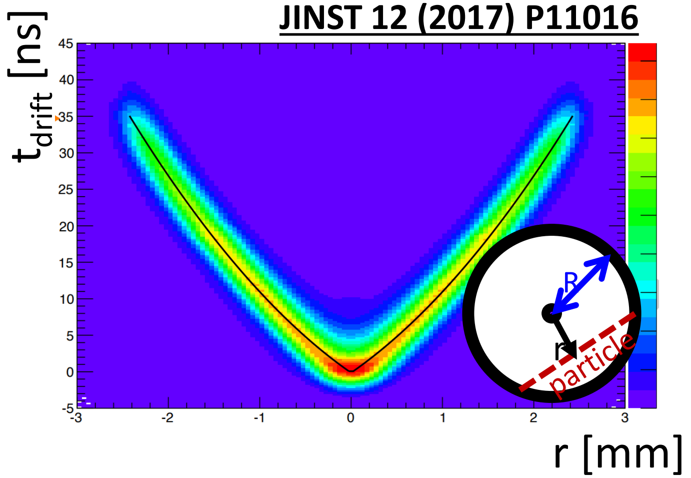

Time-of-flight measurement at LHCb

$$t_{drift} = t_{TDC} - t_{TOF} - t_{prop}$$

- t_{TOF} calculated in the β=1 hypothesis. Residual between t_{TDC} and $t(r)$, expected arrival time for fitted track, is proportional to β_{real}
  → Some capabilities for proton ID with TOF

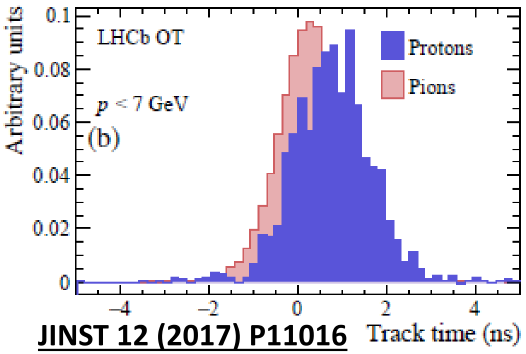

JINST 12 (2017) P11016

In principle, time resolution enough up to 10 GeV/c

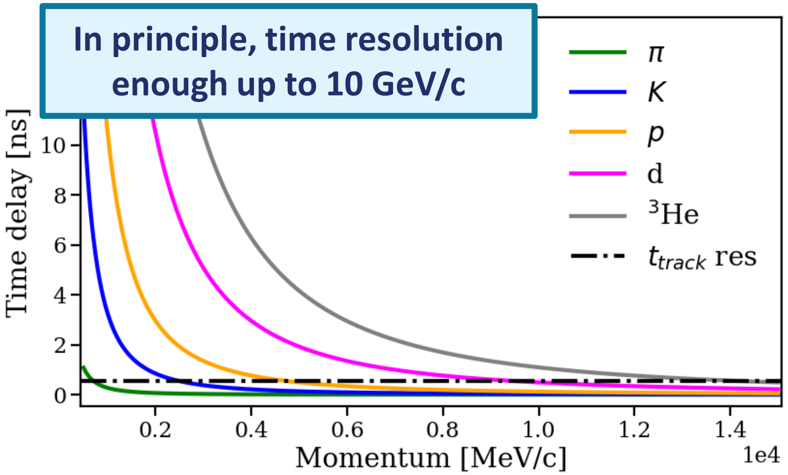

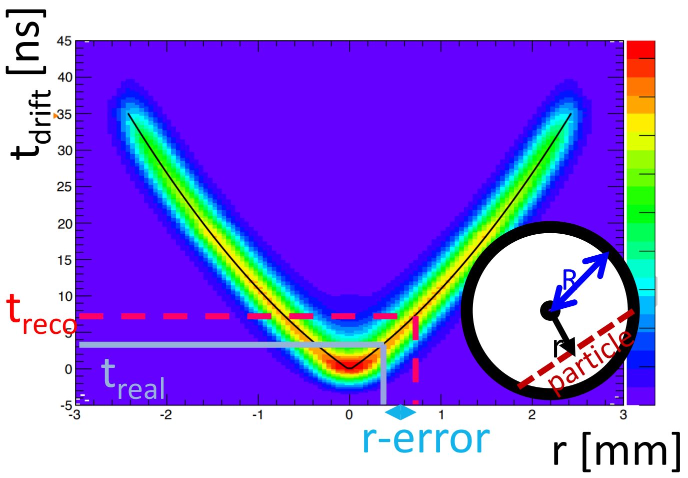

- **For β<1: $t_{TOF,reco} < t_{TOF,real} \implies t_{drift,reco} > t_{drift,real}$**
  $\implies$ error in r determination

Low d reconstruction efficiency at low momentum

- For $\bar{d}$ at p<3 GeV/c, r shifted more than 1 mm wrt real particle track.
- Hits discarded or fit χ^2 too large because of error on r

Need new reconstruction algorithm and PID strategy

Time-of-flight reconstruction algorithm

LHCb-FIGURE-2023-017

Target: Correct hits position to recover reconstruction efficiency

Modify the reconstruction algorithm to take into account β<1

Recovered efficiency at low *p*

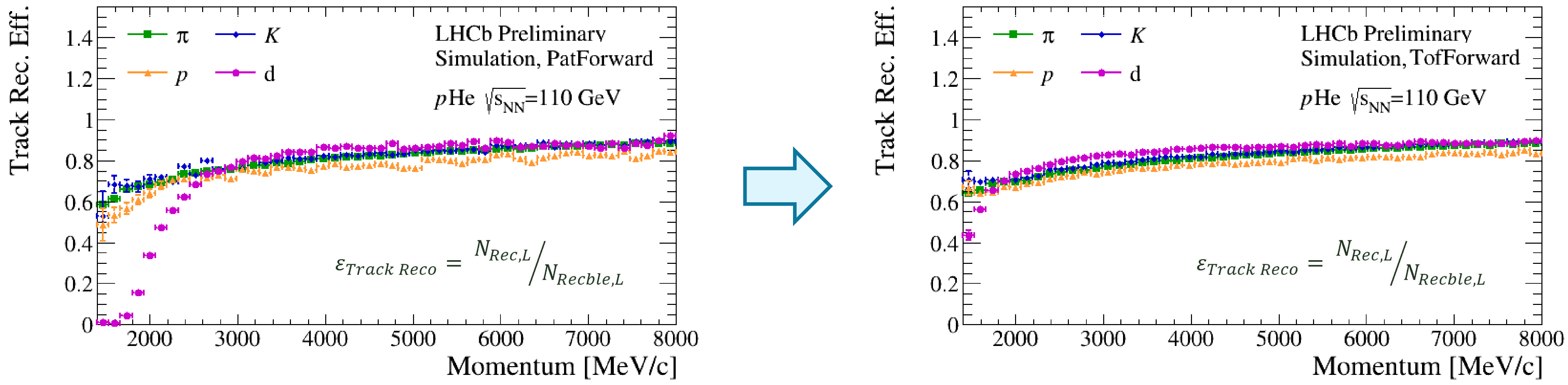

MC sample:

QGSJET for *p*He + **coalescence afterburner** (1 coal x event)

Time-of-flight reconstruction algorithm

Additional degree of freedom: possible increase of tracks reconstructed from random combinations of hits (ghost rate)

→ **Same ghost rate as standard reconstruction**

Recovered efficiency at low *p*
preserving reconstruction quality

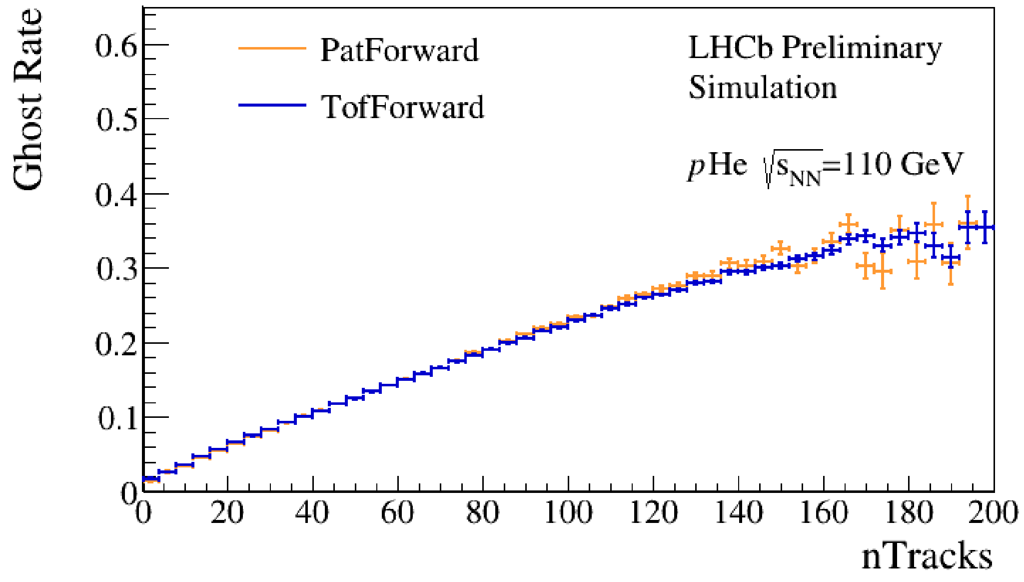

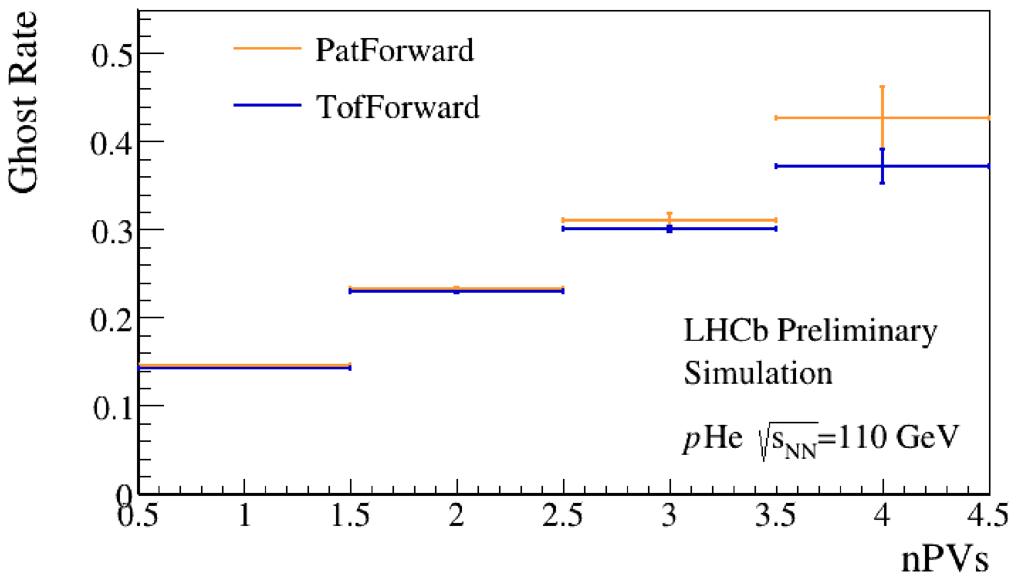

MC sample:
QGSJET for pHe + **coalescence afterburner** (1 coal x event)

Time-of-flight particle identification

Given the reconstructed tracks, developed an offline tool to determine β

Target: refit reconstructed tracks to determine β

Iterative procedure rerunning fit with different β hypothesis

Fit around minimum to estimate β_{reco} and $\sigma(\beta)$ from fit around minimum of χ^2_{fit}

Good agreement between β_{reco} and $\beta(p)$

MC sample:
QGSJET for *p*He + **coalescence afterburner** (1 coal x event)

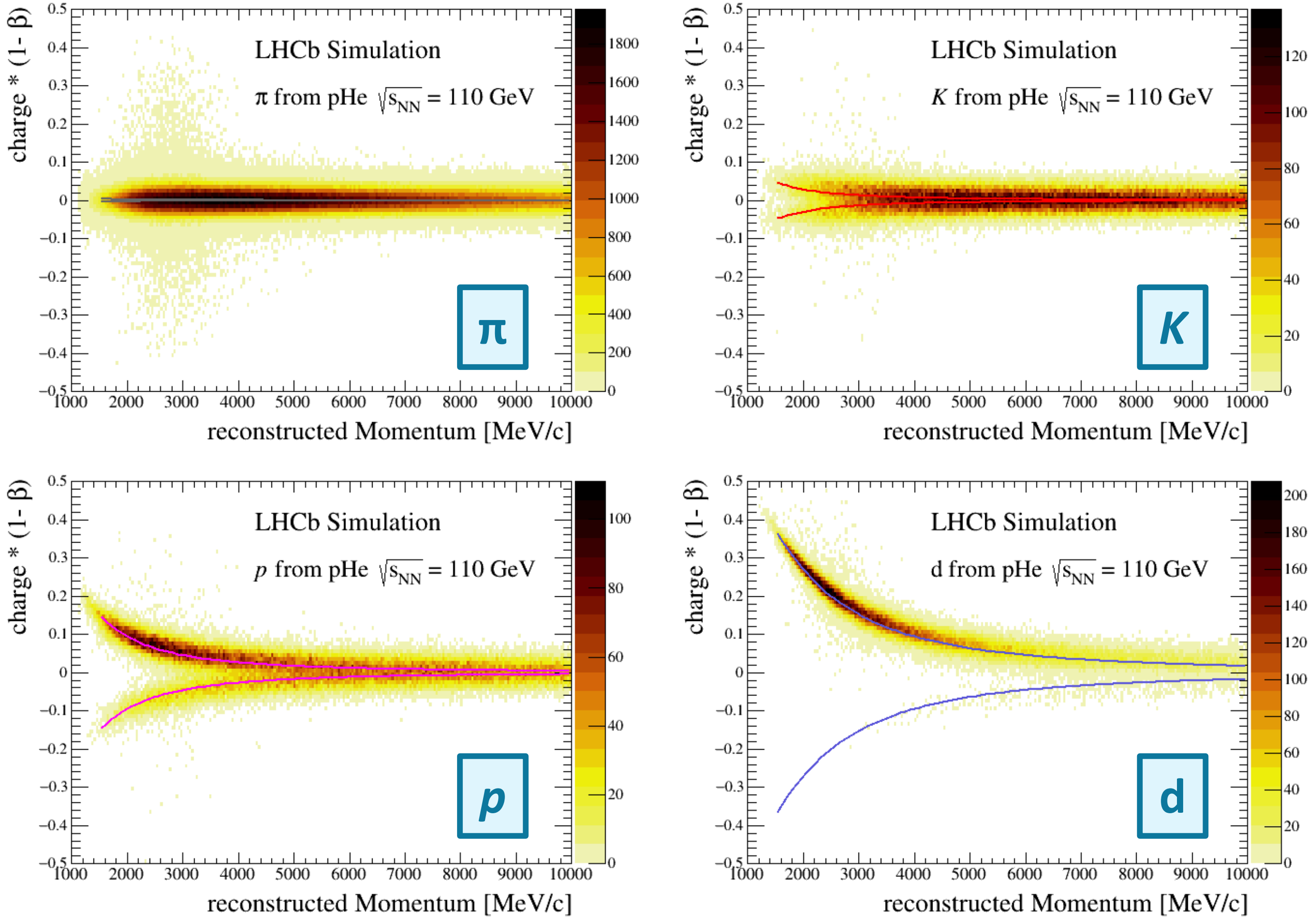

LHCb-FIGURE-2023-017

(Anti-)deuteron identification

- **SMOG *p*He** ($\sqrt{s_{NN}} = 110$ GeV) dataset reconstructed with time-of-flight reconstruction → Preliminary results

First deuteron candidates observed in *p*He data!

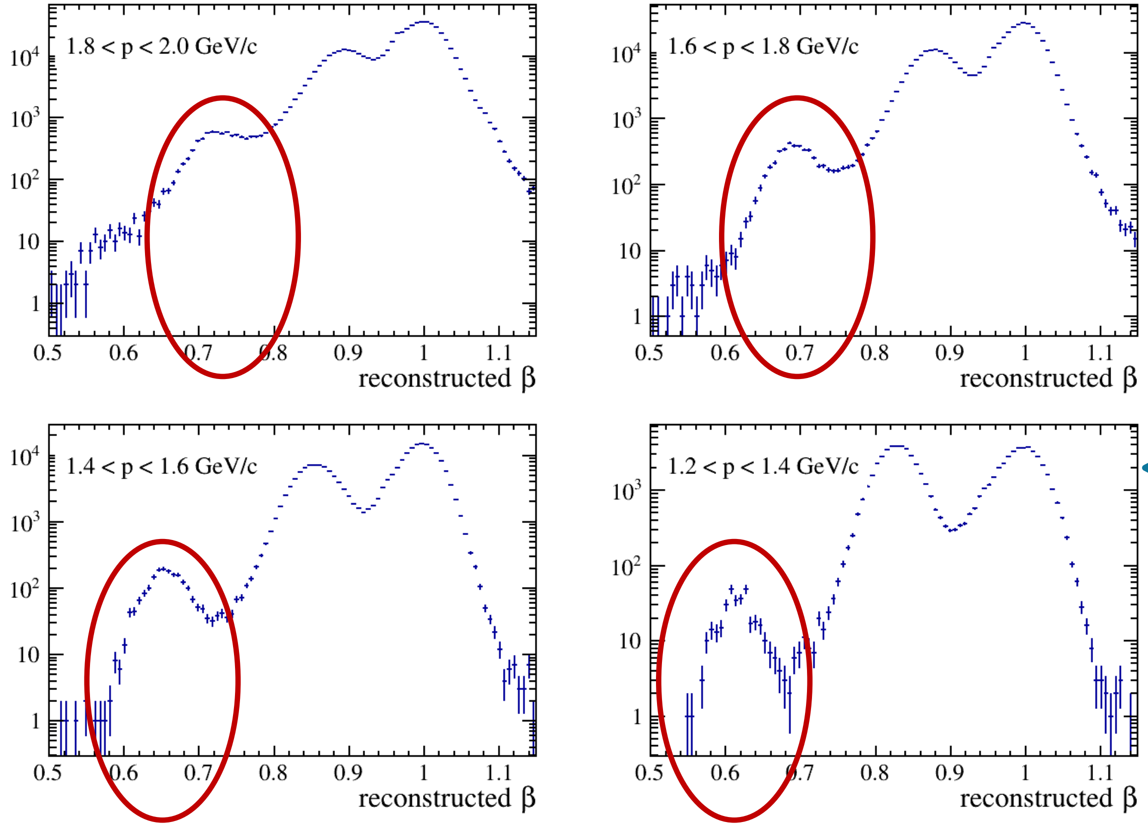

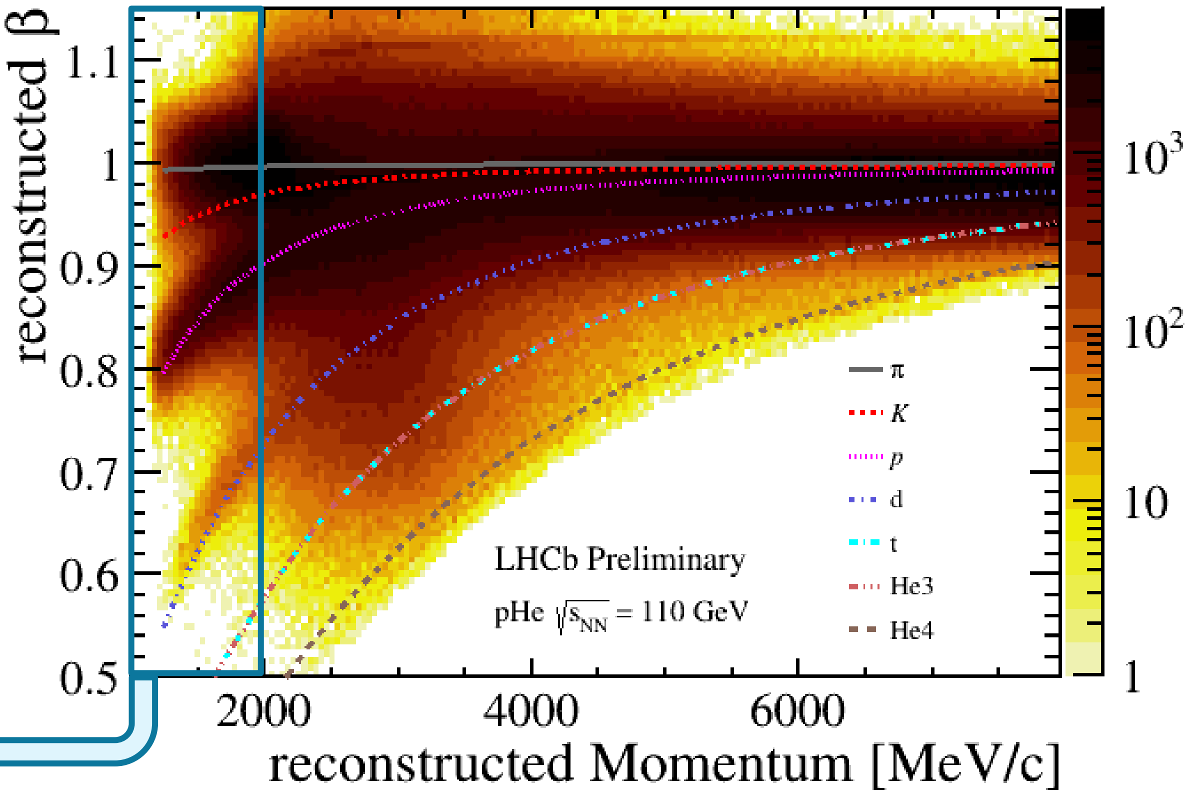

Work in progress:
- Develop MVA-based filter to improve background suppression
- Efficiencies and systematics studies

Fixed-target upgrade and gas flow studies

SMOG upgrade: SMOG2

SMOG: unique opportunity at LHC, but some limitations highlighted by analysis:

- **Limited statistics** as data collected only in dedicated periods without *pp* physics or with beam-empty LHC bunch crossing (10% of total)
- **Limited variety of collision systems**
- **Limited measurement precision**

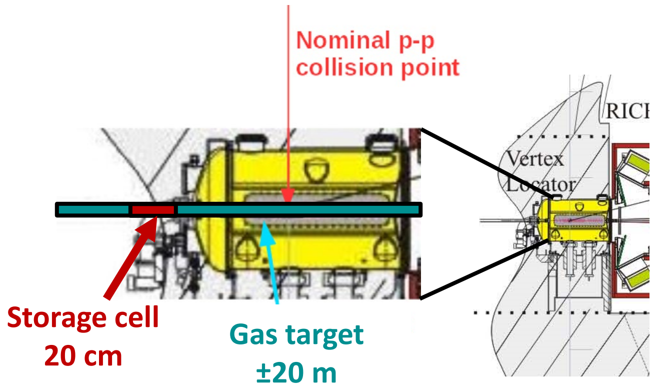

SMOG2: gas injected in a 20 cm long storage cell upstream the interaction point:

- Gas accumulates in limited region
  → **Limited contamination of beam line**
  → **x100 average pressure** with same gas flow.
  → Wider choice of injectable gases: **H_2, D_2, N_2, O_2**, Kr, Xe (+He, Ne, Ar)
- Direct and precise gas pressure and temperature measurement.
  → **Injected flux and luminosity directly measured at % level**
- Fixed-target and *pp* interaction region separated
  → **Simultaneous *pp* + fixed-target data taking**
- New gas feed system with more gas recipients
  → **Fast switch between gas** from remote (no access required)

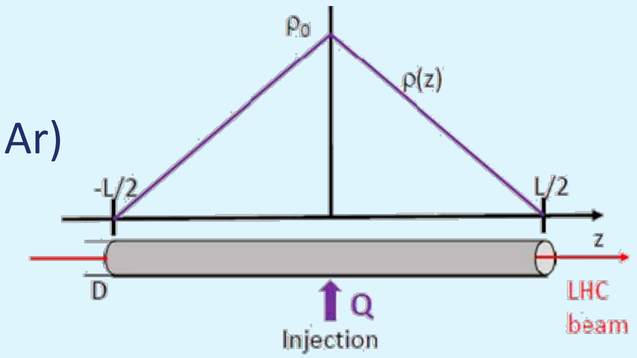

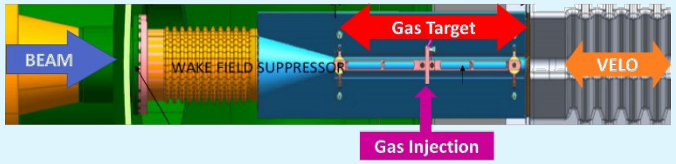

Physics opportunities with SMOG2

Unique physics opportunities never explored at LHC:

- **Charmonium, bottomonia and exotica production** from H_2 to Kr.
- **Flow measurements** at low energy over wide pseudorapidity range.
- **Ultra-peripheral collisions** in *p*A and PbA.
- *p*H_2, *p*He, *p*D_2, *p*O_2 and OH_2 collisions to extend **modelling of productions of CR interest.**

SMOG (★) and SMOG2 (★)

★2) $p\,p\,(H_2) \rightarrow \bar{p}$ to test scaling violation in forward hemisphere

★3) $p\,d \rightarrow \bar{p}$ to test isospin effects

★4) $p\,p,\ p\,He \rightarrow \bar{d},\ \overline{He}$ to determine coalescence momentum

★5) $p\,p,\ p\,He \rightarrow \pi,\ K$ to model positron source term

Martin Winkler at 2nd LHCb Heavy Ion workshop

★ H_2, O_2, N_2 for atmospheric CRs physics

Physics opportunities with SMOG2

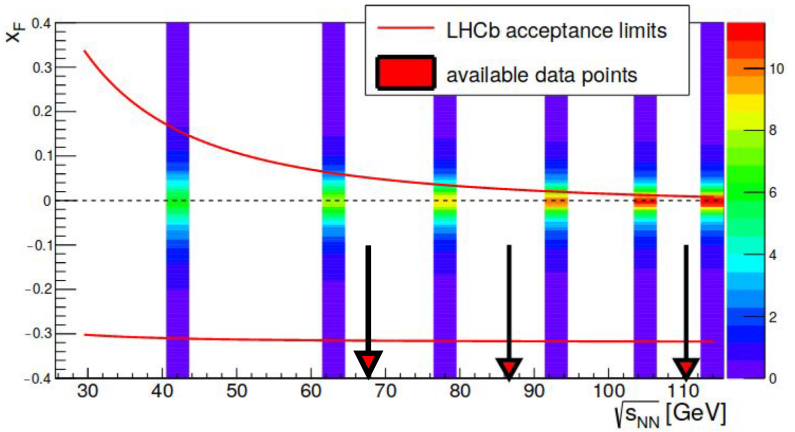

- At lower energies to test scaling violation in forward hemisphere → @87 GeV for SMOG *p*He, @68 GeV for SMOG2 during *pp* ref run
- With **H_2 injection**: $\boldsymbol{\sigma(pp \longrightarrow \bar{p}X)}$ and $\boldsymbol{\sigma(pHe \longrightarrow \bar{p}X)/\sigma(pp \longrightarrow \bar{p}X)}$ to constrain the production cross section.
- With **D_2 injection**: $\boldsymbol{\sigma(pD \longrightarrow \bar{p}X)/\sigma(pp \longrightarrow \bar{p}X)}$ to test for isospin violation and constrain the $\bar{n}$ production.
- With O_2 target and O beam: OO_2, pO_2 and OH_2 collisions to study **air showers and contribute to understand the muon puzzle**

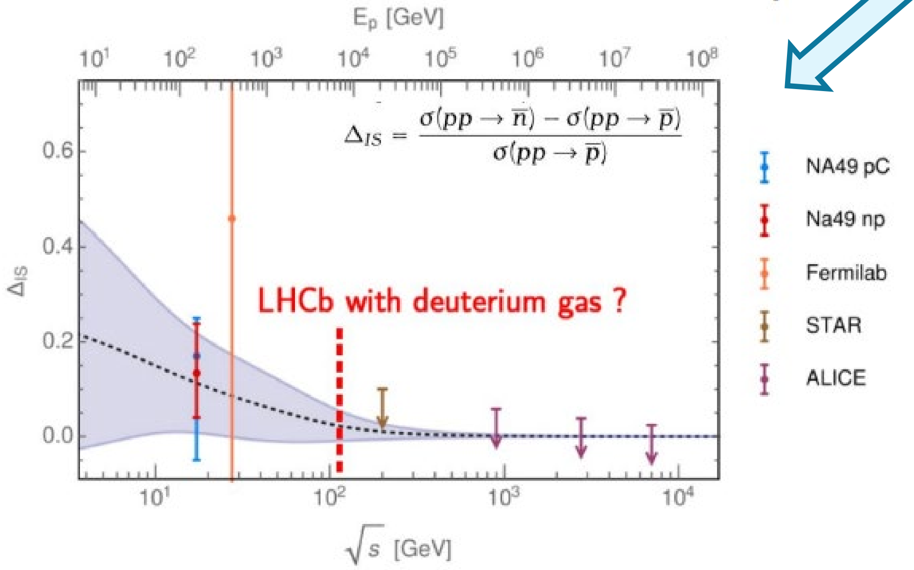

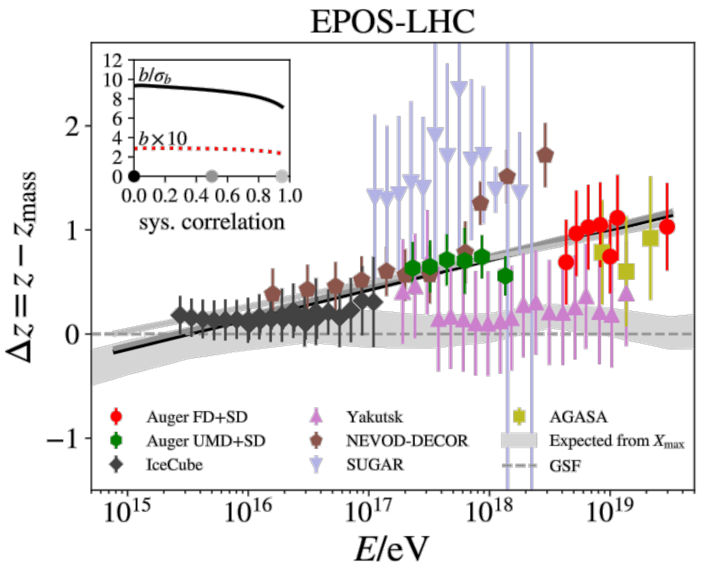

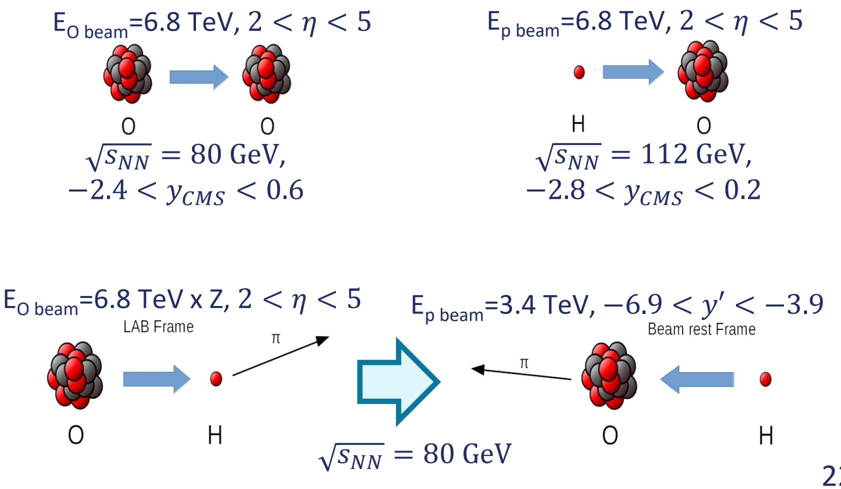

SMOG upgrade: SMOG2

Many challenges to be overcome in preparation and during operation of SMOG2

During my PhD, I took care of addressing these crucial points:

1. The storage cell is open-ended, therefore the gas flows continuously in the VELO vessel until it is extracted by the pumps.
   → **How does the non-noble gas interact with the detector material?**
2. For production measurements, the luminosity needs to be precisely known
   → **How can we calculate the luminosity for fixed-target datasamples?**
3. The SMOG2 apparatus is a new subsystem that needs to be integrated into the LHCb control system
   → **What do we need to implement for a smooth day-to-day operation by non-experts?**

Gas impact on LHC

Understand and quantify impact on LHC machine to set limits to the new gas flux injection.

The beam presence can induce desorption/emission phenomena from the surfaces exposed to it.

→ Beam pipe surface coated with Non-Evaporable Getter (NEG): thin (~µm) TiZrV film

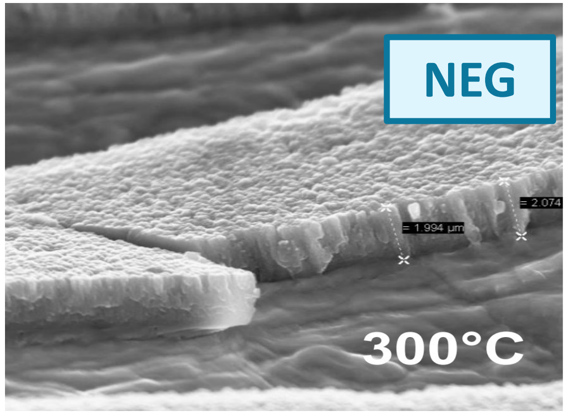

NEG coating works as a pump, adsorbing molecules on its surface through chemisorption:

- **Sticking coefficient s** (=pumping speed): probability to capture a molecule impinging on the NEG surface.

Gas can be classified according to their behaviour on NEG:

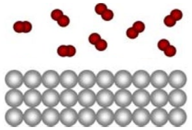

- **Noble gases** (He, Ne, Ar, Xe and Kr): not pumped by NEG, they diffuse freely.

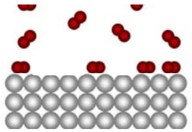

- **Getterable gases** – Non hydrogen-like (N_2 and O_2): pumped on the NEG surface. Sticking coefficient depends on available pumping sites → Progressive **saturation** of NEG (i.e. s=0).

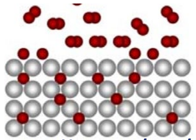

- Getterable gases – **Hydrogen-like** (H_2 and D_2): dissociate on NEG surface and diffuse into the bulk → Slow saturation of NEG, but **embrittlement** if H_{atom}/NEG_{atom} in bulk too high.

Molflow+ simulation

Impact of gases higher in the vicinity of the gas injection point
→ **VELO RF Foil**

Beam pipe + RF foil + Storage cell: complicated geometry
→ Molecular flow simulation needed to study gas injection effects:

- Detailed geometry model.
- Update NEG properties dynamically during simulation.

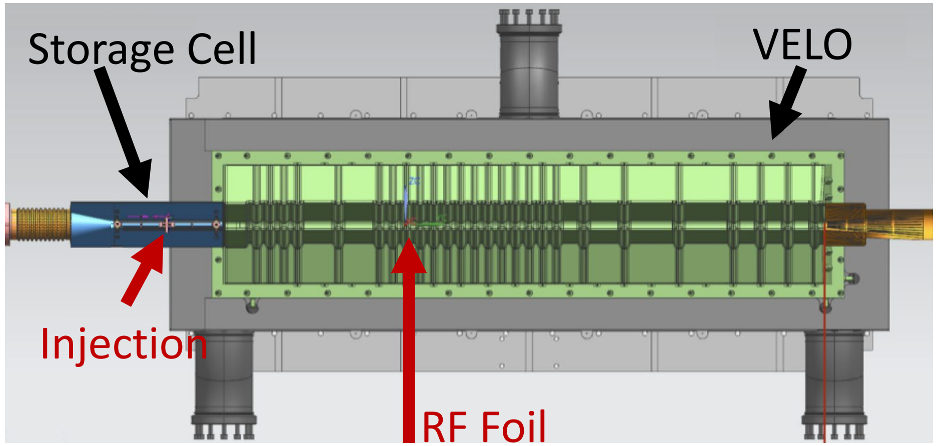

Molflow+:

- Steady-state molecular flow simulation software

Modified time-dependent simulation:

- Total simulation divided into time steps.
- NEG properties (sticking coefficient, total sorbed particles) updated after each step based on step results.

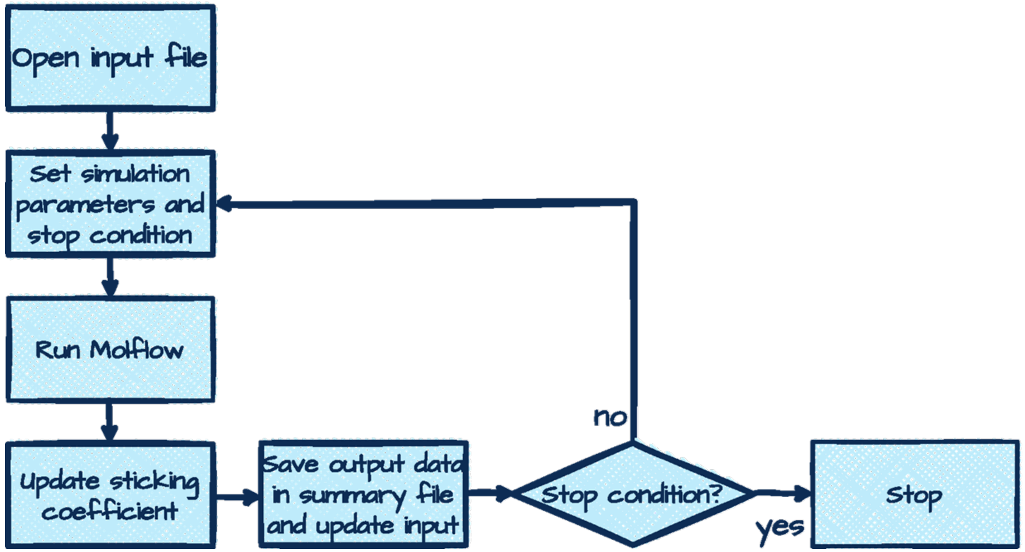

Results

TARGET: Understand the level of degradation of the NEG coating and its propagation in time and space.

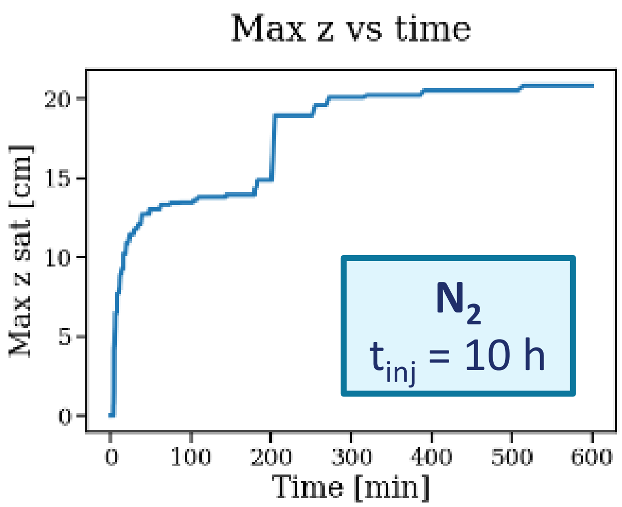

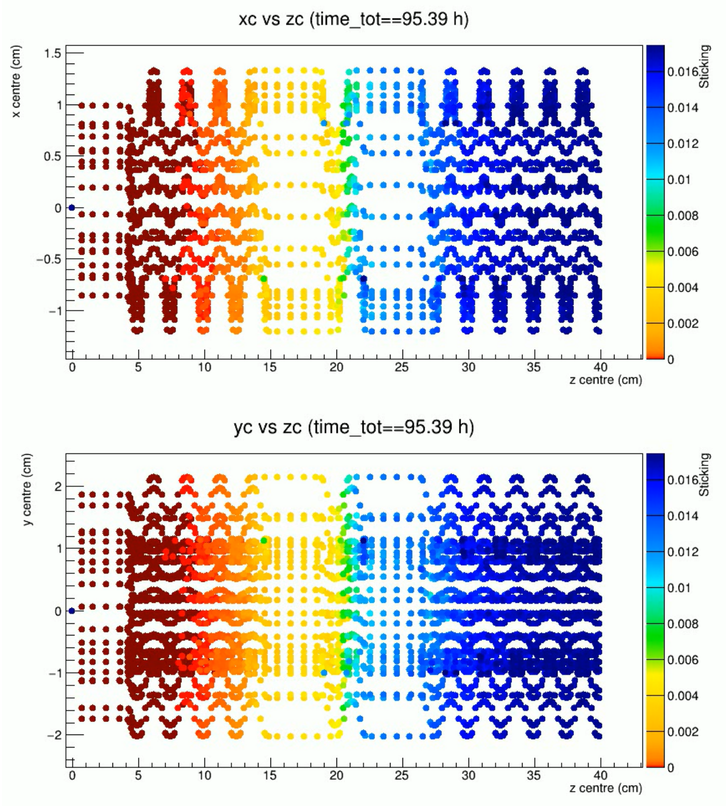

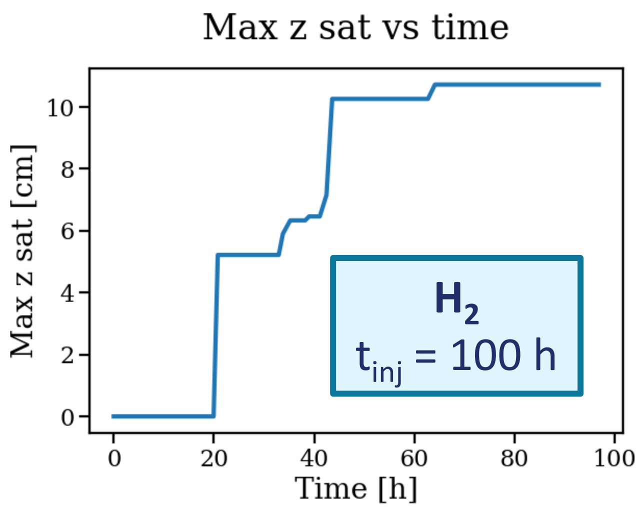

- Level of **saturation** during Run3 injections **acceptable** for LHC operation
- **No embrittlement** is expected

Approval to inject of non noble gases! First H_2 injection in November 2022

Luminosity measurement in SMOG2

Luminosity fundamental for production measurements: ${dN}/{dt} = \mathcal{L}\sigma$

→ Required precision at the percent level

In fixed-target: $\boldsymbol{\mathcal{L} = \nu_{rev} N_p \theta}$, where θ is the gas areal density

Areal density depends on **injected flux Q** and **conductance** of system **C.**

ν_{rev} = rev frequency of LHC beams
N_p = number of circulating protons
L = cell lenght
ρ_0 = maximum gas density at cell centre
Q = gas flux
k_B = Boltzmann constant
T = gas temperature
C = geometry conductance

Cylindrical cell,
injection in the middle

Triangular profile:

$$\boldsymbol{\theta = \frac{L\rho_0}{2} = \frac{LQ}{2k_B TC}}$$

$$\boldsymbol{C = 2 \cdot 3.81 \frac{D^3}{L/2 + 4D/3} \sqrt{\frac{T}{M}}}$$

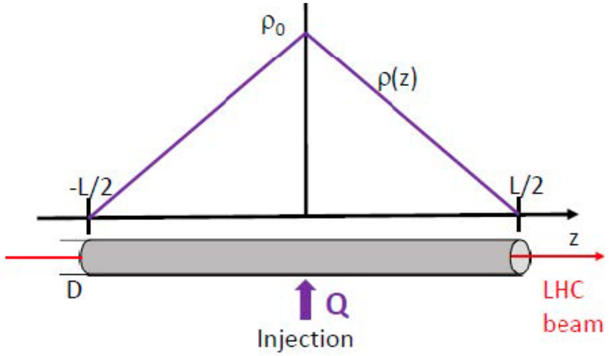

- Real cell is interfaced with a complex geometry that changes effective conductance of system
  → **Correction factor K to take into account real configuration**

$$\boldsymbol{\mathcal{L} = \mathrm{K} \cdot \nu_r N_p \cdot \frac{L}{2} \cdot \frac{1}{2 \cdot 3.81} \frac{L/2 + 4D/3}{D^3} \sqrt{\frac{M}{T}} \cdot \frac{Q}{k_B T}}$$

Luminosity: geometry impact

Molflow+ simulation to evaluate K: three geometries considered to evaluate effect of **injection point, RF foil, interfaces**

$$\mathbf{K} = \boldsymbol{\theta_{simu}/\theta_{ideal}}$$

Isolated cell, capillary injection:

- Cusp under injection point
- No impact on areal density

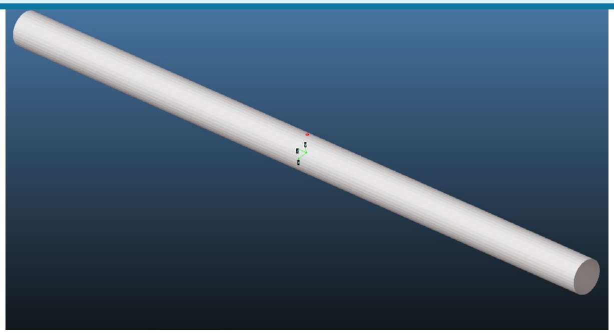

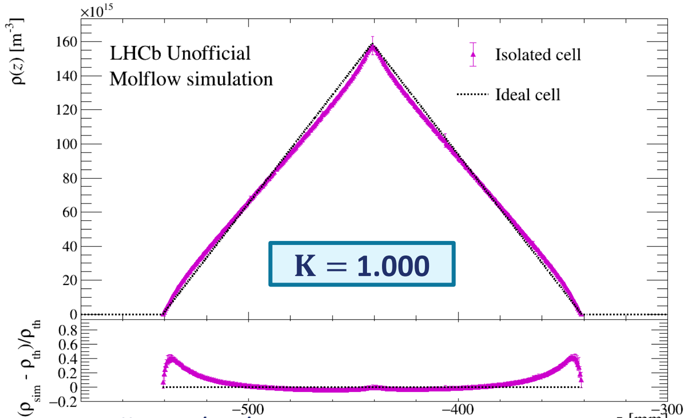

Cell + RF foil:

- Gas tail towards RF foil due to lower conductance of RF foil

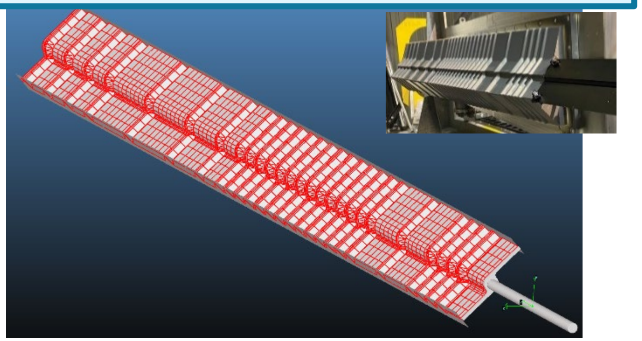

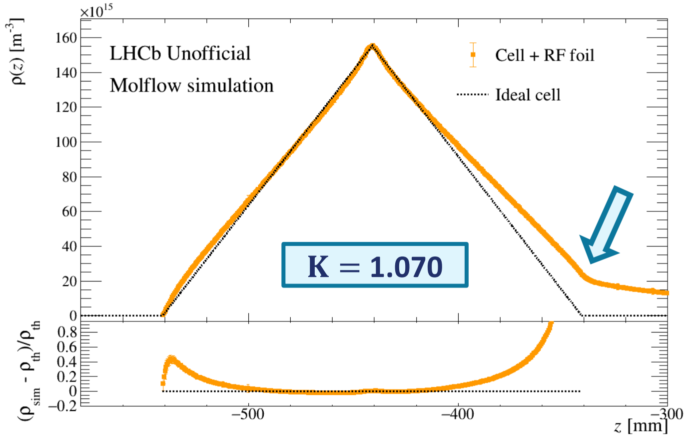

Cell + RF foil + interfaces:

- Smooth transition to 0 both upstream and downstream

Total correction factor K = 7%

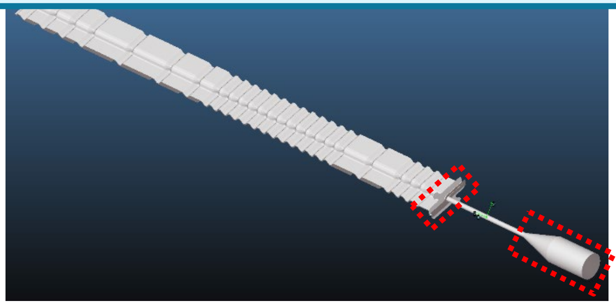

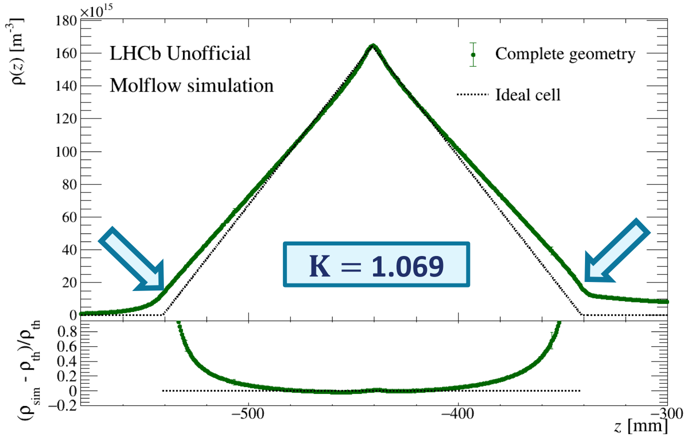

Gas flux measurement: theory

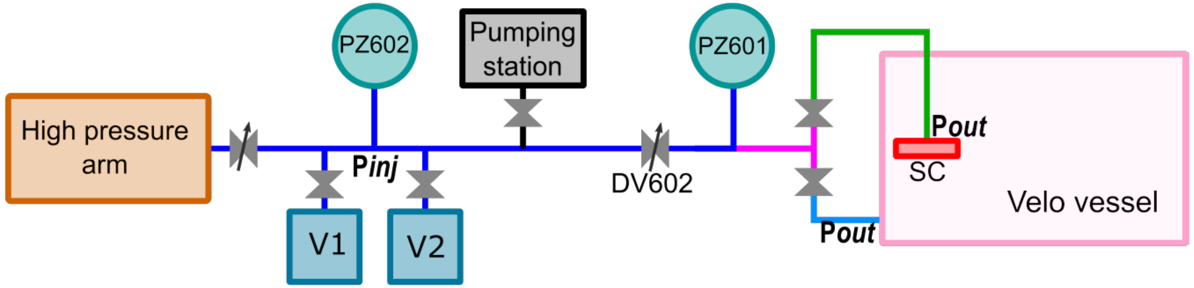

$Q = C_{inj} \times \Delta P$

- $\Delta P = P_{inj} - P_{out}$ is the pressure drop between the injection and the extraction point

$P_{inj} = 10$ mbar, $P_{out} < 10^{-4}$ mbar → $\Delta P = P_{inj}$

- C_{inj} is the conductance of the GFS line and it determines time dependence of $P_{inj}(t)$:

$$P_{inj}(t) = P_{inj}(0)e^{-t \cdot C_{inj}/V_{inj}} \quad \Longrightarrow \quad \frac{dP_{inj}(t)}{dt} = -\frac{C_{inj}}{V_{inj}} P_{inj}(t) \quad \Longrightarrow \quad \mathbf{Q} = -\frac{dP_{inj}(t)}{dt} \mathbf{V_{inj}}$$

Gas flux measured from pressure decrease in time

Online flux and lumi measurement

Online flux Q and luminosity determination:

- P_{inj} from PZ602 acquired every 10 s
- **Q from linear fit to pressure drop** over last 15 min
    - Strong instability over first 10-15 points (∼2 min).
    - Stable within expected decrease levels over the injection duration.
- **Instantaneous luminosity** from $\mathcal{L} = \mathbf{k} \cdot \nu_r N_p \cdot \frac{L}{2} \cdot \frac{1}{2 \cdot 3.81} \frac{L/2+4D/3}{D^3} \sqrt{\frac{M}{T}} \cdot \frac{Q}{k_B T}$
- Integration performed per-run as for *pp* and persisted in RunDB

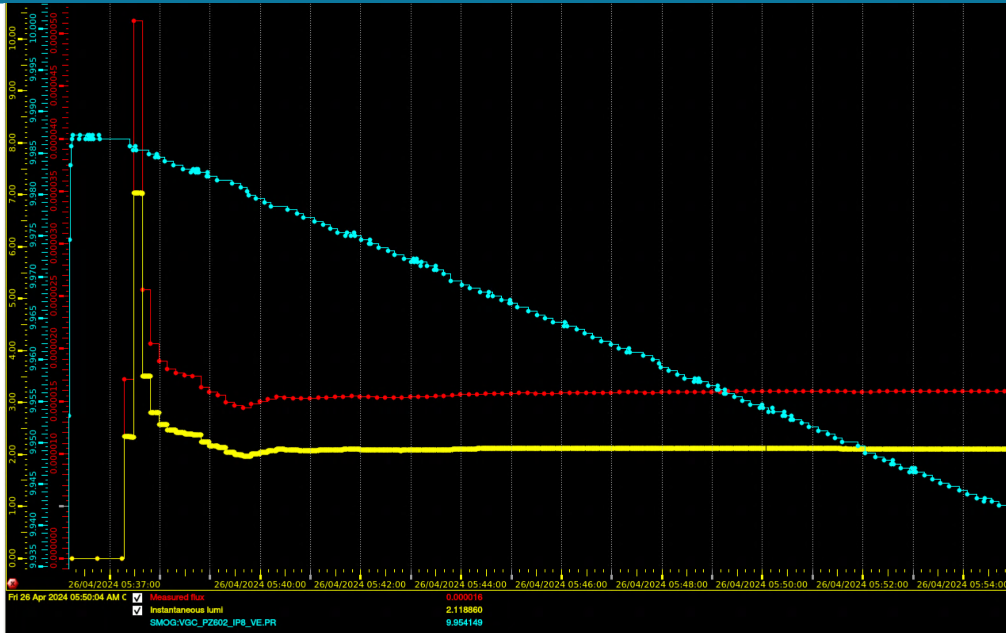

RUNID	FILLID	PARTITION: SUBDETECTORS	RUNTYPE / ACTIVITY	TCK	PHYSSTAT	STATE / DESTINATION
292195	9565	LHCb: **all but** UT_A	COLLISION24 PHYSICS	0x1000104A	0	DEFERRED OFFLINE

Beam Energy	Start Lumi	End Lumi
6800.0	0.0	932874.88451525

CalibSettings	LHCState	SMOG	SMOGLumi	avHltPhysRate	avL0PhysRate	avLumi
30, 1689, 858, 2616	PHYSICS	SMOG2_HELIUM	1463.48412397	499494.64892805	22586411.368421	892.72216044387

- **Real-time check of agreement between target and measured flux:**
    - At the moment tolerance 20% to mitigate effect of decreasing flow with time, work in progress!

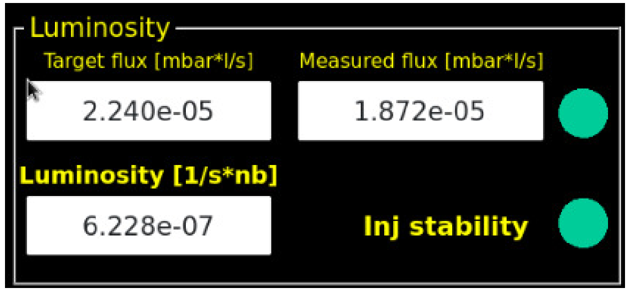

Offline flux and lumi measurement

Offline re-evaluation required to reach target precision (<2%) and evaluate related uncertainties:

- **Exponential fit to PZ602 to get C_{inj}:** $P_{inj}(t) = P_{inj}(0)e^{-t \cdot C_{inj}/V_{inj}}$
  - $P_{inj}(0)$ measured at start of each injection
  - V_{inj} measured by LHC vacuum group on GFS
- **Instantaneous Q from:** $Q(t) = -\frac{dP_{inj}(t)}{dt}V_{inj} = C_{inj}P_{inj}(t)$
- Luminosity per-run re-calculated and persisted in LumiDB
- Offline analysis not started yet, but first test on 6 hr 2023 Ar injection
  - Q decreases 2% per hour (but it depends on the gas type)
  - Average difference with **online measurement** of 5%

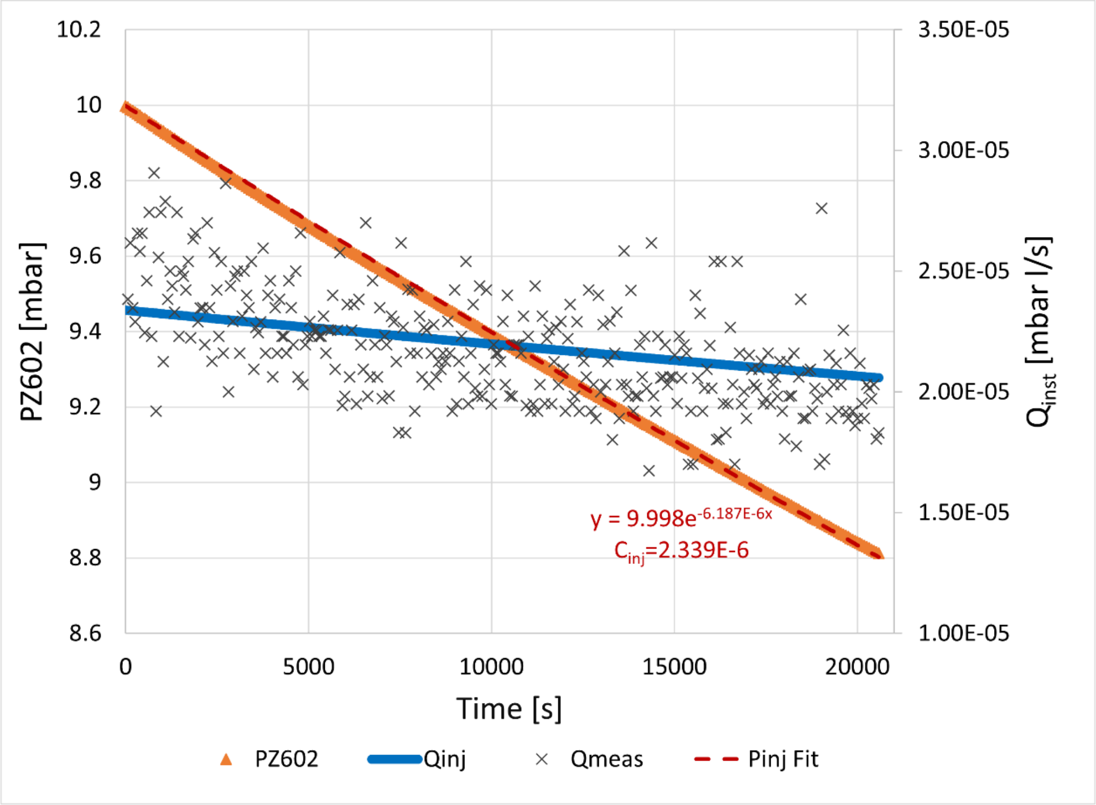

To be done:

- Validate correction factor K (from simulation)
- Validate luminosity results performing *p-e* elastic scattering measurement

SMOG2 operations

The injection in the storage cell (and all related operations) is controlled through a complex gas feed system.

- Multi-gas injection system with variable conductance to allow controlled fluxes.
- Remotely controlled valves and pumping groups to ensure purity of injected gas.

Many new exciting opportunities, much more complicated operations and control system!

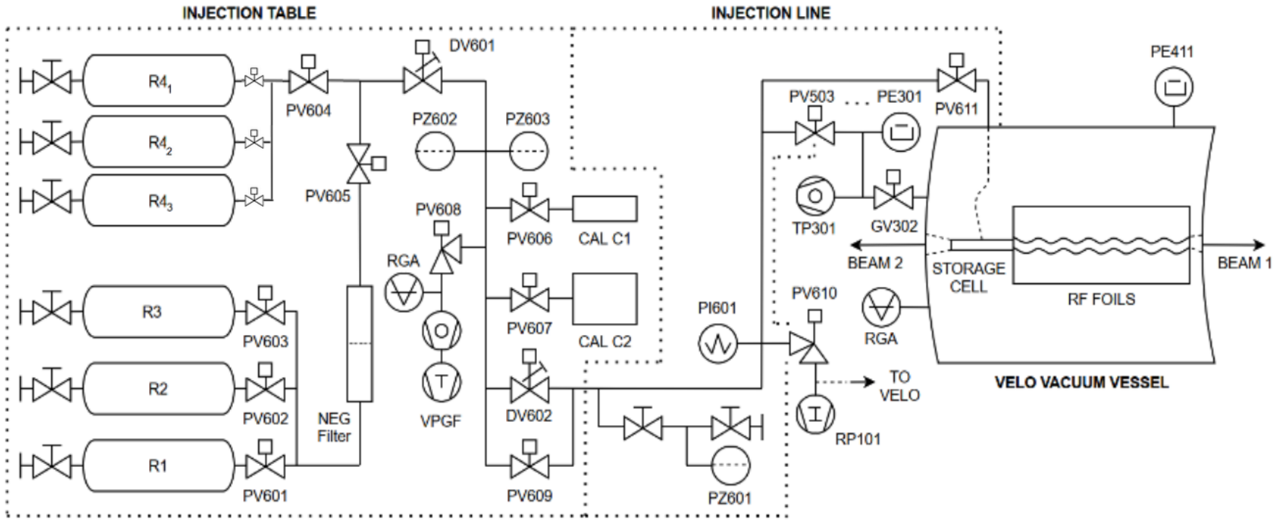

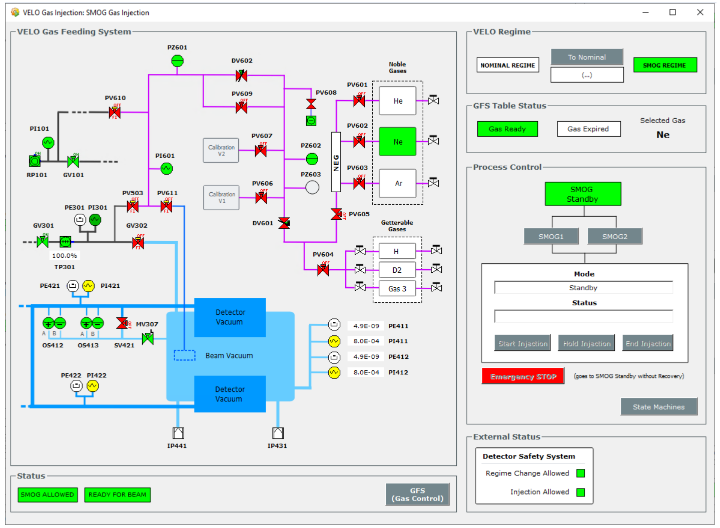

GFS controlled automatically via FSM:

Operators select which gas to inject and when start/stop the injection, pumps and valves are automatically configured by the FSM

Bucket List for a fully operational SMOG2 subsystem:

- Monitoring panel for operators and experts
- Interface with central LHCb control system

GFS monitoring panel

Injected Gas & GFS status

Valves status & SMOG regime

Flux & Lumi & Injection stability

System status, screenshot to logbook, link to instructions

Injection type

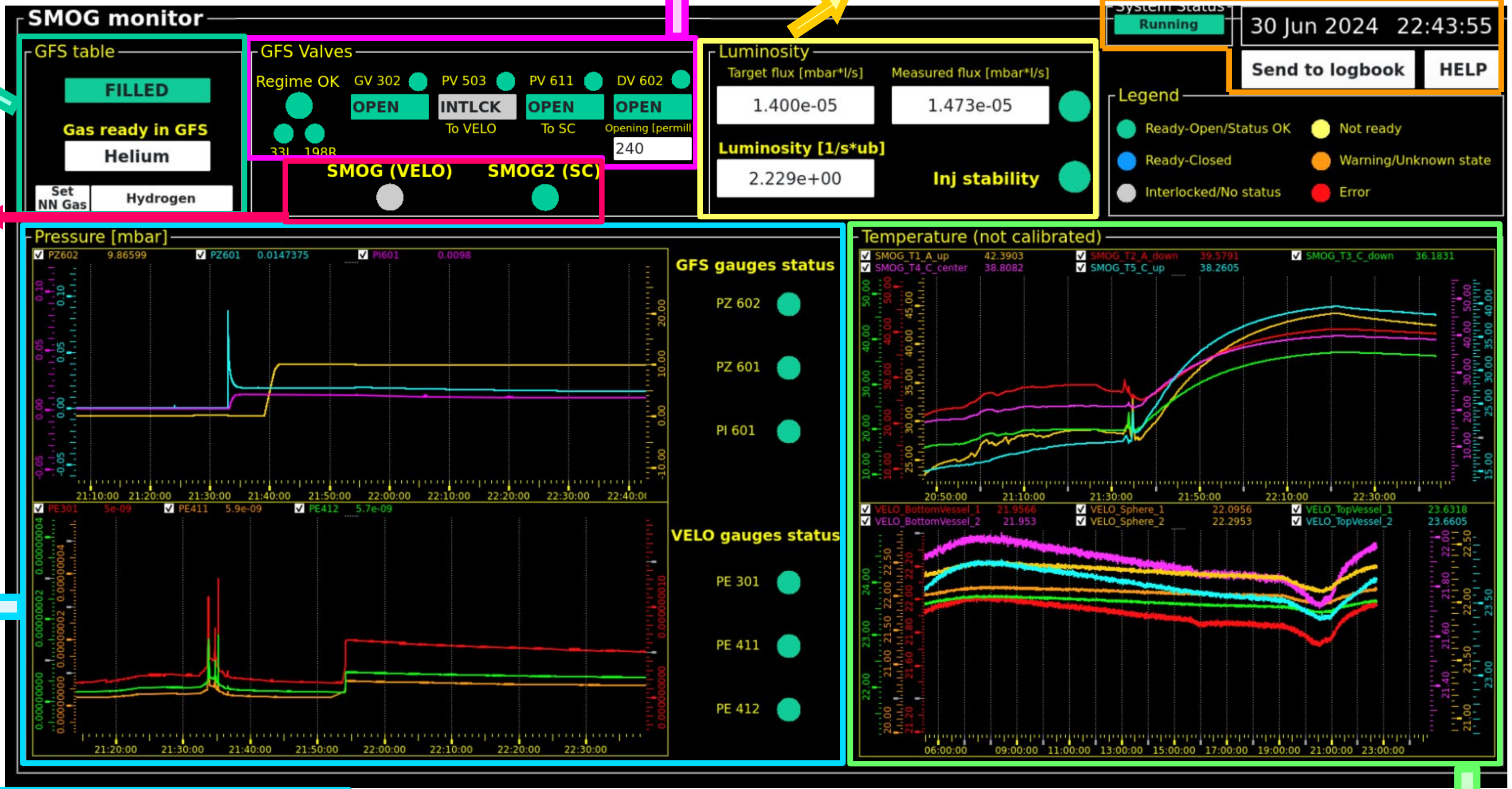

Target:

- One place with all essential operational information
- Fast identification of problems

Pressure trending plot and gauges status

Temperature trending plot

Automatic alarms for:

- Warnings/errors
- Conditions that need manual intervention

SMOG2-LHCb control interface

- LHCb operators in Control Room have to be able to easily access the status of SMOG2.
- Injection conditions (mode, gas, stability) should be stable during each run and easily accessible for analysts

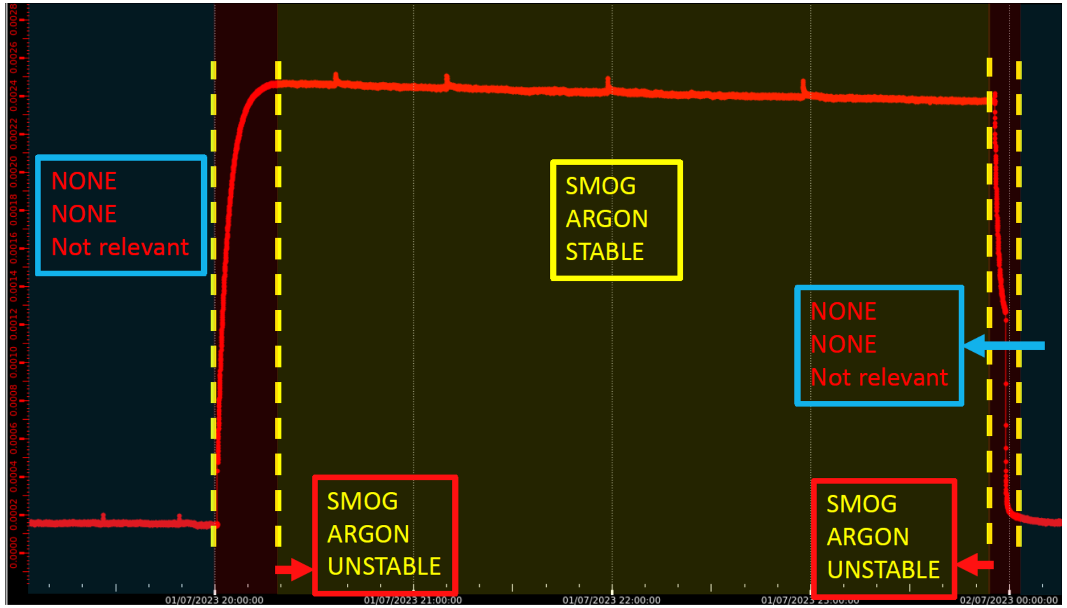

FSM to trigger run change when injection mode (NONE/SMOG/SMOG2) or status (STABLE,UNSTABLE) change.

Propagation of injection conditions to

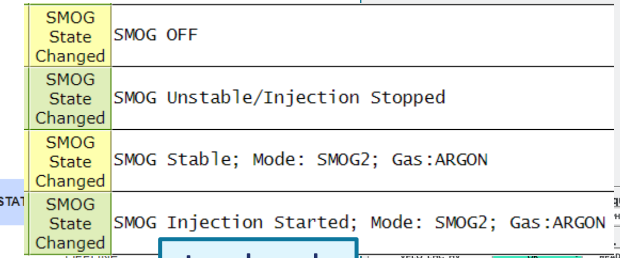

Logbook

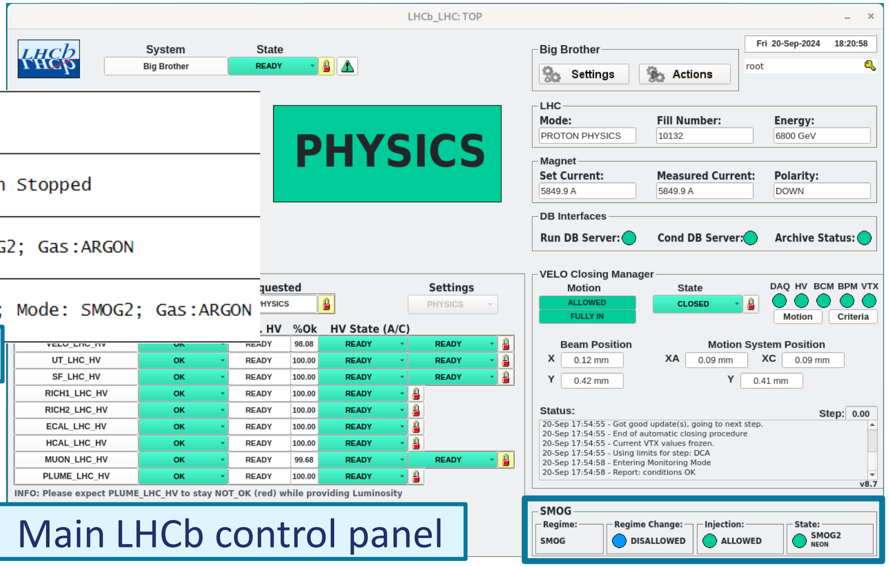

Main LHCb control panel

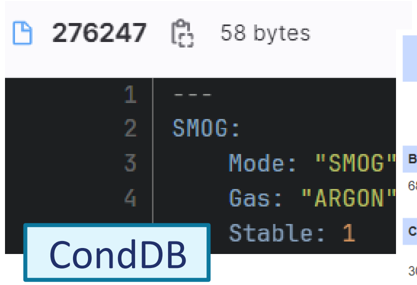

CondDB

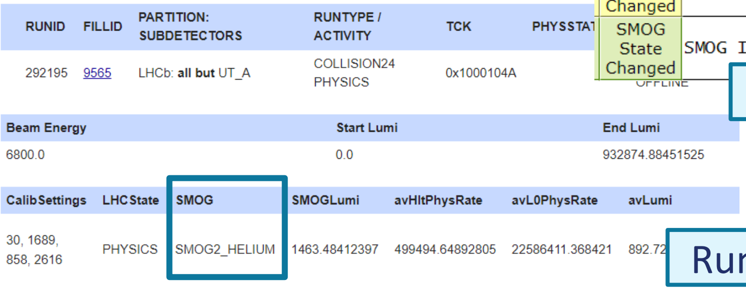

RunDB

Validation on data

Injections in SMOG2 as default since May 2024, already collected hundreds of hours for all available gases
→ **H_2 regularly injected in LHC!**

Efficient separation between *pp* and *p*Ar

→ **Operating simultaneously in collider and fixed target mode with two colliding system and energies!**

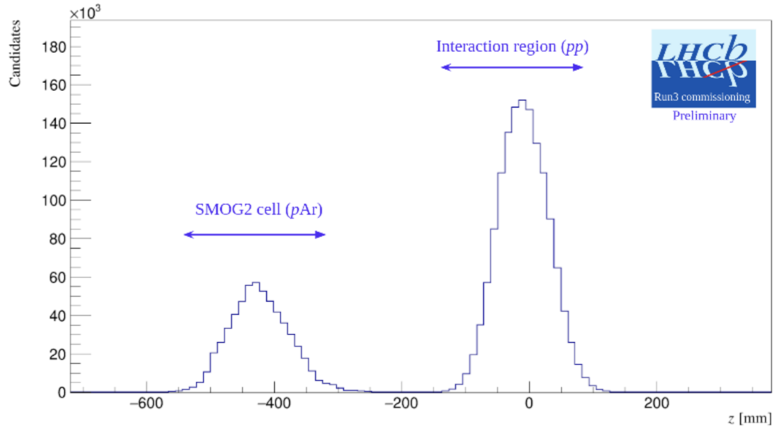

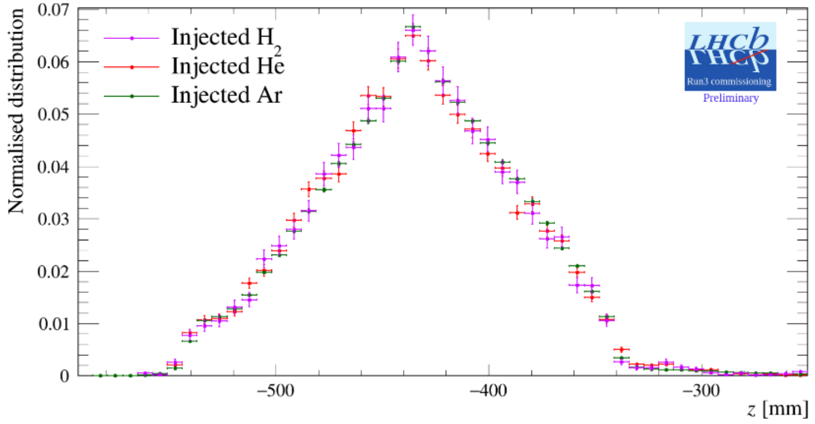

Gas density profile follows a **triangular shape, independent from gas type**

Large statistics of signals already collected!

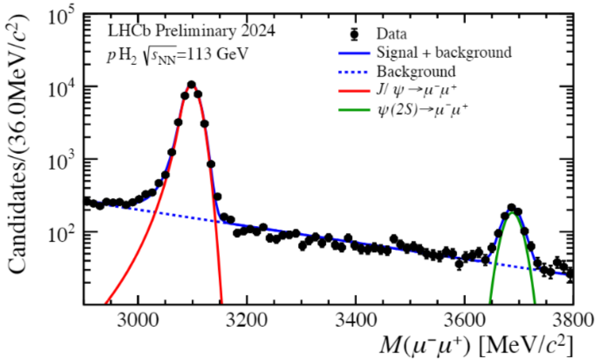

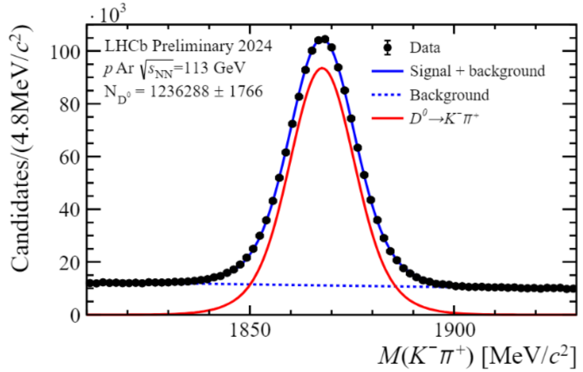

Conclusions

LHCb fixed-target programme is continuously expanding its physics reach

- New time-of-flight based technique to reconstruct and identify low momentum (anti-)deuterium

  → **First deuteron candidates observed in LHCb!**

- Gas flow simulation studies for upgraded SMOG2 system to:
  - control systematics on density profile for precise luminosity measurement

    → **Systematic on luminosity from density profile within percent level**

  - demonstrate the feasibility of injecting non-noble gases: H_2, N_2, O_2

    → **First H_2 injection in November 2022, regularly performed since May 2024**

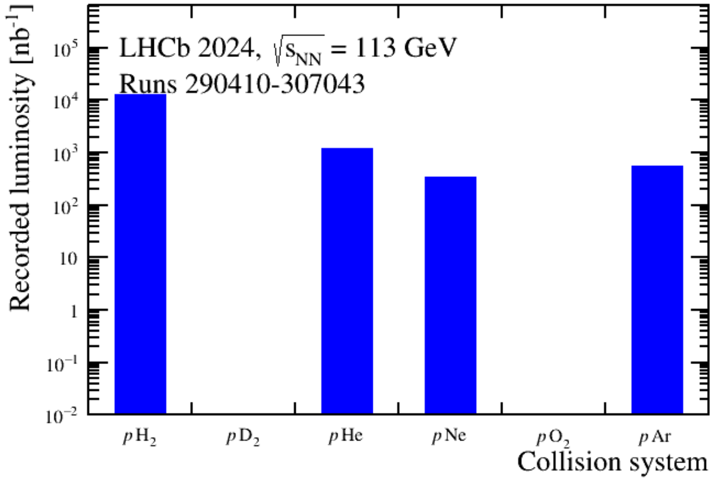

Exiting new physics results expected with data collected in 2024 and 2025

Thanks for the attention

BACKUP

LHCb fixed-target apparatus

Unique physics opportunities at the LHC

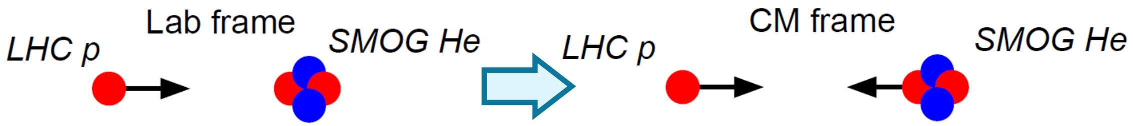

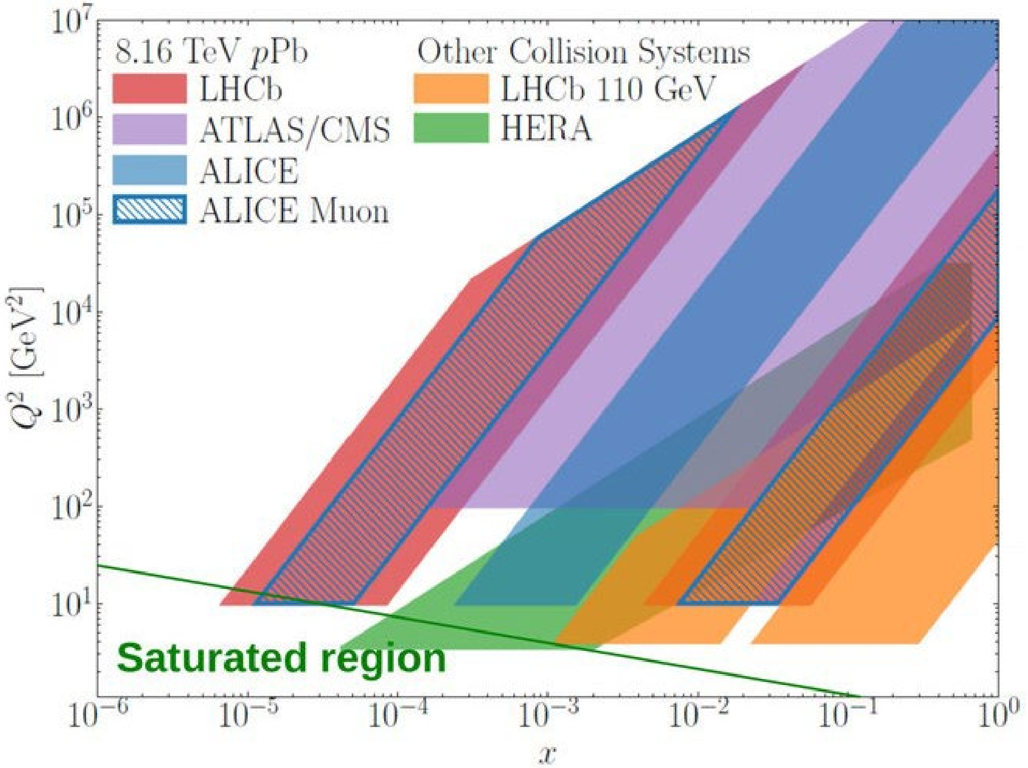

LHCb-PUB-2018-015

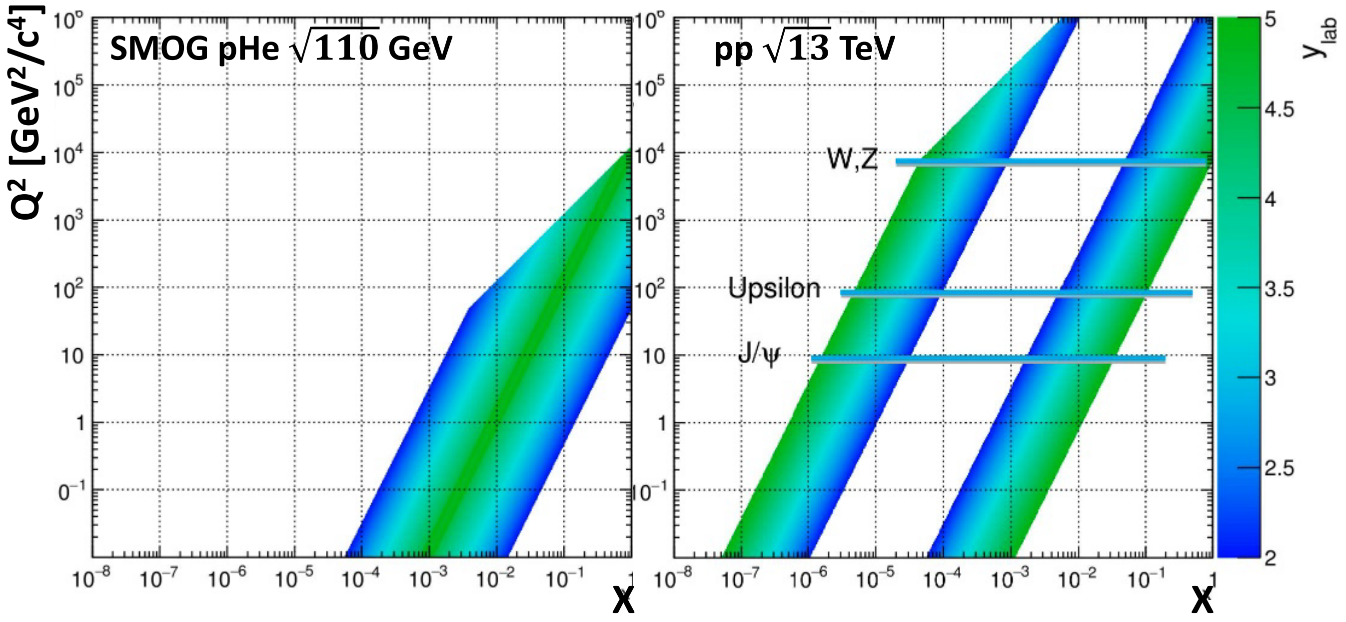

Prompt antiproton production

PRL 121 (2018) 222001

First measurement of $\sigma(pHe \to \bar{p}_{prompt}X)$ at $\sqrt{s_{NN}} = 110\ GeV$:

- $\bar{p}$ reconstructed in the kinematic region ($p \in [12,110]\ GeV/c$, $p_T \in [0.4, 4]\ GeV/c$) to optimize reconstruction and particle identification efficiencies.
- **Only $\bar{p}$ promptly produced** considered
  → detached component reduced cutting on the impact parameter wrt the primary vertex.
- $\bar{p}$ number from simultaneous fit to PID variables in (p, p_T) bins.
- Luminosity from ***pe* elastic scattering** with gas atomic electrons.

  → **Dominant contribution to systematic:**

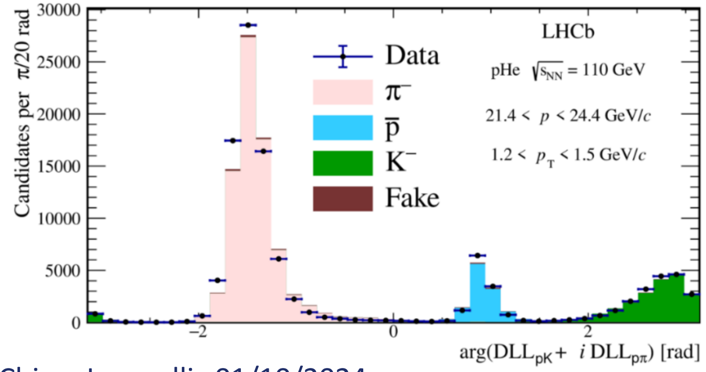

- **Luminosity measurement:** injected gas pressure not precisely measured.
- **Particle identification performance:** poor calibration statistics.

- Result on XS is compared to different MC event generator.
- **Experimental uncertainties (<10%) are lower than the spread among theoretical models.**

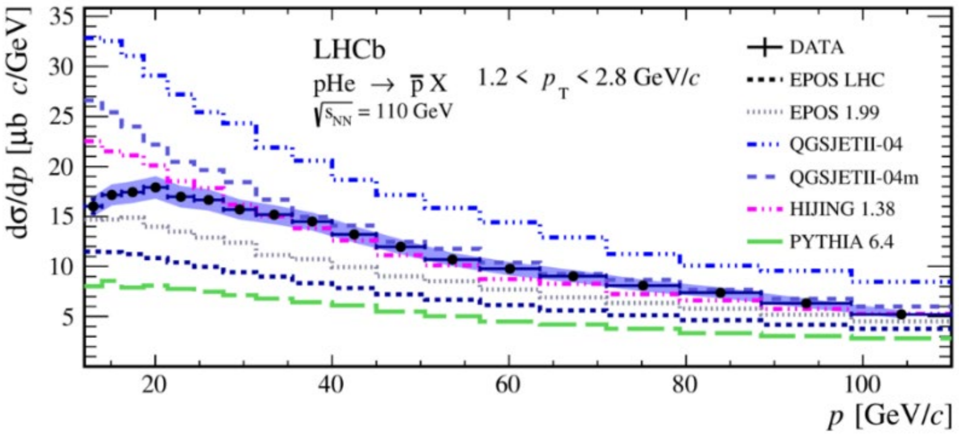

Luminosity measurement in SMOG data samples

PRL 121 (2018) 222001

SMOG is not equipped with precise gauges for the gas pressure:

→ Luminosity is determined through ***pe* elastic scattering** with gas atomic electrons.

- pe events are identified as an isolated low-energy electron track.
- Charge symmetric background is evaluated through positron yield and subtracted from electron yield.
- Poor electron reconstruction efficiency (16%) → 6% uncertainty on luminosity

Dominant contribution to systematic uncertainty on σ!

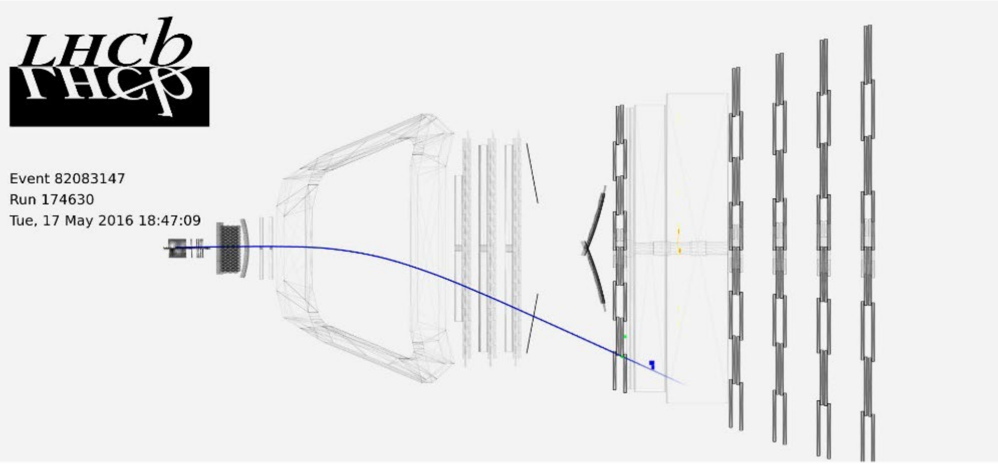

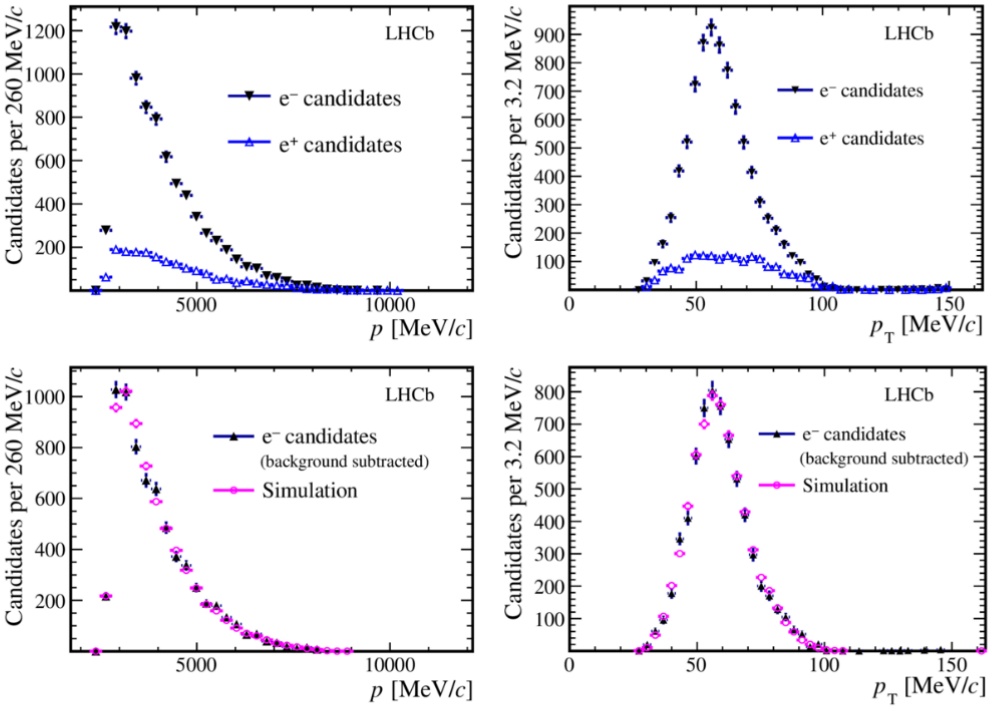

Detached antiproton production

- Around **20-30% of $\overline{p}$ production** comes from anti-hyperon decays → Dedicated measurement to the component from anti-hyperon decays in *p*He, extending first LHCb result only dealing with prompt processes

$$\bar{\Lambda}^0_{\text{prompt}} \to \bar{p}\pi^+ \qquad \bar{\Sigma}^- \to \bar{p}\pi^0 \qquad \bar{\Xi}^+ \to \bar{\Lambda}\pi^+ \qquad \bar{\Xi}^0 \to \bar{\Lambda}\pi^0 \qquad \bar{\Omega}^+ \to \bar{\Lambda}K^+$$

- Available data indicate strangeness enhancement but **large spread among different theoretical models**

→ **LHCb SMOG measurement can constrain the models**

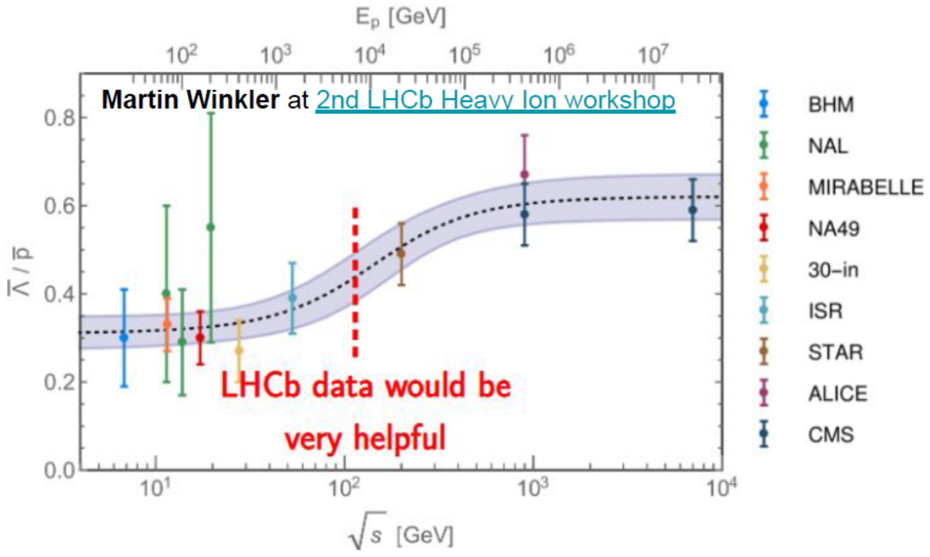

CERN-THESIS-2021-313

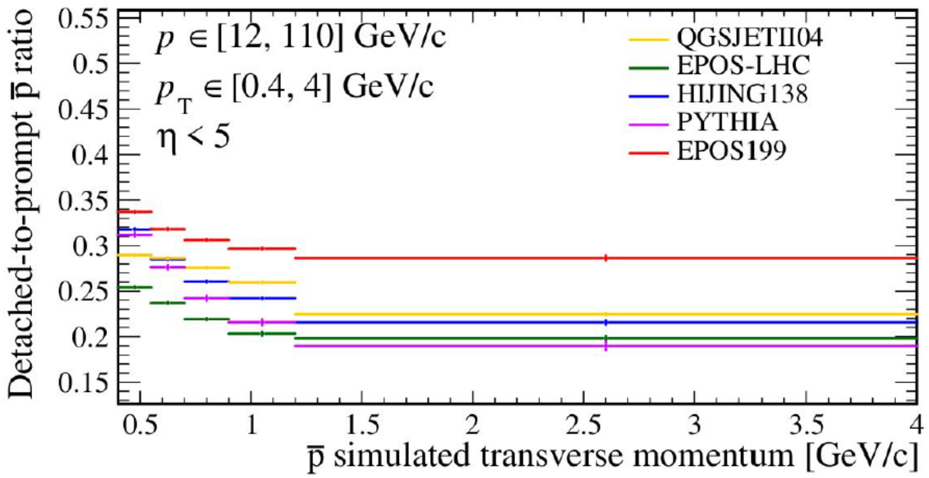

Analysis strategy

Eur. Phys. J. C83 (2023) 543

Analysis for secondary-to-primary $\bar{p}$ ratio $\boldsymbol{R = \sigma_{sec}/\sigma_{prim}}$ following **two complementary approaches**:

- **Exclusive approach**: $$R_{\bar{\Lambda}} = \frac{\sigma(p\text{He} \to (\bar{\Lambda}_{\text{prompt}} \to \bar{p}\pi^+)X)}{\sigma(p\text{He} \to \bar{p}_{\text{prompt}}\, X)}$$
  - Measure $\boldsymbol{\bar{\Lambda} \longrightarrow \bar{p}\pi^+}$, dominant detached component.
  - Identifying decay exploiting LHCb **excellent mass resolution** (no PID info).

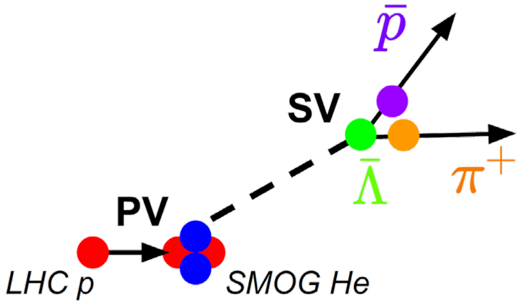

- **Inclusive approach**: $$R_{\bar{H}} \equiv \frac{\sigma(p\text{He} \to \bar{H}X \to \bar{p}X)}{\sigma(p\text{He} \to \bar{p}_{\text{prompt}}X)},\ \bar{H} = \bar{\Lambda}, \bar{\Sigma}, \bar{\Xi}, \bar{\Omega}$$
  - Focused on **all detached components.**
  - Selecting **antiproton with PID information** and distinguishing between prompt and detached $\bar{p}$ via excellent VELO IP resolution.

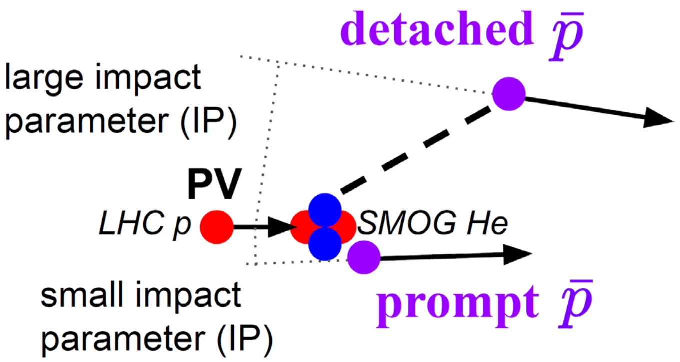

Exclusive approach

[Eur. Phys. J. C83 (2023) 543]

Measure antiprotons from $\overline{\Lambda}_{prompt}$: $R_{\bar{\Lambda}} = \dfrac{\sigma(p\mathrm{He} \rightarrow (\bar{\Lambda}_{\mathrm{prompt}} \rightarrow \bar{p}\pi^+)X)}{\sigma(p\mathrm{He} \rightarrow \bar{p}_{\mathrm{prompt}}\ X)}$

- Event selection via **kinematic description in the Armenteros plot** and **impact parameters to select signal decays**.
- Most systematic uncertainties (luminosity, reco, …) **cancel in the ratio**.

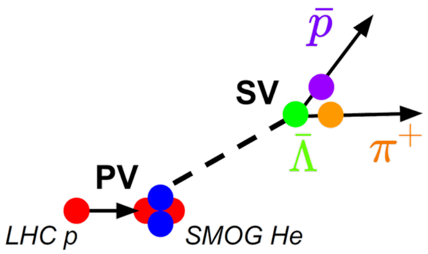

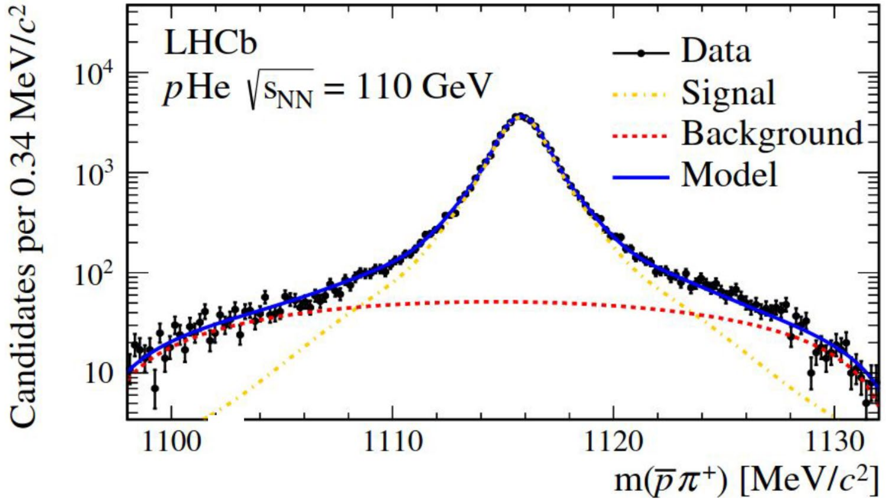

Larger contribution measured wrt all most widely used theoretical models

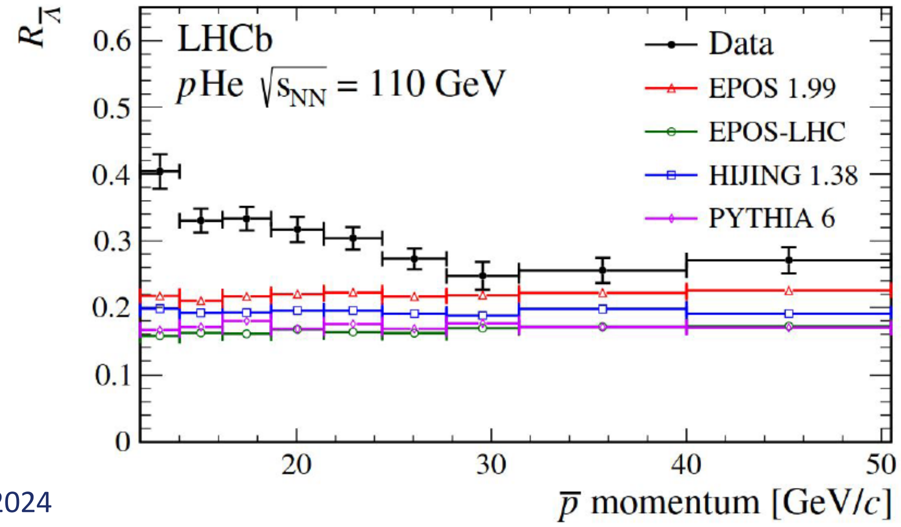

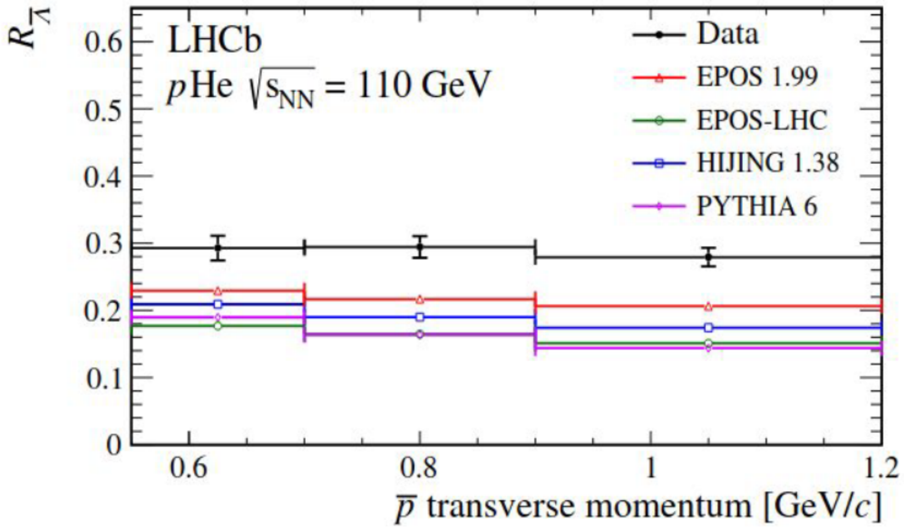

Inclusive approach

Eur. Phys. J. C83 (2023) 543

Measure antiprotons from all detached components: $R_{\bar{H}} \equiv \frac{\sigma(p\mathrm{He} \to \bar{H}X \to \bar{p}X)}{\sigma(p\mathrm{He} \to \bar{p}_{\mathrm{prompt}}X)}$, $\bar{H} = \bar{\Lambda}, \bar{\Sigma}, \bar{\Xi}, \bar{\Omega}$

- Sample enriched with $\bar{p}$ **selected with tight PID cuts**.
- Components statistically separated as **prompt**, **detached** and **secondary** with a **fit to the *p*He data impact parameter with the composition of templates** (Gaussian compositions applied to simulation).

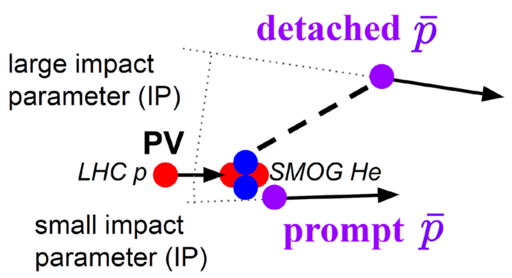

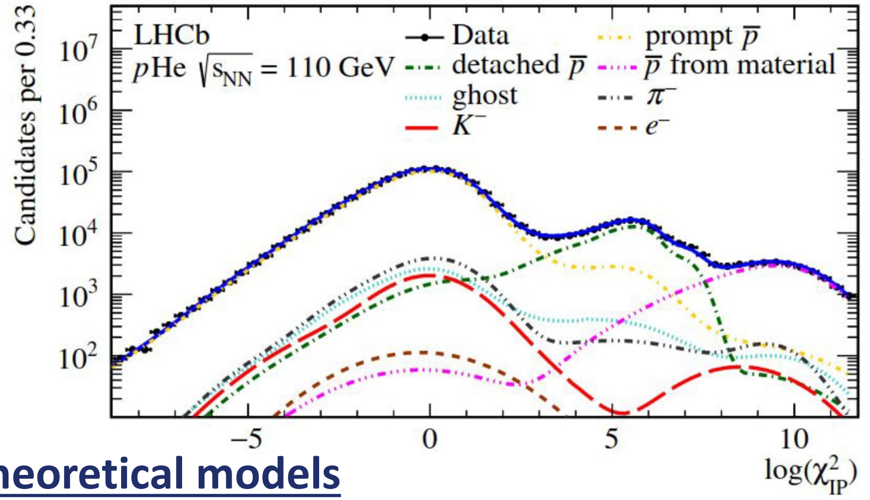

Larger contribution measured wrt all most widely used theoretical models

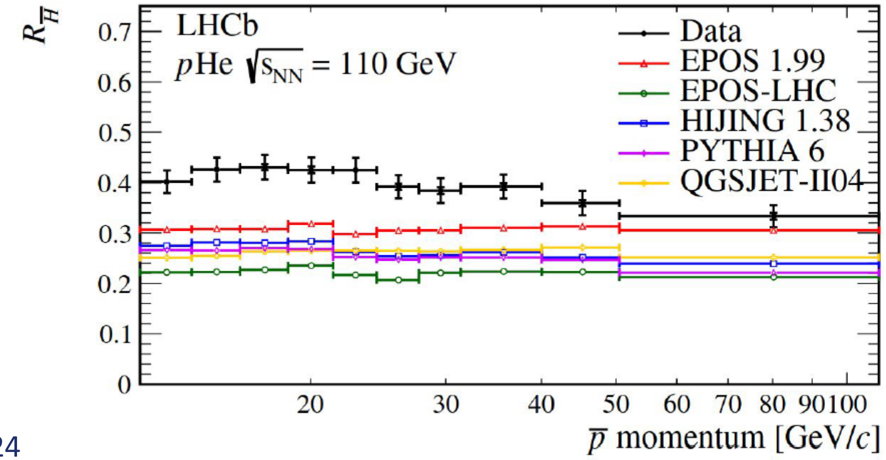

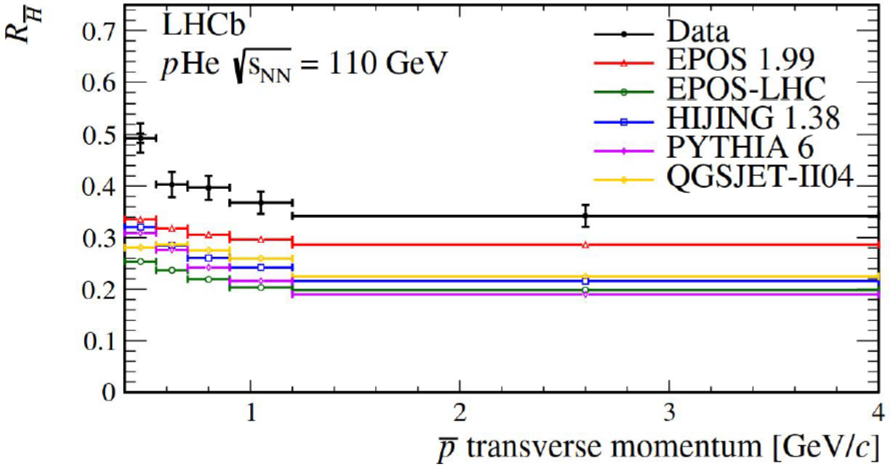

Comparison between the approaches

Eur. Phys. J. C83 (2023) 543

- Ratio of the results is expected to be **predicted more reliably** than the single terms (depends only on the hadronization).
- Results mutually cross-checked since found to be **consistent with EPOS-LHC prediction.**

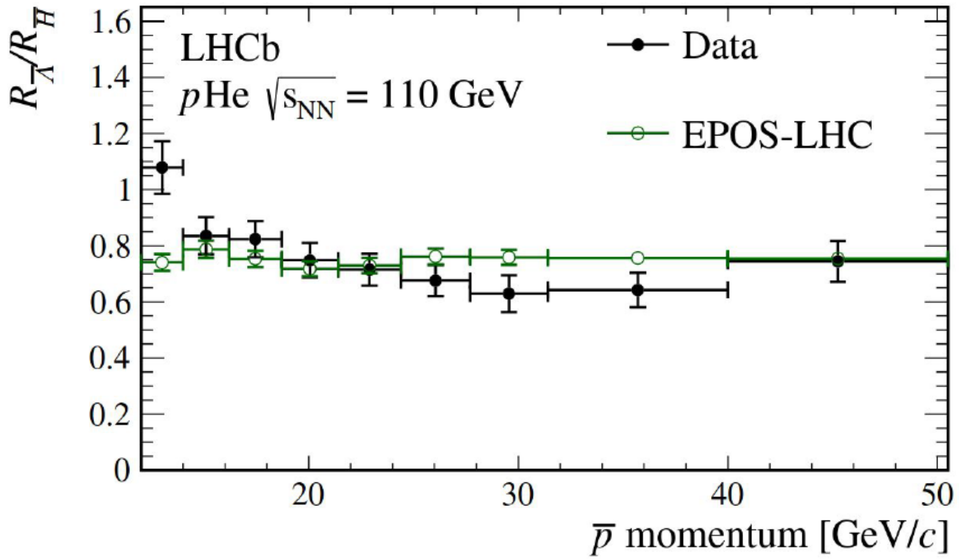

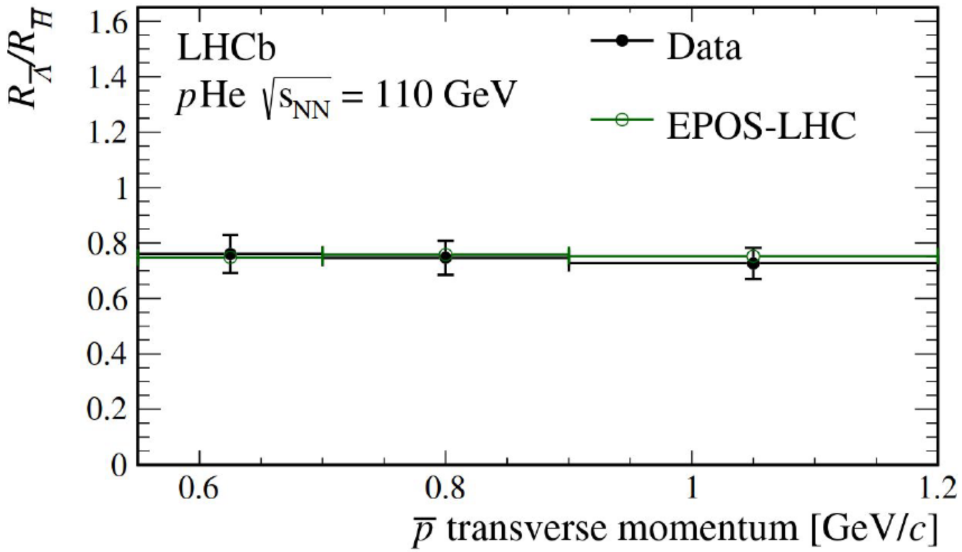

Anti-nuclei production

- Main channels for indirect DM measurements are e^+ and $\bar{p}$ but limited in accuracy by the knowledge of background from secondary production (e^+, $\bar{p}$) and standard primary sources (e^+).
- Anti-nuclei production cross section (SM) scales with mass number A: $\sigma_{anti\text{-}N}/\sigma_{anti\text{-}p} = (10^{-3})^{A-1}$

  → $\bar{d}$ and $\overline{^3He}$ are ideal channels but it's necessary to predict with high precision the secondary flux.

⇩

Coalescence model:

An anti-nucleus is produced if the nucleons are sufficiently close in phase space: **B_A coalescence probability**.

- Experimental data suggest that B_A depends on the **type of reaction** (*pp*, *p*A or AA) and on the **incident particle momentum** (p_{lab}).
- **No comprehensive theoretical model** to explain from first principles (anti-)nuclei production in hadronic interactions

  → Phenomenological models tuned on data

⇨ **More direct measurements in the interesting system and energy range are needed.**

Coalescence model

$\bar{d}$ formation is described via the coalescence of a $\bar{p}$-$\bar{n}$ pair:

$$\gamma_{\bar{d}} \frac{d^3 N_{\bar{d}}}{d^3 k_{\bar{d}}}(\vec{k}_{\bar{d}}) = \frac{4}{3}\pi p_0^3 \cdot \gamma_{\bar{p}} \gamma_{\bar{n}} \frac{d^3 N_{\bar{p}} d^3 N_{\bar{n}}}{d^3 k_{\bar{p}} d^3 k_{\bar{n}}} \left(\frac{\vec{k}_{\bar{d}}}{2}, \frac{\vec{k}_{\bar{d}}}{2} \right) \quad (1)$$

Factorization hypothesis and *isospin invariance* hypothesis:

$$\gamma_{\bar{d}} \frac{\mathrm{d}N_{\bar{d}}}{\mathrm{d}^3 k_{\bar{d}}}(\vec{k}_{\bar{d}}) = R_n(\sqrt{s + m_{\bar{d}}^2 - 2\sqrt{s}E_{\bar{d}}}) \cdot \frac{4}{3}\pi p_0^3 \cdot \left[\gamma_{\bar{p}} \frac{\mathrm{d}N_{\bar{p}}}{\mathrm{d}^3 k_{\bar{p}}} \left(\frac{\vec{k}_{\bar{d}}}{2} \right) \right]^2 \quad (2)$$

where R_n is associated to the reduction of the phase space after the production of the first nucleon.

For an anti-nucleon with mass number A, under the same hypotesis:

$$\gamma_A \frac{\mathrm{d}N_A}{\mathrm{d}^3 k_A}(\vec{k}_A) = R_n(\sqrt{s + m_A^2 - 2\sqrt{s}E_A}) \cdot \left(\frac{4\pi}{3} p_0^3 \right)^{(A-1)} \cdot \left[\gamma_{\bar{p}} \frac{\mathrm{d}N_{\bar{p}}}{\mathrm{d}^3 k_{\bar{p}}} \left(\frac{\vec{k}_A}{A} \right) \right]^A \quad (3)$$

Alternative parameter: $B_A = \frac{A}{m_p^{A-1}} \left(\frac{4\pi}{3} p_0^3 \right)^{A-1}$

Coalescence model: results

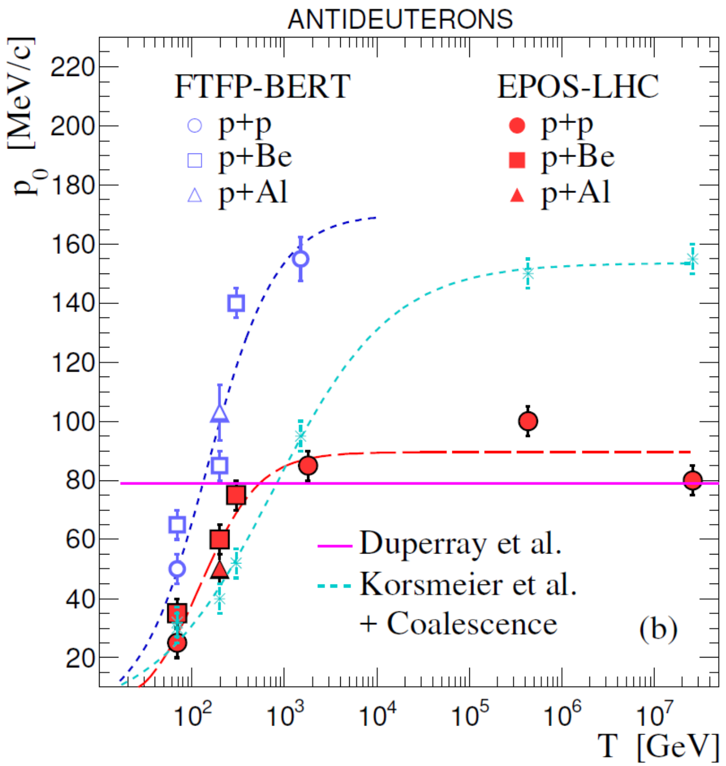

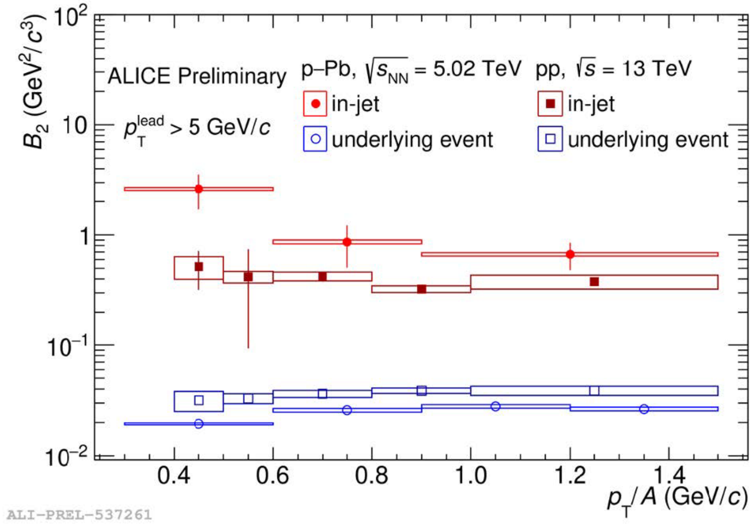

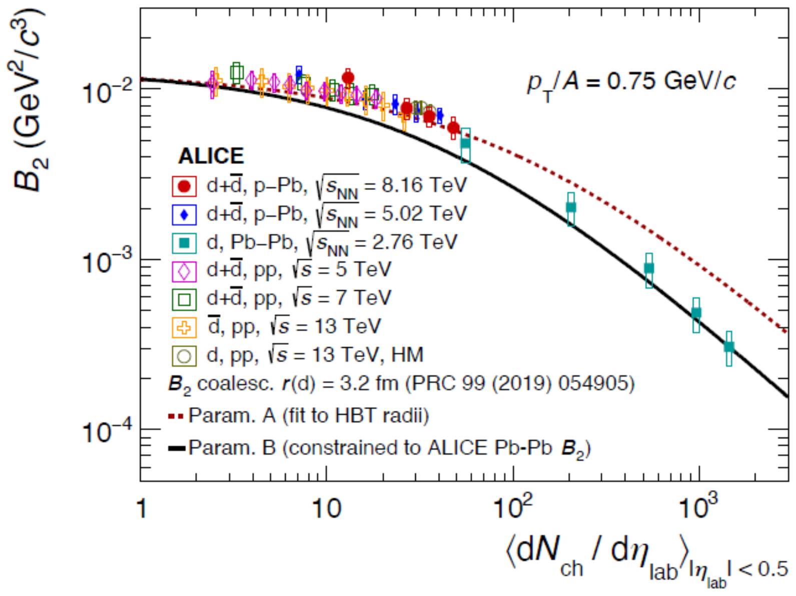

Expected anti-nuclei in SMOG dataset

Is the luminosity of the Run2 *p*He ($\sqrt{s_{NN}}$= 110 GeV) dataset sufficient?

Estimation of expected number of $\bar{\mathrm{d}}$ in dataset

B_A = coalescence probability

- EPOS-LHC simulation of *p*He ($\sqrt{s_{NN}}$= 110 GeV) collisions: 1<*p*<100 GeV/c, p_T<3 GeV/c, 2<η<5.
- **Afterburner for $\bar{d}$ production: coalescence model (*A*=2)** ⇨ $E_A \frac{dN_A}{d\vec{p}_A^{\,3}}\left(\sqrt{s}, \vec{p}_A\right) = B_A \left(E_p \frac{dN_p}{d\vec{p}_p^{\,3}}\left(\sqrt{s}, \vec{p}_A/A\right)\right)^A$
- Number of prompt $\bar{p}$ observed in *p*He ($\sqrt{s_{NN}}$= 110 GeV) dataset used to normalize simulation results

	$\bar{\mathrm{d}}/\bar{p}$	$\bar{\mathrm{d}}$ yield
Total (1<*p*<100 GeV/c)	0.9×10^{-3}	**4500**
RICH (35<*p*<100 GeV/c)	1.0×10^{-3}	**2000**
TOF (1<*p*<10 GeV/c)	0.3×10^{-3}	**300**

Around 4500 candidates in LHCb acceptance

⇩

Expected 300 candidates in Time-Of-Flight region (1<*p*<10 GeV/c)

Future possibilities: expand searches for $\overline{\mathrm{He}}$

Anti-nuclei distributions

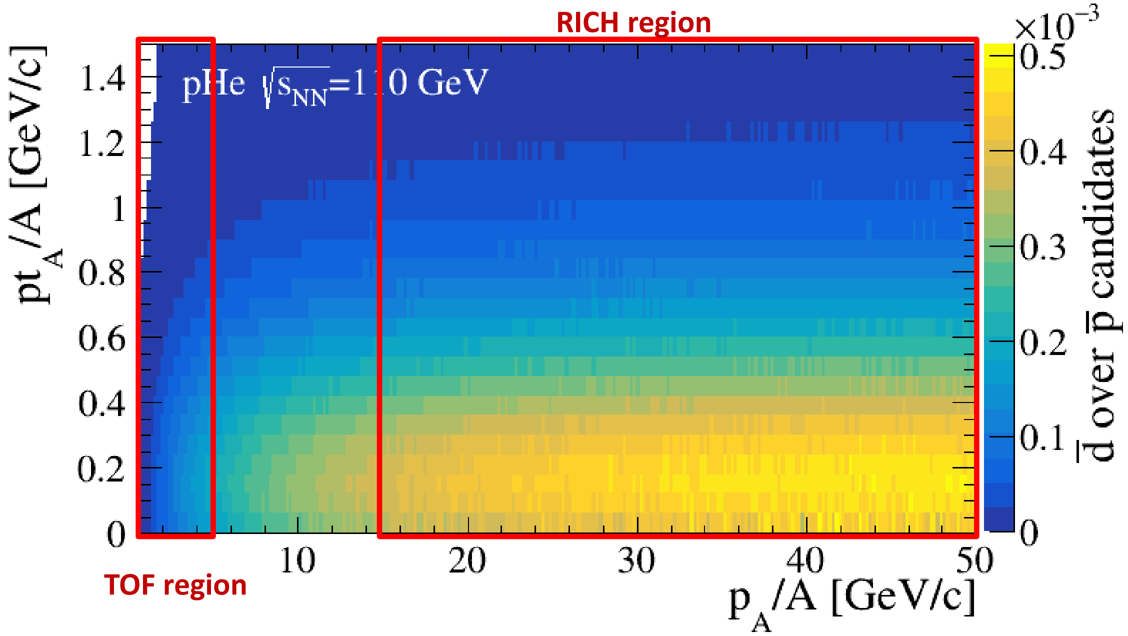

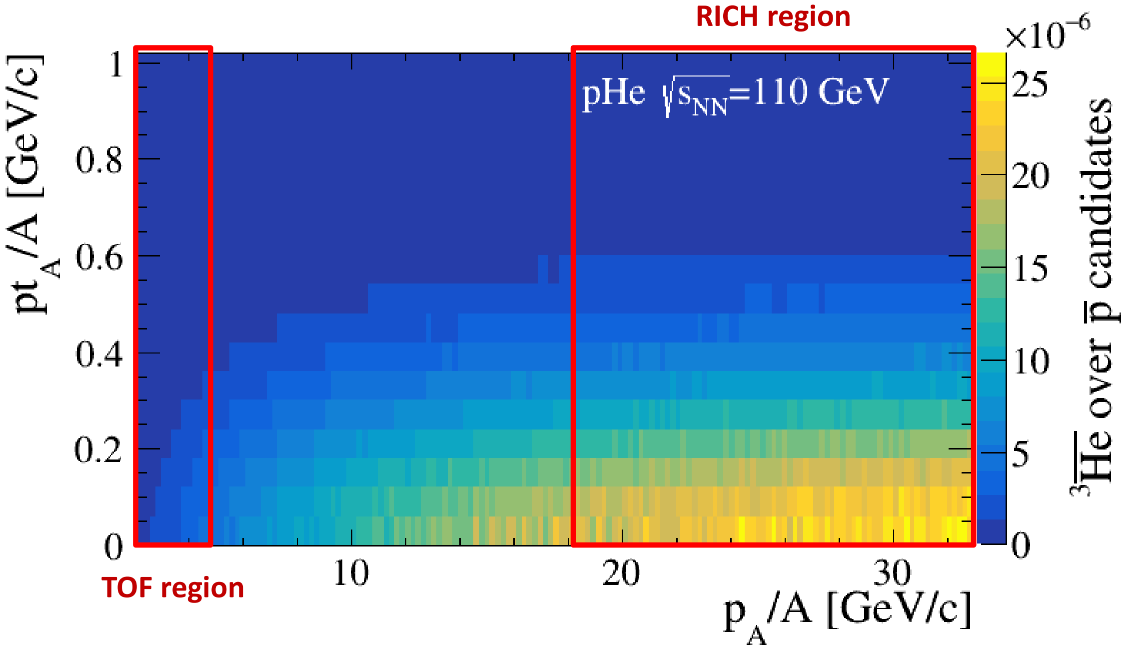

Anti-d distributions

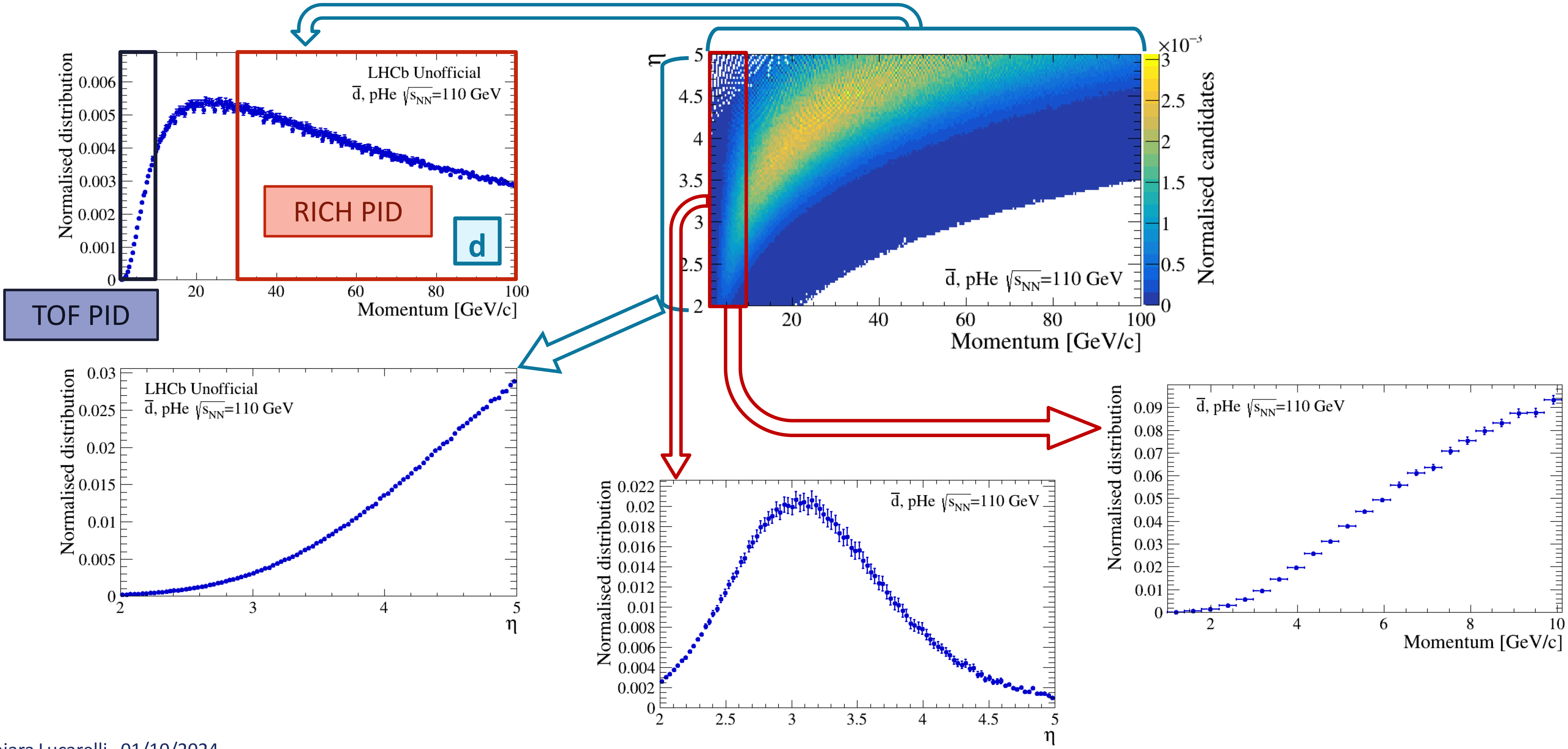

Anti-He distributions

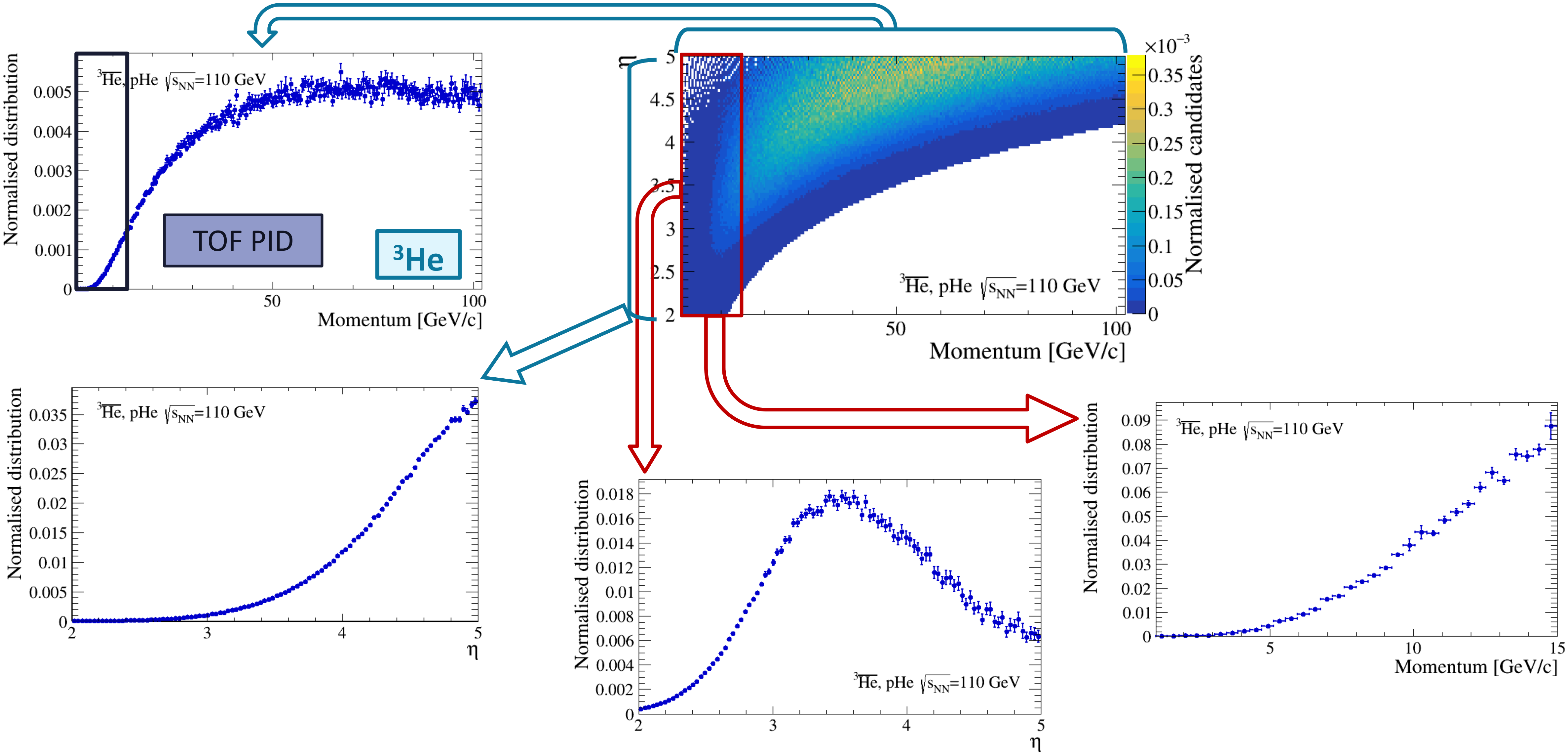

$\bar{d}$ identification with OT Track Time

Hits position determined from TR relation (calibrated on data):

$$t_{drift} = t_{TDC,corr} - t_{TOF} - t_{prop},$$
$$t_{drift}(r) = \left(21.3\frac{|r|}{R} + 14.4\frac{|r|^2}{R^2}\right)\ \text{ns}$$

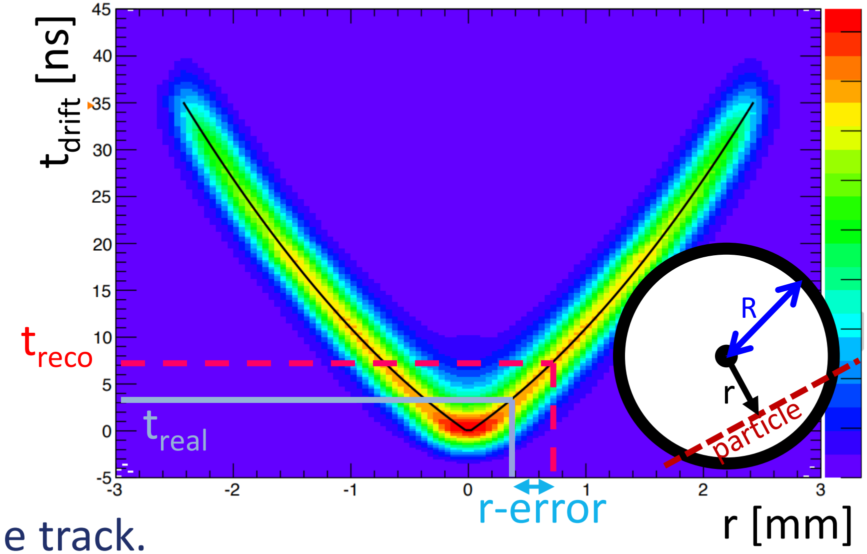

For β<1: $t_{TOF,reco} < t_{TOF,real}$ ⟹ $t_{drift,reco} > t_{drift,real}$ ⟹ error in r determination

For $\bar{d}$ (p<3 GeV/c), hits position wrong of the order of 1mm wrt real particle track.

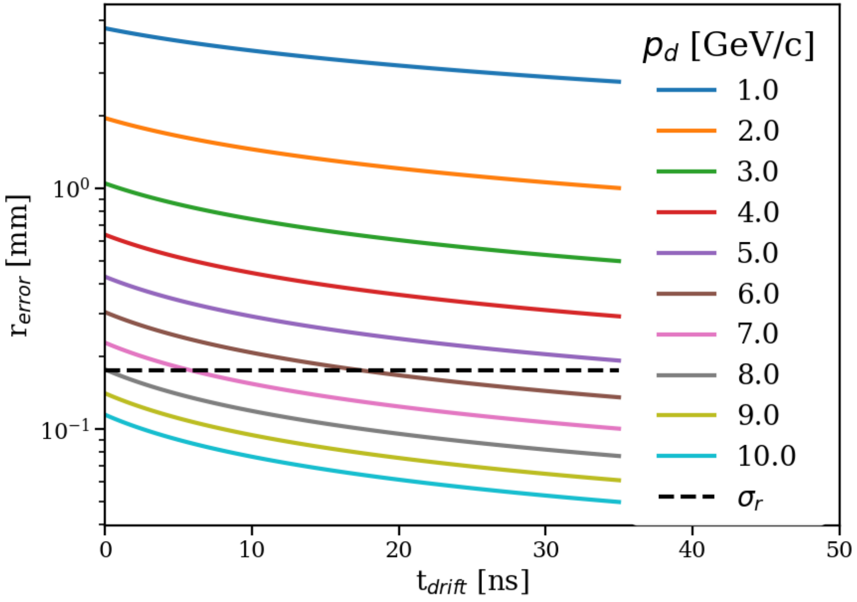

Low d reconstruction efficiency at low momentum

TOF Forward reconstruction algorithm

Modify the reconstruction algorithm to take into account β

Target: Correct hits position to **recover reconstruction efficiency**

Loop on β $\in \left[1/\sqrt{1+M_{max}^2/p^2}\,,1\right]$ **and save track with best fit** χ^2

- **PreLoop with no OT drift time**: hit position at center of straw, σ_{hit} = 2.5 mm
  1. If no candidate track, stop algorithm
  2. If no OT hit, run regular reconstruction
  3. If track with OT hit, use track *p* to set β range for loop
- **Loop on β**: for each step, correct hits position for β value and perform fit
- **Select candidate track with best** χ^2

Efficiency at low *p* recovered

MC sample:
QGSJET for *p*He + **coalescence afterburner** (1 coal x event)

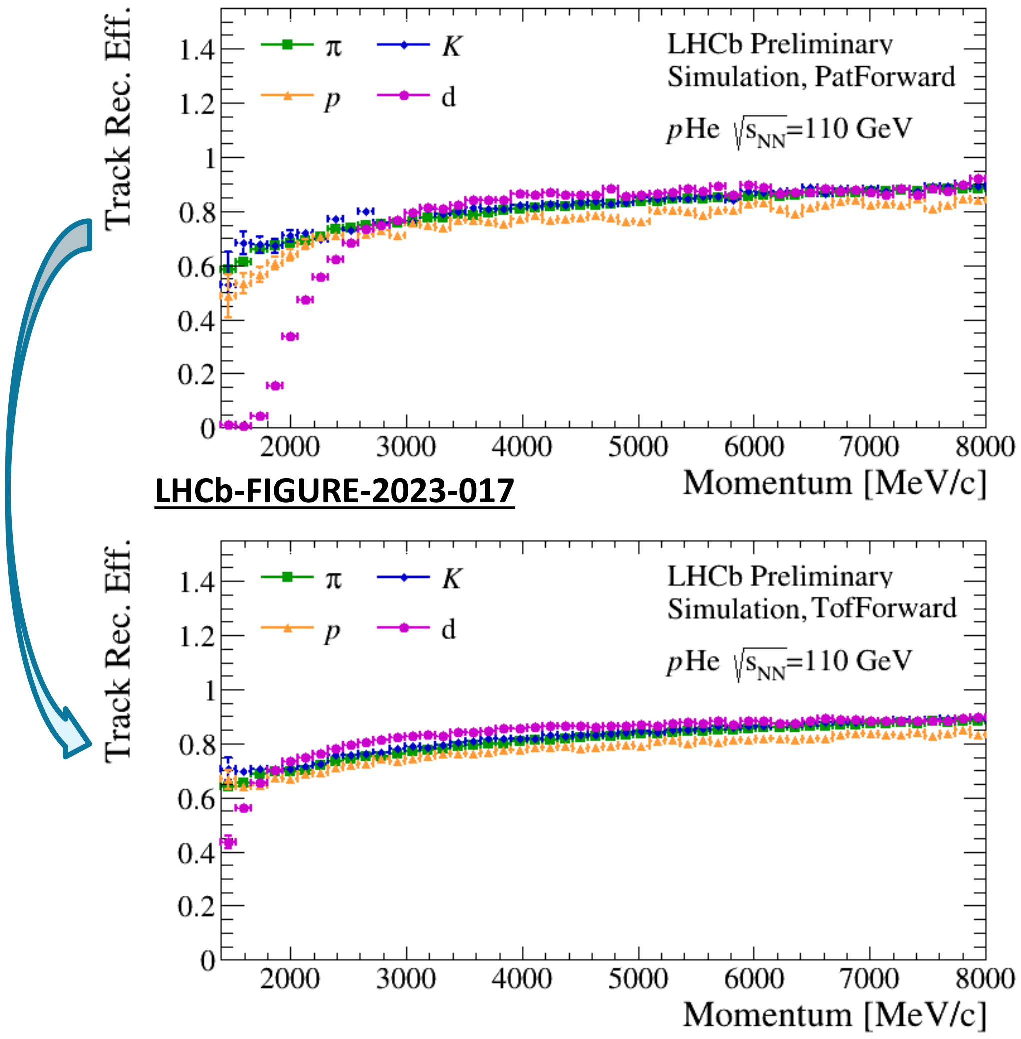

OT standard reconstruction

$$t_{drift} = t_{TDC,corr} - t_{TOF} - t_{prop}$$

Standard reconstruction algorithm:

1. Check for hits on the X planes of OT compatible with VELO seed
   1. Simple correction of t_{drift} for TOF with β=1 → Flight distance from IP to centre of straw, straight line. ⇐ Correct TOF with β≠1.
   2. From VELO seed, y of track on every planes → Correct t_{drift} for propagation on wire ⇐ Correct TOF for straight line to right y
   3. Project hits from t_{drift} on reference plane to select hit clusters compatible with VELO seed projection

2. Compatible hits fitted and excluded based on contribution to χ^2
   1. From candidate track parametrization based on VELO seed and central hit of cluster, correct t_{drift} for adjusted propagation ⇐ Correct TOF for adjusted track length
   2. Fit candidate track with cluster hits
   3. Remove outlier (hit with highest χ^2) → stop loop when reached good quality

OT standard reconstruction

$$t_{drift} = t_{TDC,corr} - t_{TOF} - t_{prop}$$

Standard reconstruction algorithm:

3. Track candidates with minimum OT hits and maximum χ^2 extended with compatible hits from stereo planes
   1. Candidate track parametrization from fit used to extract x,y position from stereo hits ⇐ Correct TOF for adjusted track length
   2. Project hits from t_{drift} on reference plane to select hit clusters compatible with VELO seed projection

4. Parabolic fit of x information and linear fit of y information performed to exclude hits with largest χ^2 contribution
   1. Repeat x fit from step 2 including x component of stereo hits
   2. Straight line fit for y component of stereo hits (same steps as x fit)
   3. Based on new y parametrization of track, update hits and repeat y fit ⇐ Correct TOF for adjusted track length

5. Quality variable based on momentum, χ^2 and number of hits defined, to be used in best track selection ⇐ Based on NN tuned on high momentum pp, changed to χ^2

TOF Forward performance studies

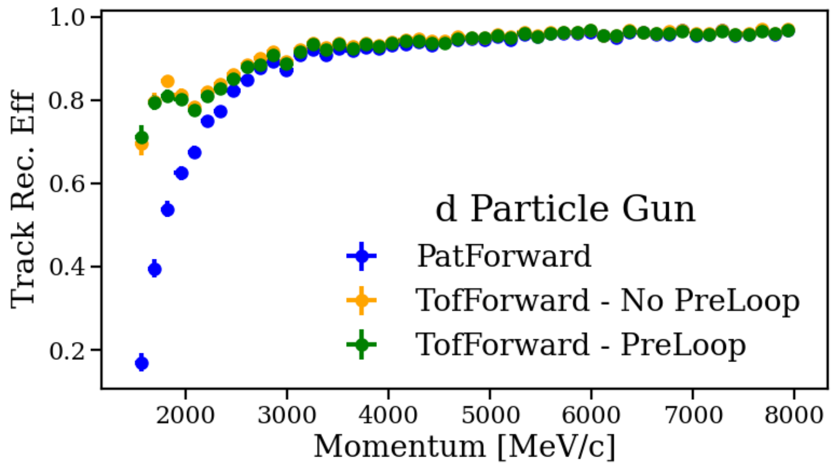

PreLoop:
- no impact on efficiency
- Reduce reco time by factor 3 wrt no PreLoop

Step size:
- Negligible impact on efficiency and β resolution
- Reco time significantly increase reducing step:
  - 0.1 step: 1.50xPatForward
  - 0.05 step: 1.65xPatForward
  - 0.01 step: 2.11xPatForward

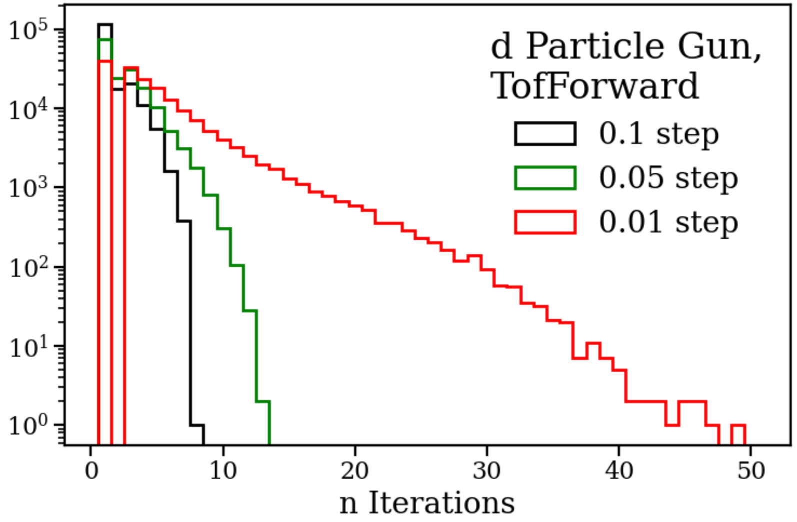

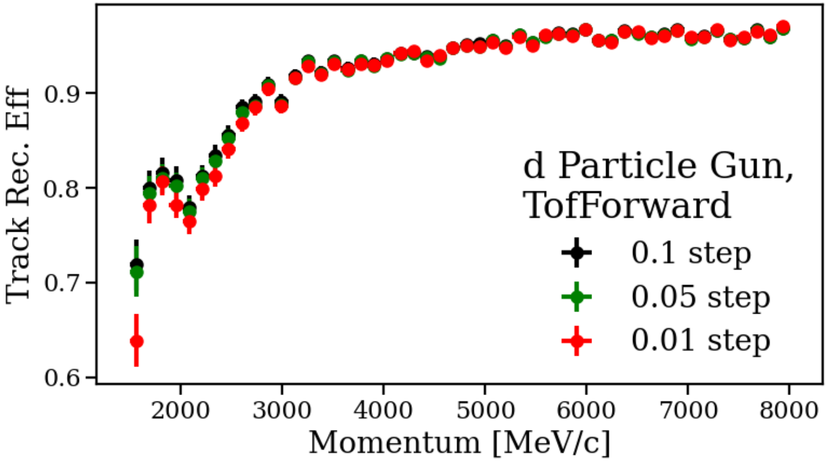

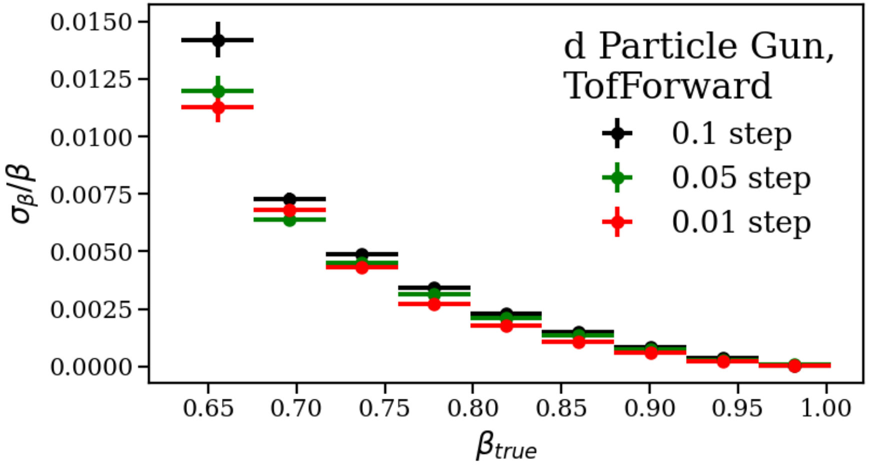

Reconstruction efficiency

$$\varepsilon_{Track\ Reco} = {N_{Rec,L}}/{N_{Recble,L}}$$

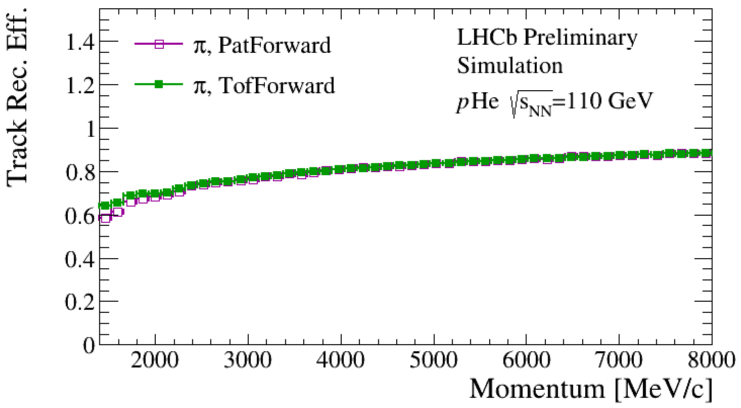

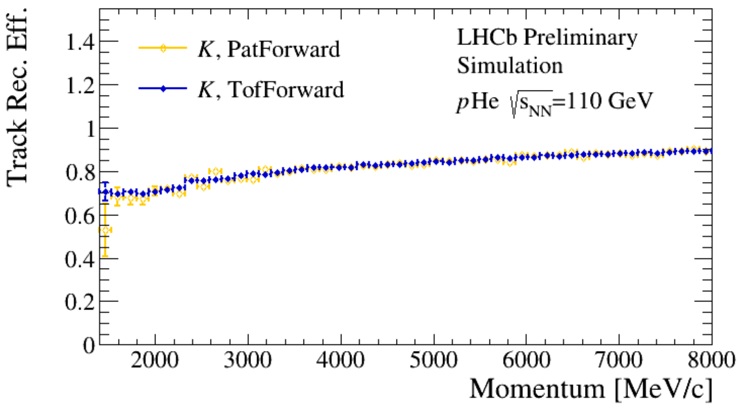

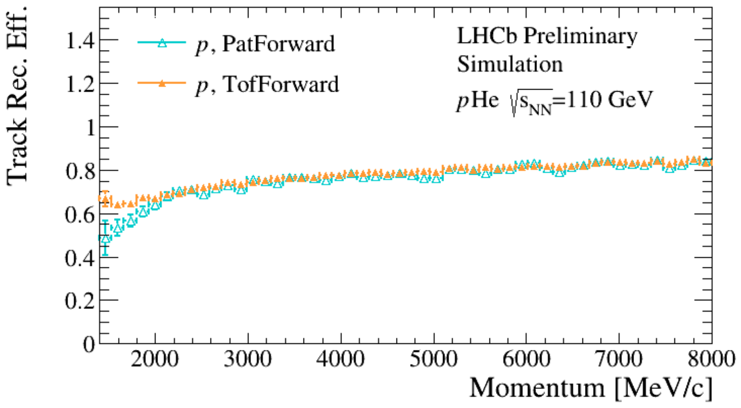

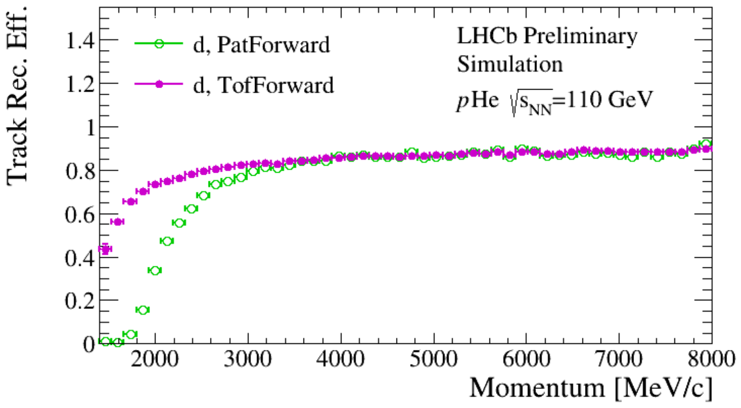

MC sample:

QGSJET for *p*He + **coalescence afterburner** (1 coal x event)

Momentum resolution

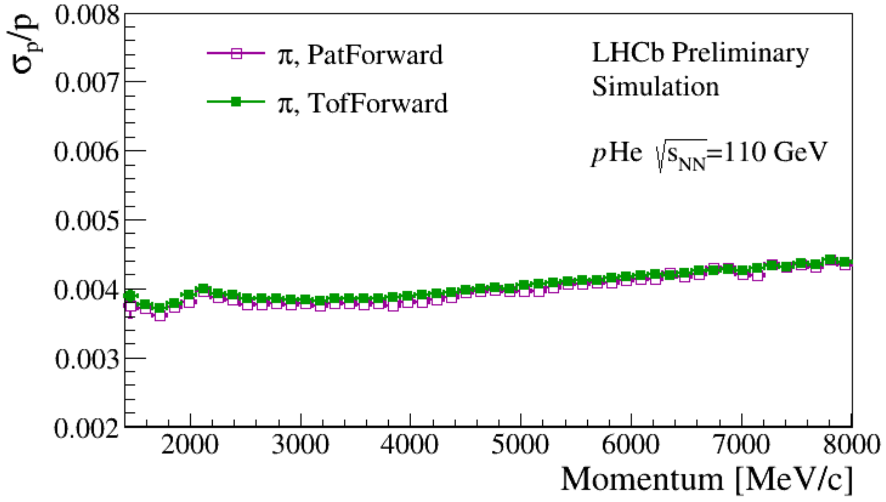

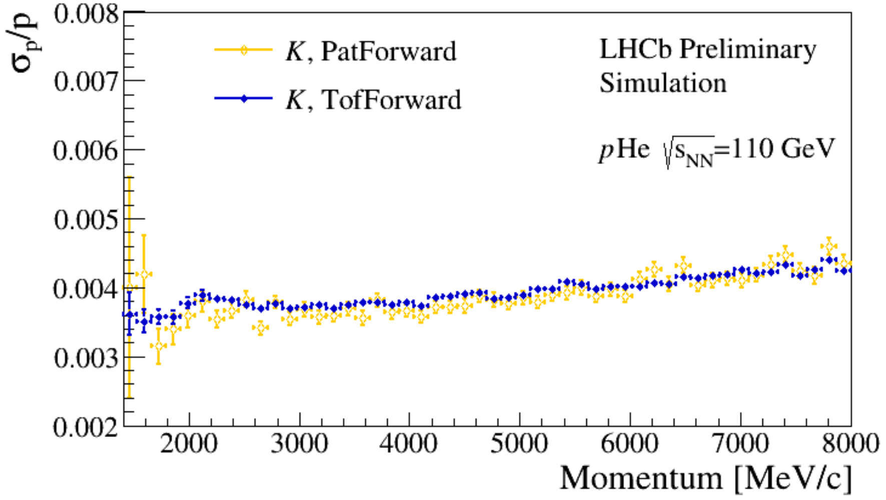

σ_p unchanged

Multiple scattering dominates σ_p over hit position

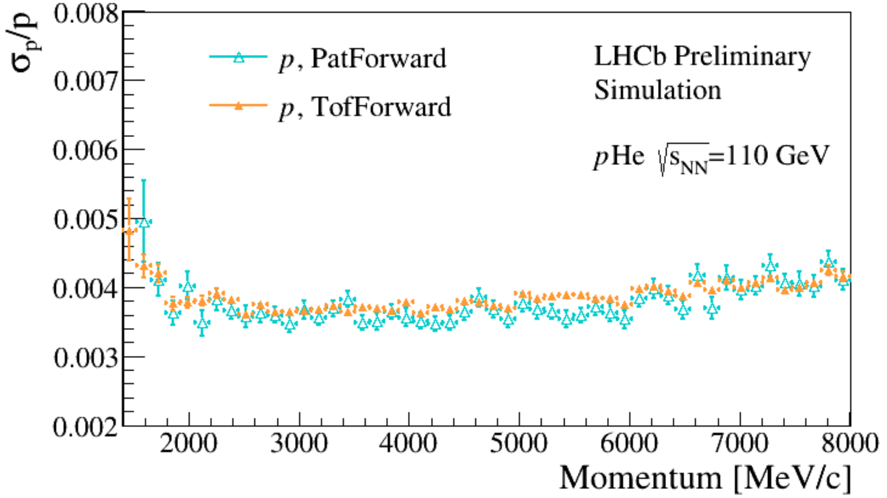

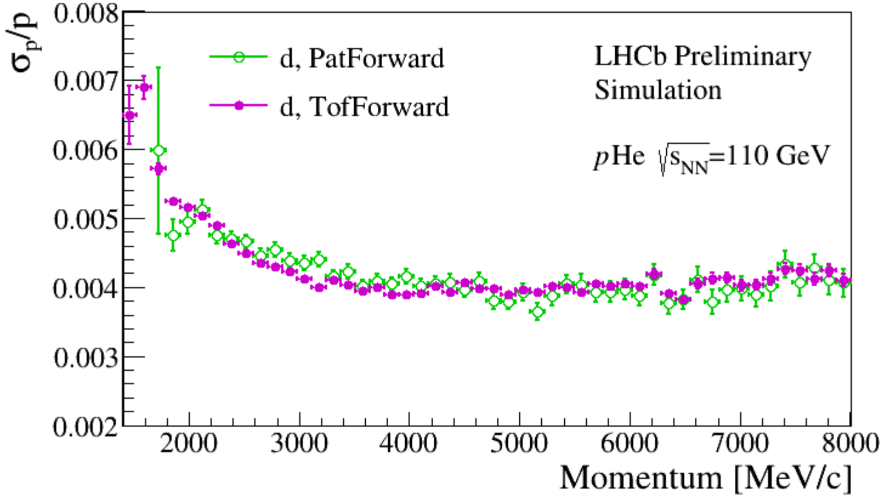

MC sample:
QGSJET for *p*He + **coalescence afterburner** (1 coal x event)

Mass reconstruction vs std OT TrackTime

Loose selection:
converged fit + σ(β)<0.06
- Clear d peak separated from background for *p*<3 GeV/c

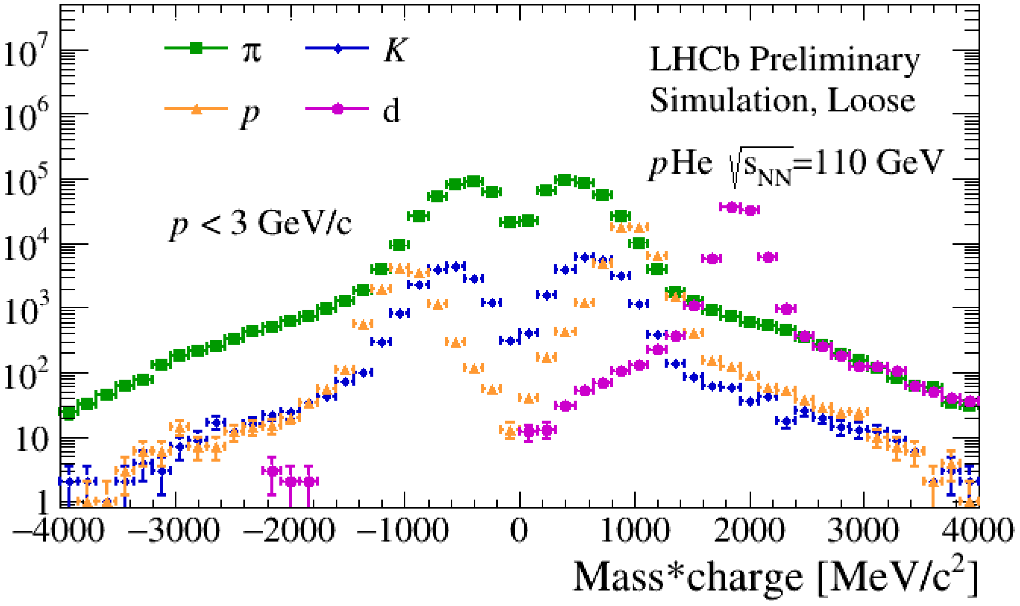

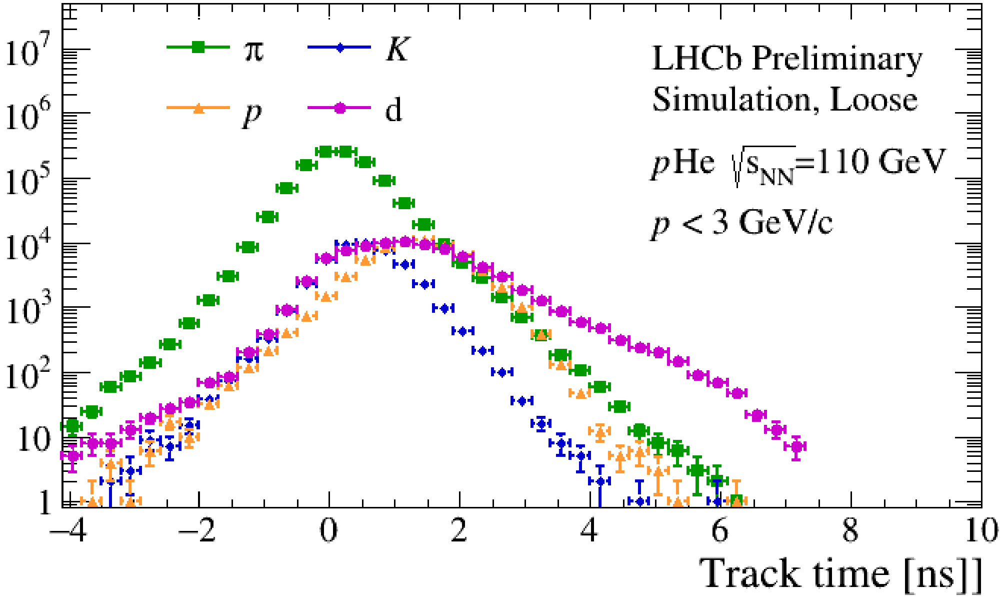

Better discrimination on mass compared to arrival time residuals

Performance on MC simulation

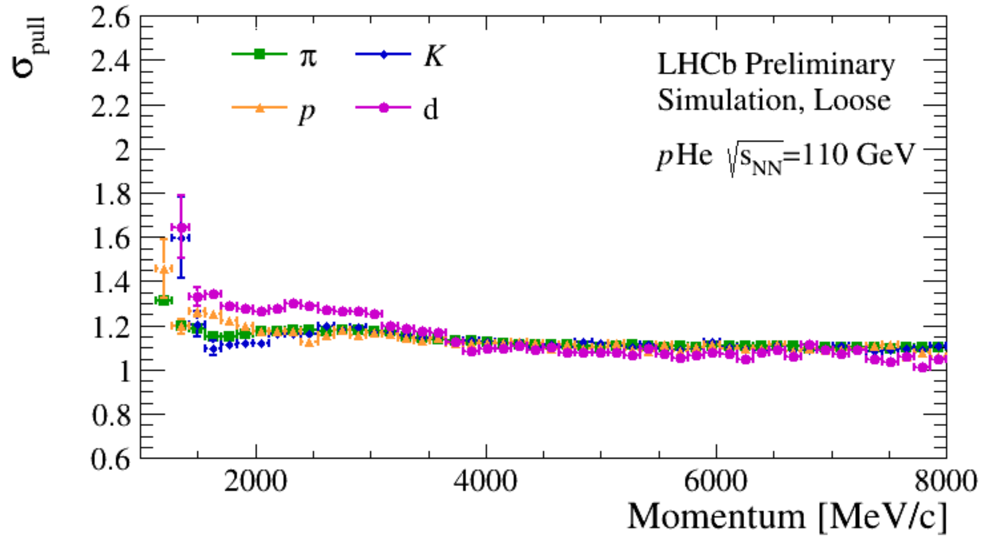

- **Correct estimation of uncertainty**

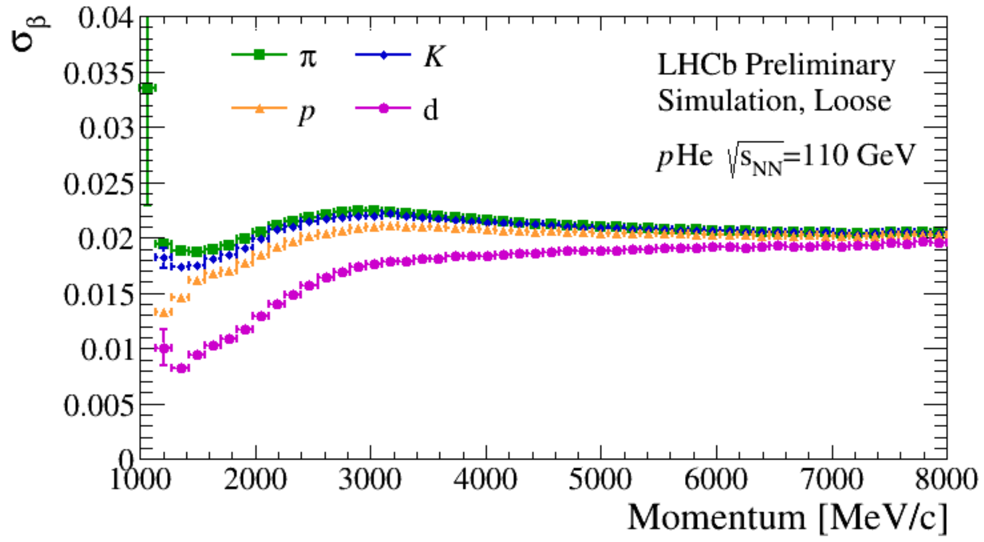

- **Precision on β better for slow tracks**
- **Some separation power as a function of *p***

Bias on β reconstruction

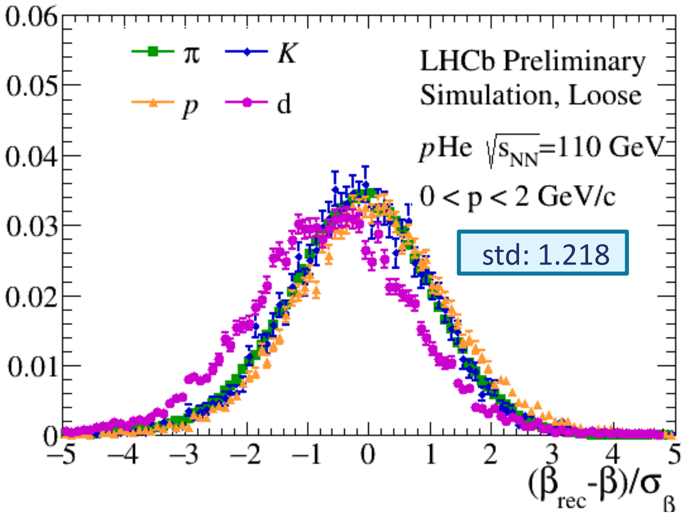

- Correct estimation of uncertainty
- Systematic underestimation of β at high momentum
- Origin of bias to be understood, could be related to approximations in TOF estimation

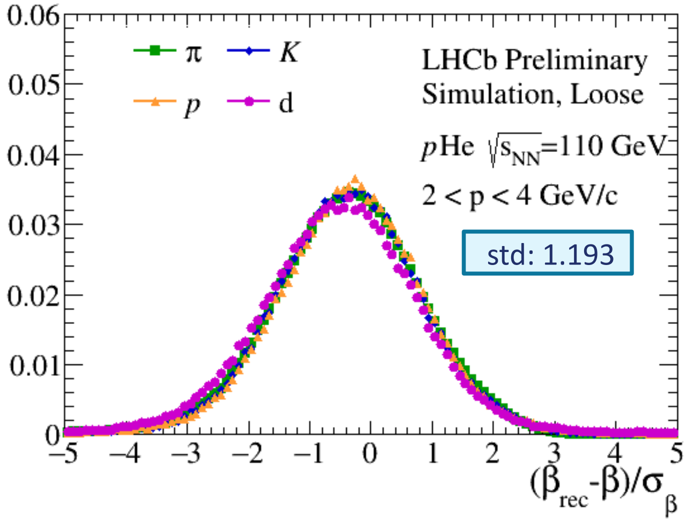

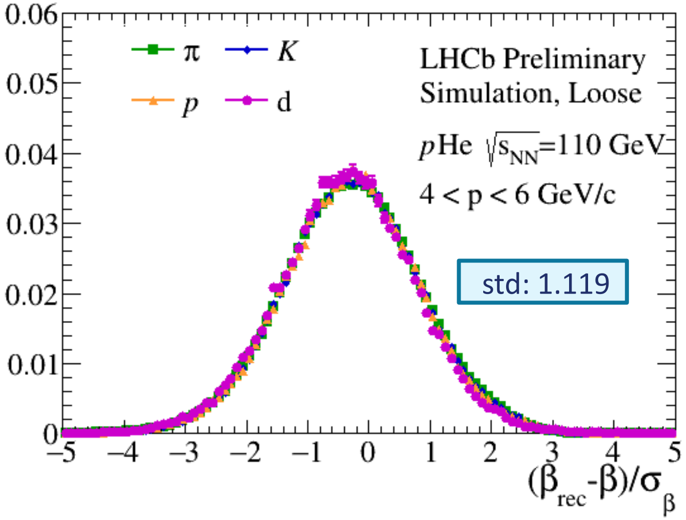

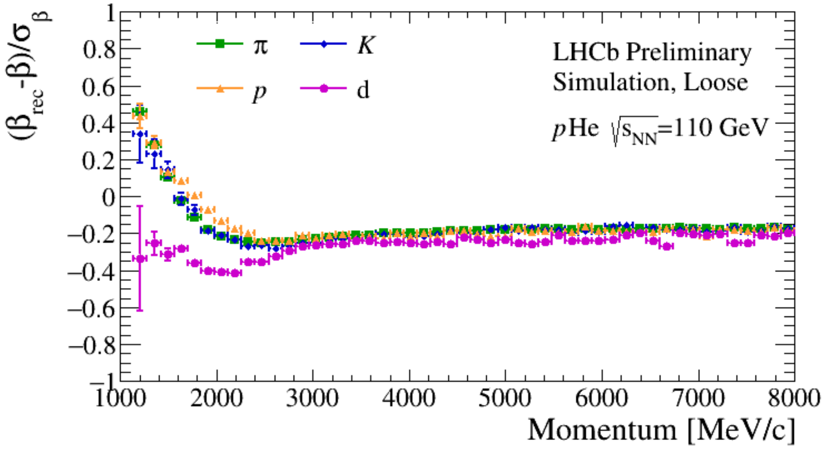

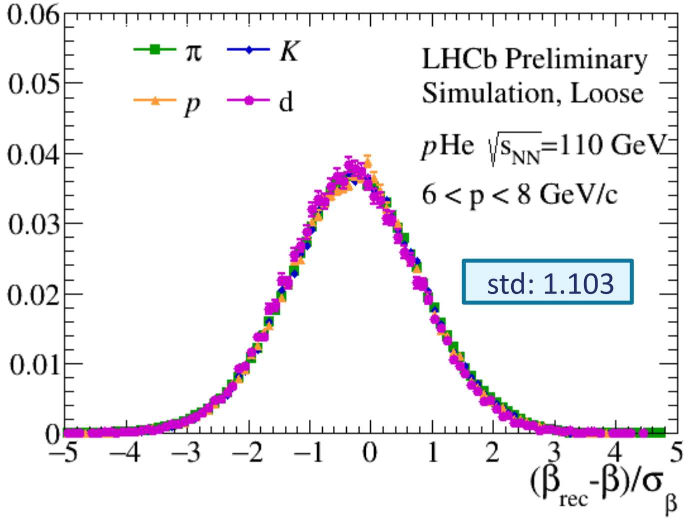

Deuteron selection

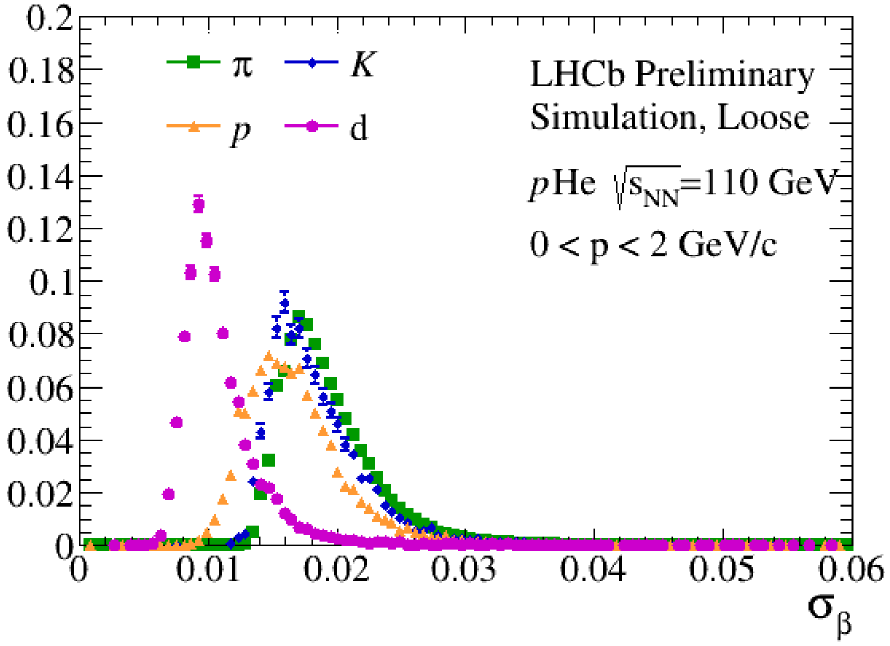

- In real data, d expected to be suppressed by $O(10^{-3})$ wrt to π

  Background suppression needed

- Exploit cuts on σ(β) and other quality-related variables:

  $\sigma(\beta) < 0.02$, $\chi^2_{OThits}/ndf < 1.2$

  → Suppressing light particles where β is largely underestimated

Selection efficiency

Efficiency for simulated deuterons

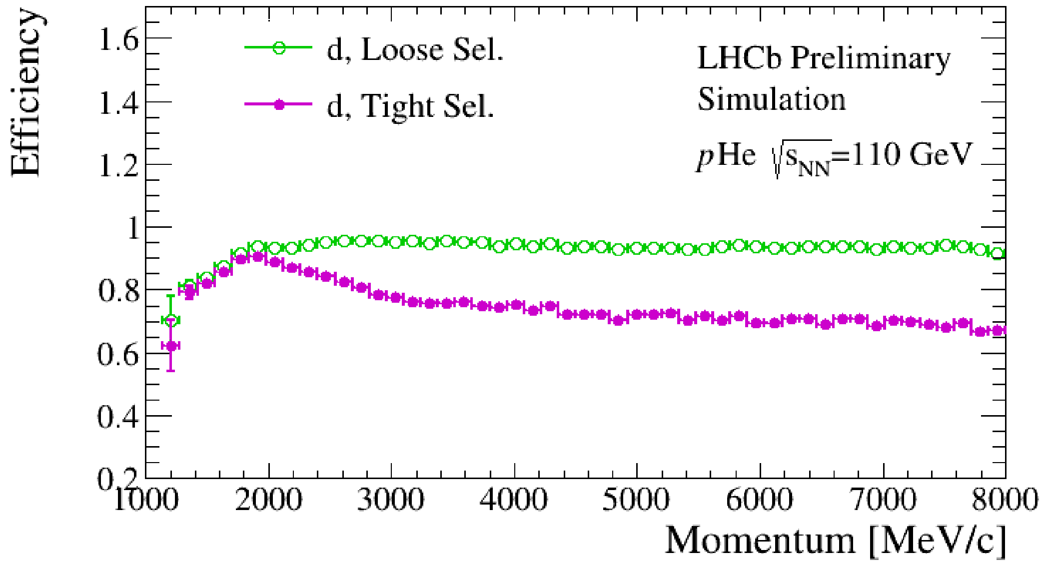

- Reduced efficiency for d with p>3 GeV/c

Efficiency for MC particles

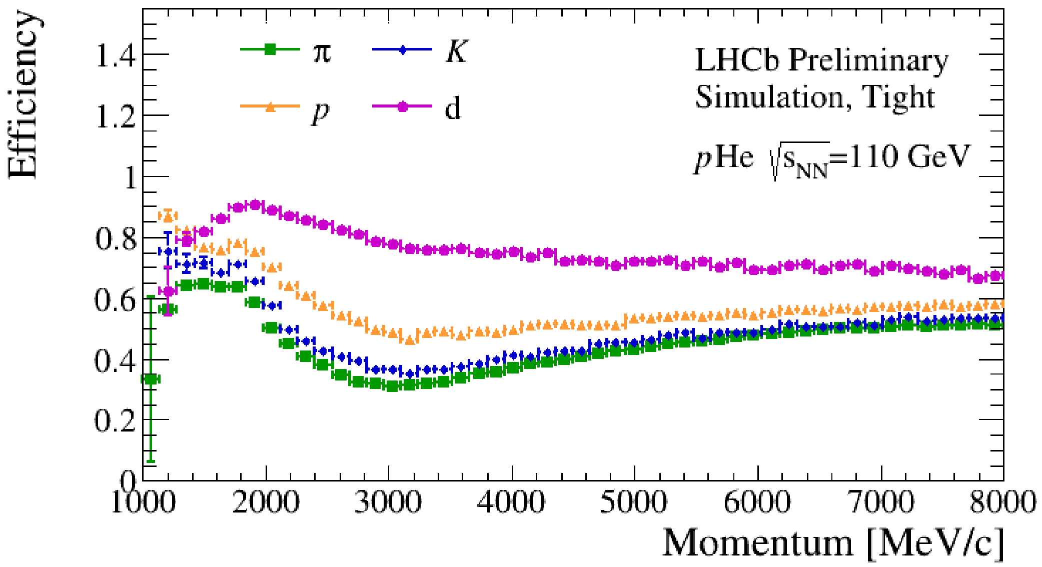

- Rejection power higher than 50% for pions and kaons.

Performance on Data

Clean samples of π and *p* from $K_S^0 \rightarrow \pi^+\pi^-$ and $\Lambda \rightarrow p\pi^- + cc$ (β_{true} known from *p*)

π

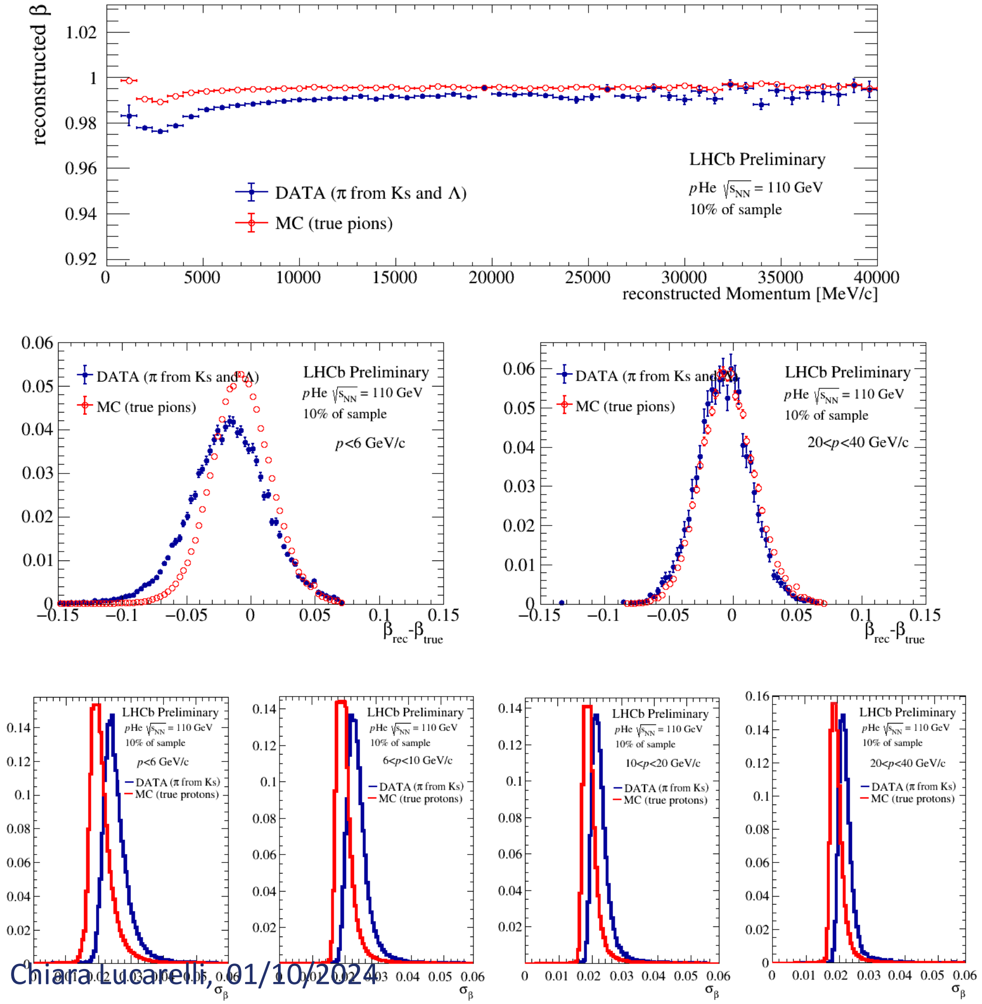

p

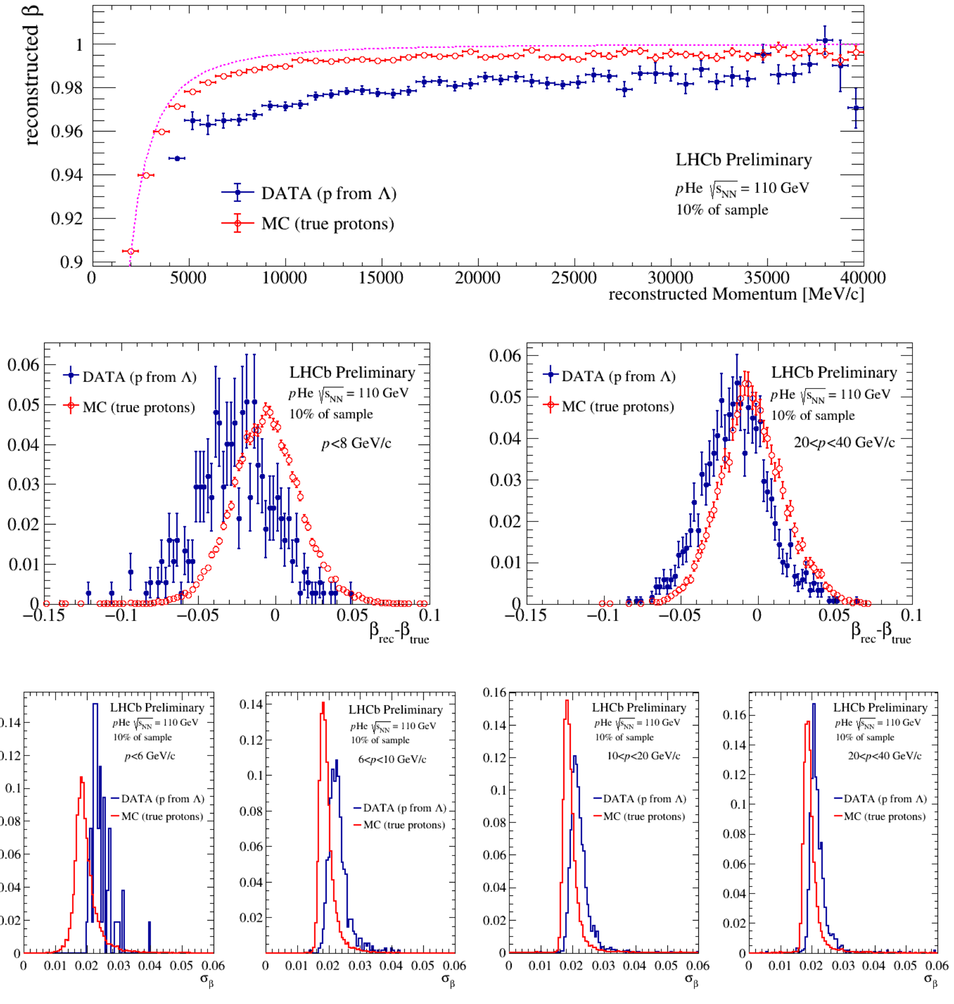

On average, larger negative bias and lower fit quality in DATA wrt MC (should depend on OT σ_t)

(Anti-)helium identification

What about (anti-)helium?

New technique developed in Aachen based on dE/dx in LHCb subdetectors

LHCb-DP-2023-002

Ionisation losses: **Z^2 dependence** in Bethe-Bloch
→ dE/dx to **identify He**

***pp* at $\sqrt{s} = 13$ TeV**, $\mathcal{L}_{int}$=5.5 fb^{-1}

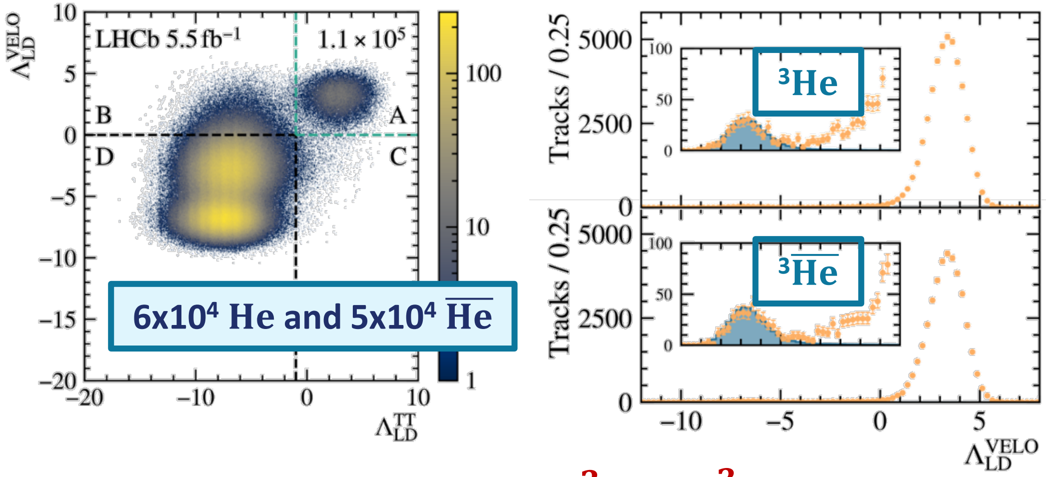

Hypertriton *pp* collisions: $^3_\Lambda\mathrm{H} \rightarrow {}^3\mathrm{He}\,\pi^- + cc$
[LHCb-CONF-2023-002]

Anti-helium from $\overline{\Lambda}_b^0$ decay: $\overline{\Lambda}_b^0 \rightarrow {}^3\mathrm{He}X$
[LHCb-CONF-2024-005]

Exploit TOF+dE/dx complementarity to distinguish
t, ^{3}He and ^{4}He

→ **Work in Progress**

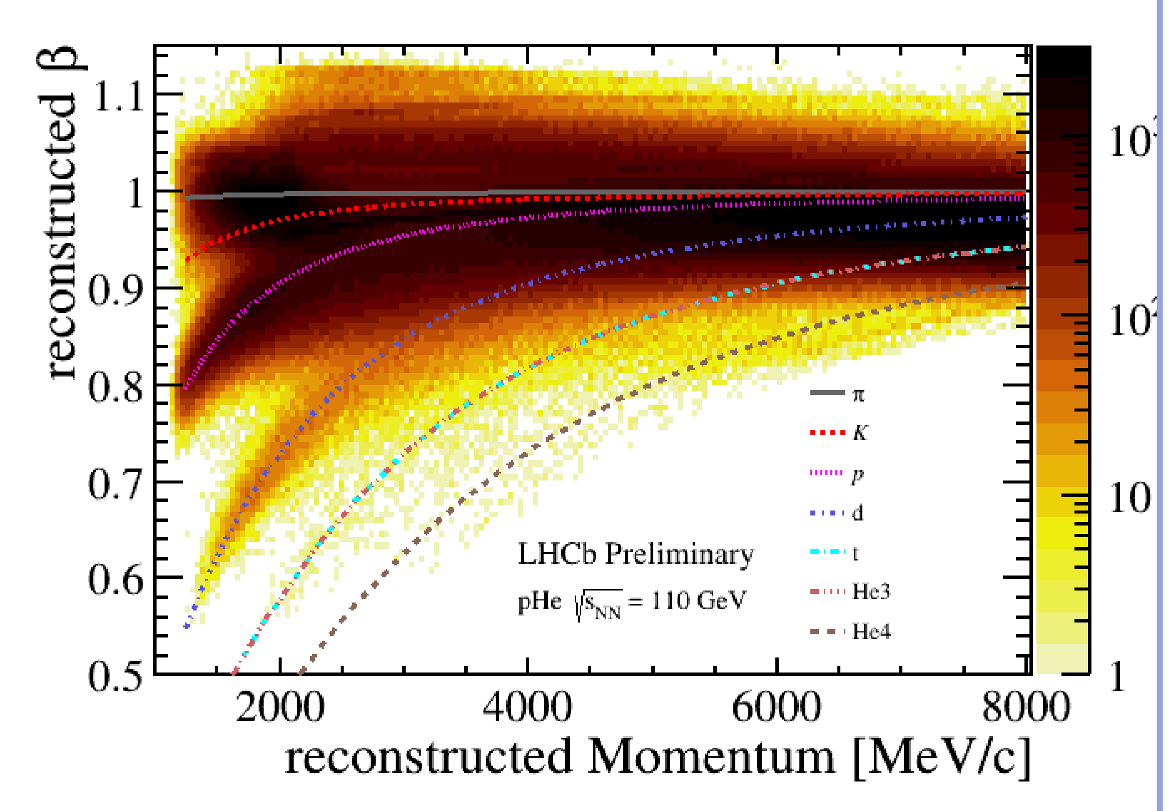

(Anti-)helium identification

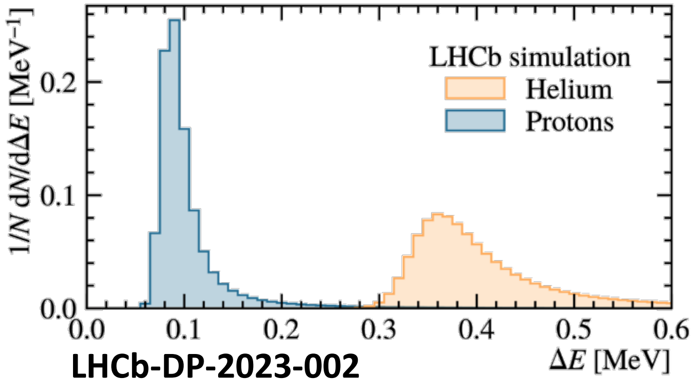

LHCb-DP-2023-002

Bethe-Bloch: Z=2 particles deposits ~4 times the energy of Z=1 particles

→ **He: higher ADC counts and wider cluster size**

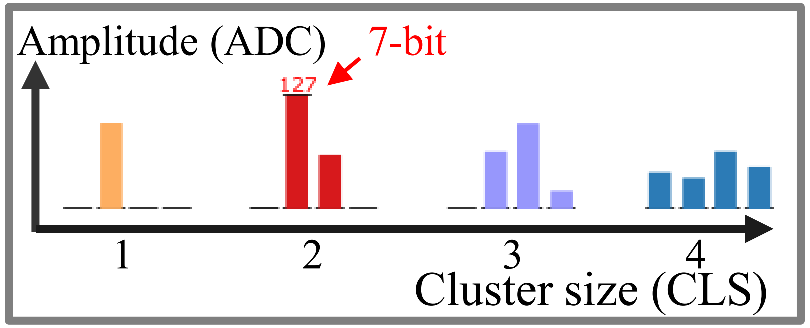

Probability Density Distributions (PDD)

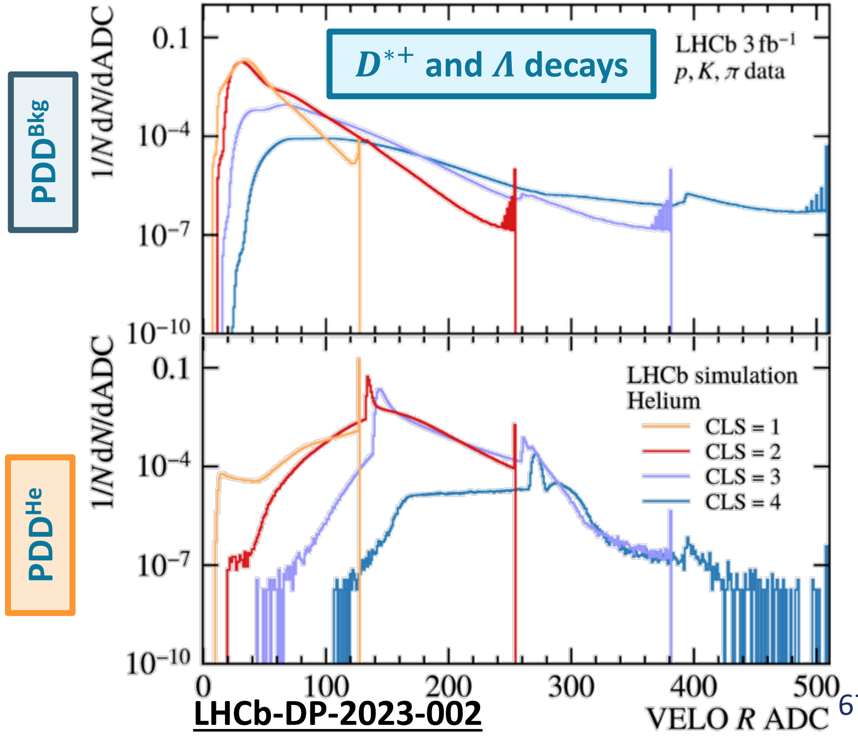

LHCb-DP-2023-002

Define Likelihood discriminators based on cluster size and ADC counts:

$$\mathcal{L}^X = \left(\prod_{i=1}^{n} \mathrm{PDD}_i^X\right)^{1/n}, X = \{\mathrm{He}, \mathrm{Bkg}\}$$

$$\Lambda_{\mathrm{LD}} = \log\mathcal{L}^{\mathrm{He}} - \log\mathcal{L}^{\mathrm{Bkg}}$$

One discriminator for each subdetector:

- $\Lambda_{\mathrm{LD}}^{\mathrm{VELO}}$
- $\Lambda_{\mathrm{LD}}^{\mathrm{TT}}$
- $\Lambda_{\mathrm{LD}}^{\mathrm{IT}}$

Prompt (anti-)helium at LHCb

Selection:

Run2 data: ***pp* collisions at $\sqrt{s} = 13$ TeV**, $\mathcal{L}_{int}$=5.5 fb^{-1}

- All trigger lines
- Prompt tracks (compatible with PV) passing through VELO, TT, and T1->T3
- Good quality tracks ($\chi^2_{track} < 3$, $N_{clusters\ X\ Si\ station}$ >2)
- $p/|Z|$>2.5 GV and $p_T/|Z|$>0.3 GV
- Λ_{LD}^{VELO}>0 and Λ_{LD}^{TT}>-1; Λ_{LD}^{IT}>-1 for IT tracks
- Rejection of photon conversions

First (anti-)helium candidates observed in *pp* in LHCb data!

LHCb-DP-2023-002

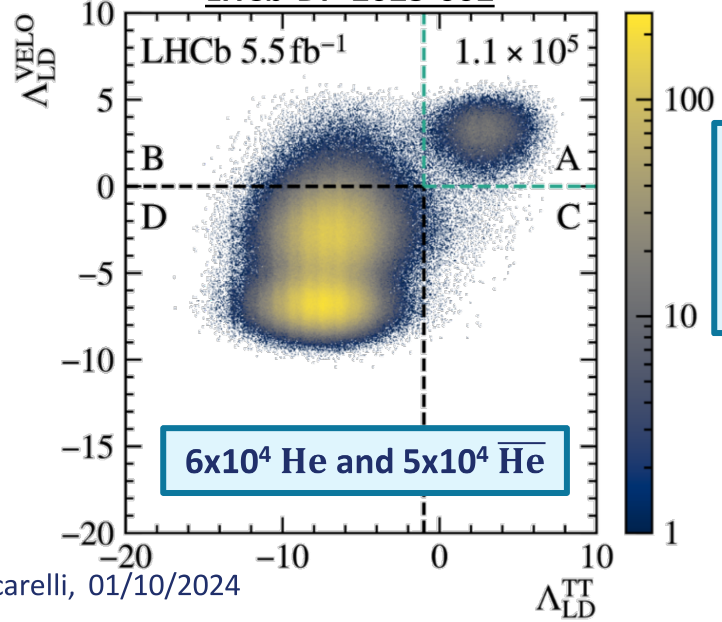

Performance:

- **MisID** probability: $\mathcal{O}(10^{-12})$
- **Signal efficiency**: ~ 50%

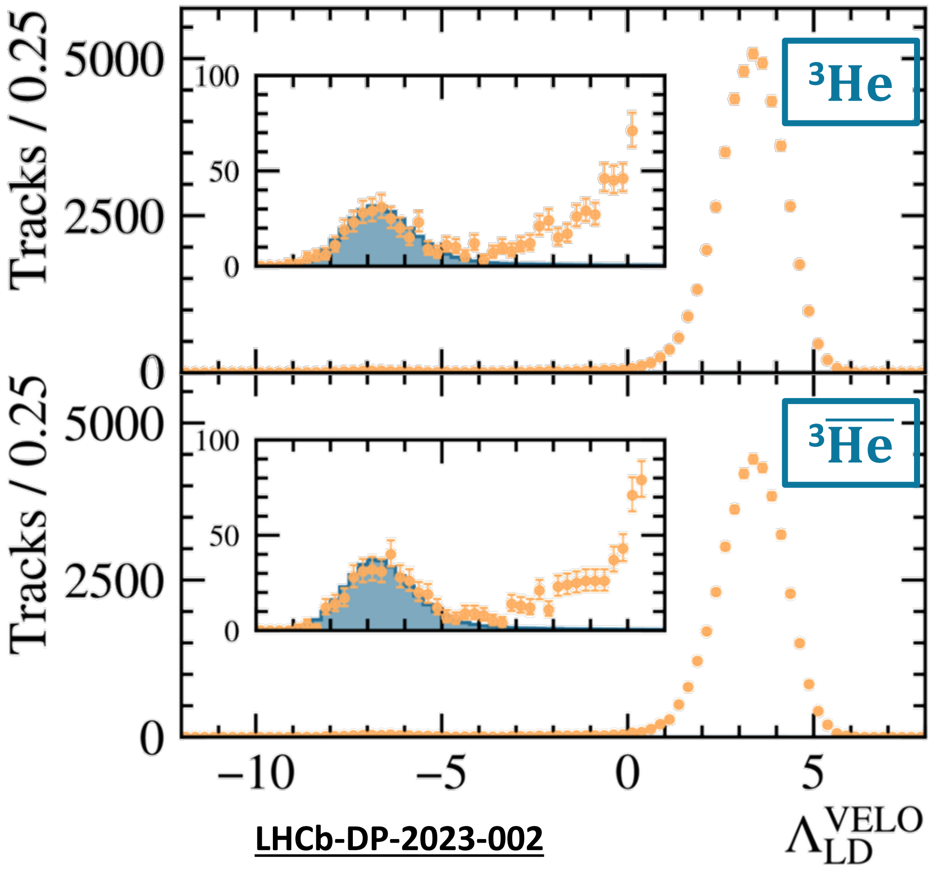

LHCb-DP-2023-002

Application: Hypertriton

- Hypertriton life-time and binding energy gives access to hyperon-nucleon interaction

  → **Constrains on maximum mass of neutron stars**

Search for 2-body decay into He:

$$^{3}_{\Lambda}\mathrm{H} \to {}^{3}\mathrm{He}\,\pi^{-} + cc$$

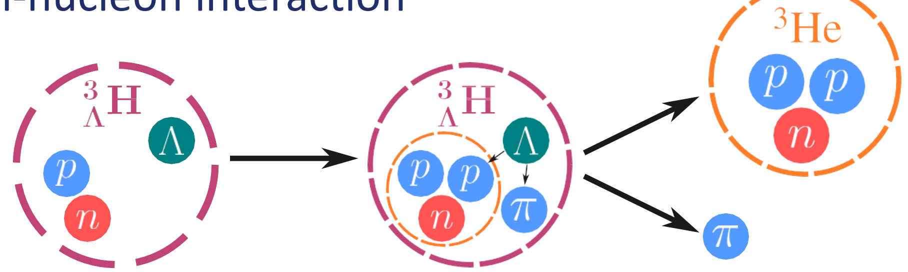

Results:

(Run2 *pp* collisions at $\sqrt{s} = 13$ TeV)

- **Yields**:
  - 61 ± 8 Hypertriton
  - 46 ± 7 anti-Hypertriton
- Statistical **mass precision**: 0.16 MeV

Under investigation:

- Systematic corrections on mass scale:
  - Charge-sign dependent energy-loss
  - Tracking corrections for Z=2
- Efficiency and acceptance corrections

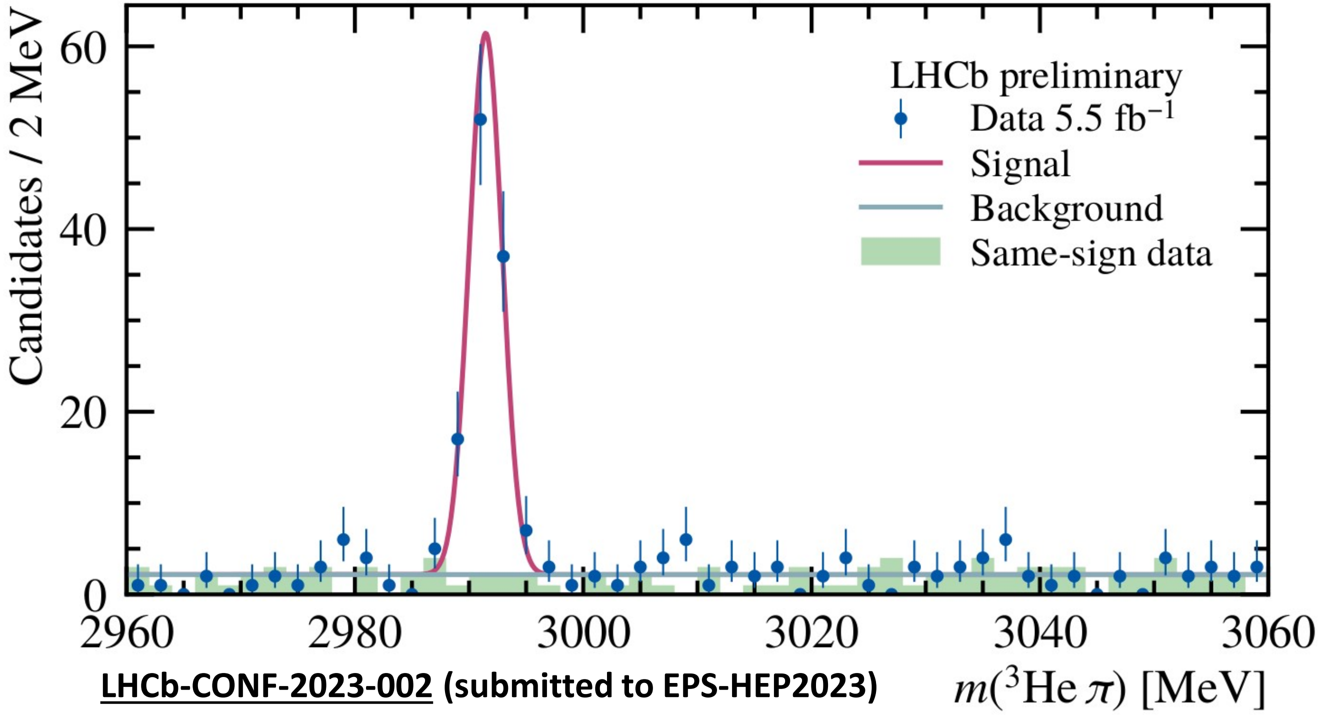

LHCb-CONF-2023-002 (submitted to EPS-HEP2023)

The LHCb experiment upgrade

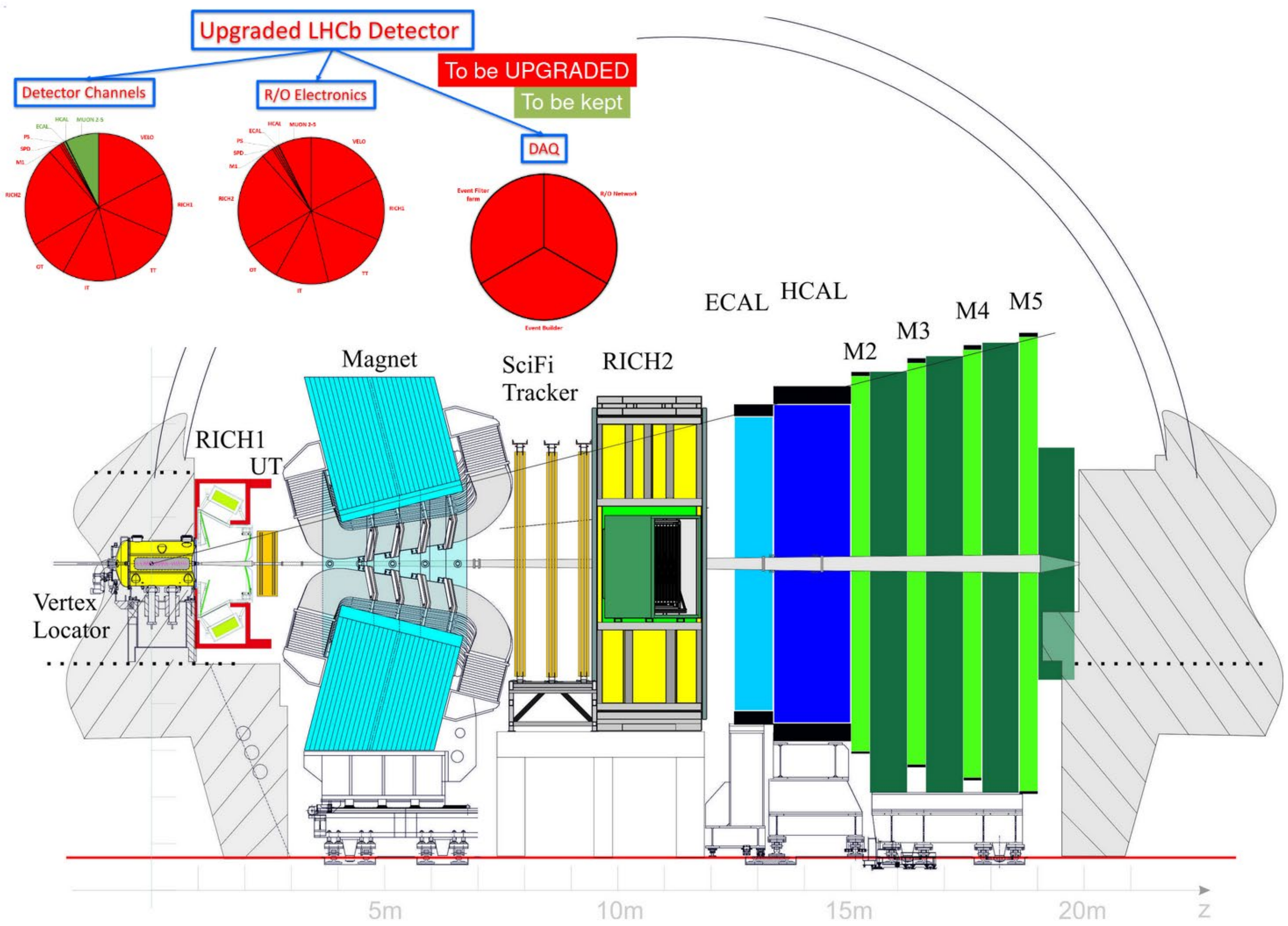

LHCb detector upgraded during 2018-2022 to extend the reach to new physics signatures and increase precision on key observables

- **Tracking system fully replaced**
- **New optics for RICH system**
- **New electronics and DAQ channels**
- **Full DAQ chain only software**:
  - First trigger level completely on GPUs, 30 MHz
  - Real-time alignment & calibration and event reconstruction & selection

SMOG upgrade: SMOG2

SMOG: unique opportunity at LHC, but some limitations highlighted by analysis:

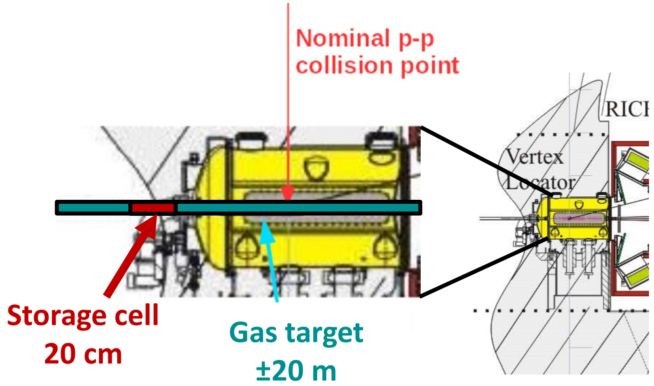

- **Limited statistics** as data collected only in dedicated periods without *pp* physics or with beam-empty LHC bunch crossing (10% of total)
  → Overlapping with *pp* luminous region problematic
  → For operation safety, max 10^{-7} mbar gas pressure
- **Limited variety of collision systems**
  → For operation safety, only noble gases
  → Gas switch requires access in the cavern
- **Limited measurement precision**
  → No direct pressure measurement to measure luminosity
  → SMOG data processing not included in "standard" *pp* analysis tool

Physics opportunities with SMOG2

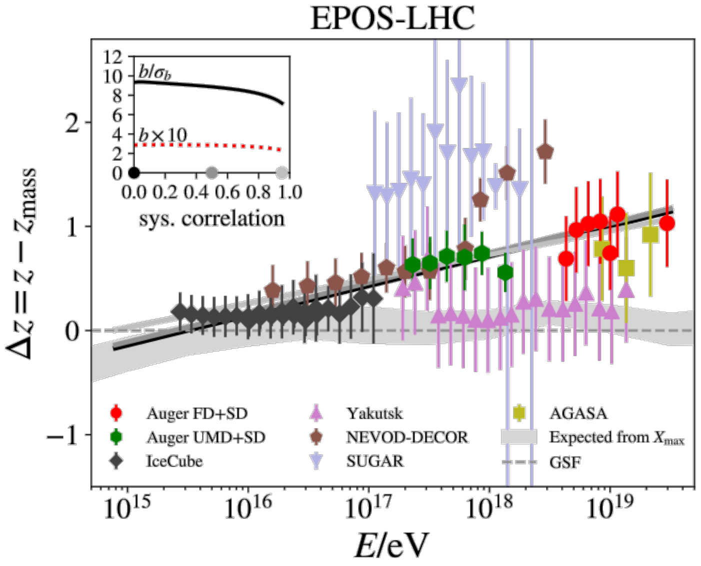

- **Ultra-high energy CRs are measured by ground-based experiments**, after full development of the shower in the atmosphere
- **Muon puzzle**: observed a muon excess with respect to model predictions.
- **Modelling of hadronic interactions in non-perturbative regime require more precise and more various experimental data.**
- **SMOG2**, accessing the poorly explored high-x and intermediate Q^2 region, can give a **unique contribution**

- With SMOG2 **O_2 target and *p* beam**: exactly reproduces CR particle impinging on the atmosphere.
- With SMOG2 **O_2 and H_2 target and O beam**: $OO_{(2)}$ simultaneously at two energy scales and rapidity; OH_2 reproduces very forward *p*O interactions in the O at rest reference.

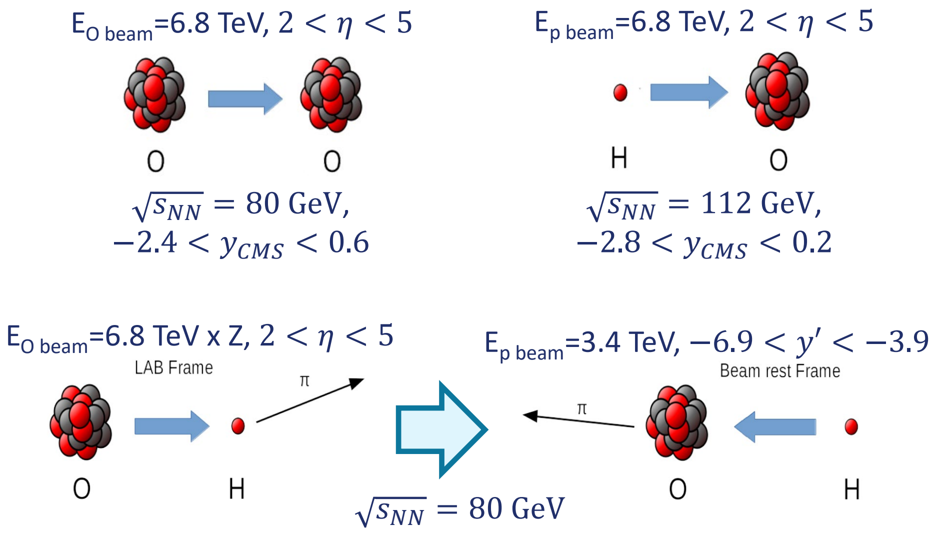

Sticking coefficient evolution model

No theoretical model to describe sticking coefficient saturation. Some general empirical models exists but parameters must be measured for each NEG film + Gas combination

→ Sticking coefficient evolution model fitted from experimental data.

H_2

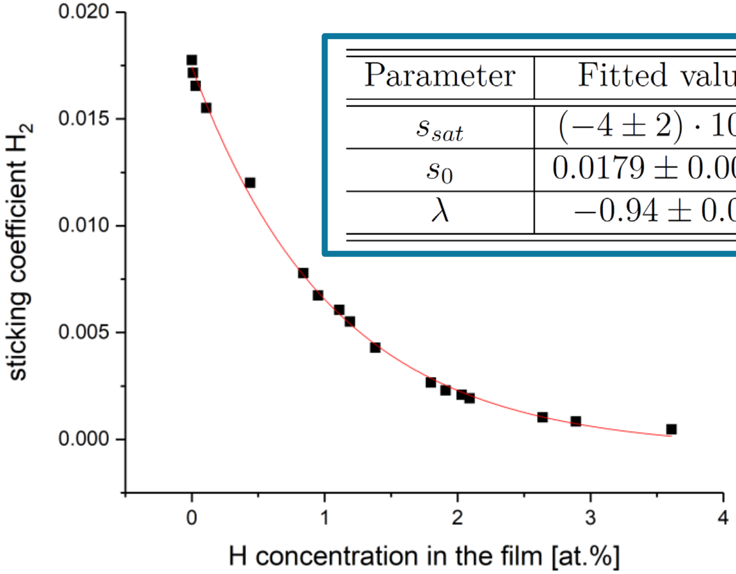

Parameter	Fitted value
s_{sat}	$(-4 \pm 2) \cdot 10^{-4}$
s_0	0.0179 ± 0.0002
λ	-0.94 ± 0.03

$$s(x_H) = s_{sat} + s_0 e^{\lambda x_H}$$

N_2

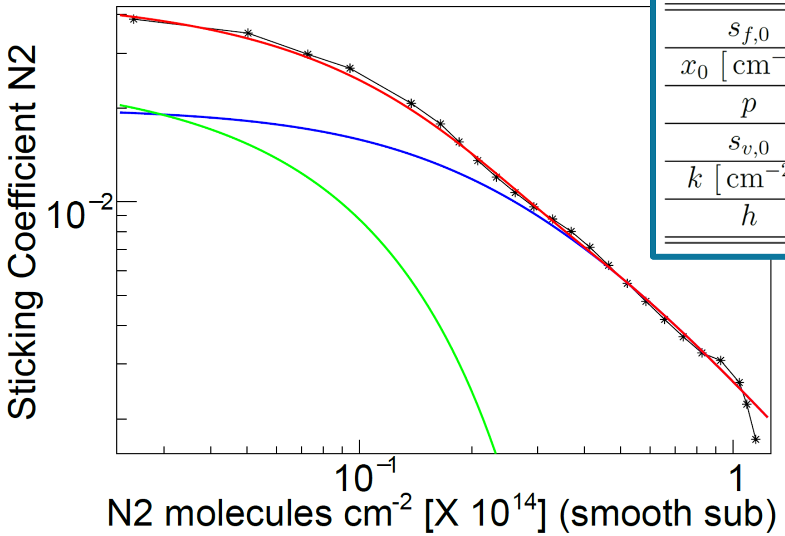

Parameter	Fitted value
$s_{f,0}$	0.0258 ± 0.0008
x_0 [cm^{-2}]	$(0.7 \pm 0.2) \cdot 10^{14}$
p	7 ± 2
$s_{v,0}$	0.020 ± 0.009
k [cm^{-2}]	$(0.26 \pm 0.16) \cdot 10^{14}$
h	1.4 ± 0.3

$$s(x) = \begin{cases} s_{f,0}\left(1 - \frac{x}{x_0}\right)^p + \frac{s_{v,0}}{1+\left(\frac{x}{k}\right)^h} & x < x_0 \\ \frac{s_{v,0}}{1+\left(\frac{x}{k}\right)^h} & x \geq x_0 \end{cases}$$

Results: N_2

- **Saturation** starts **after 3 min** of injection, total saturation of first 5 cm after 30 min
- Saturation **propagation slows down after 1 h**
- **After 10h** of continuous injection, **saturation up to ~20 cm** and total saturation up to ~13 cm.
  → **15% area saturated, 37% reduction of average s_{avg}**

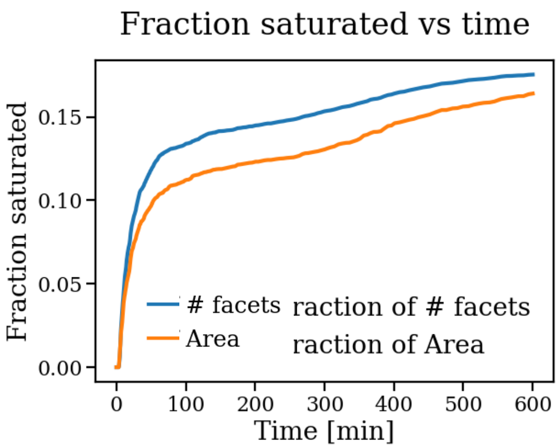

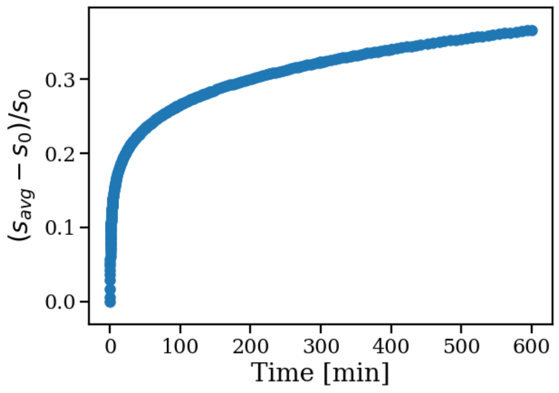

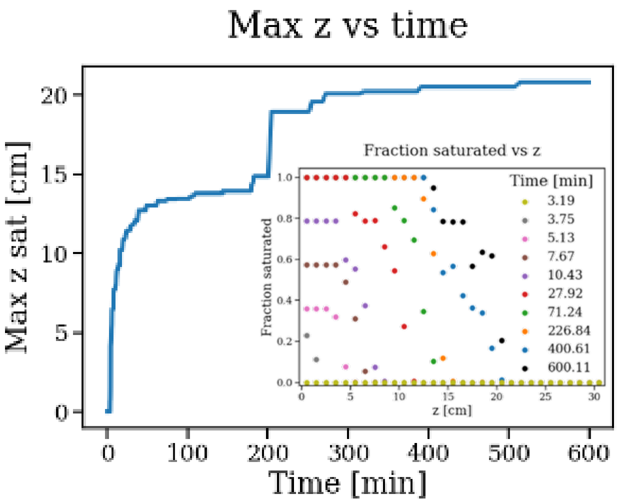

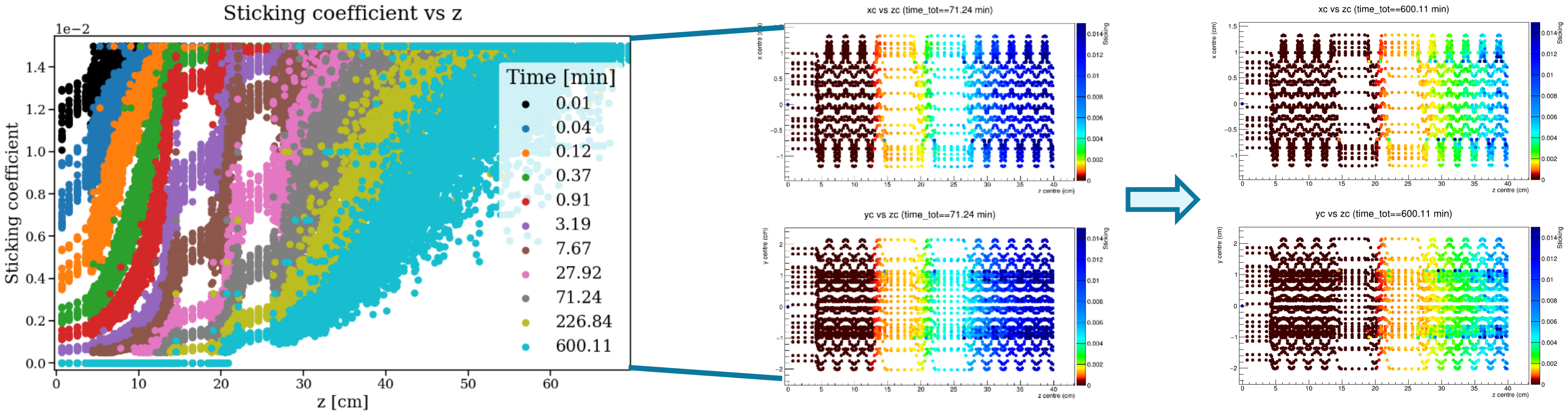

Results accuracy: N_2

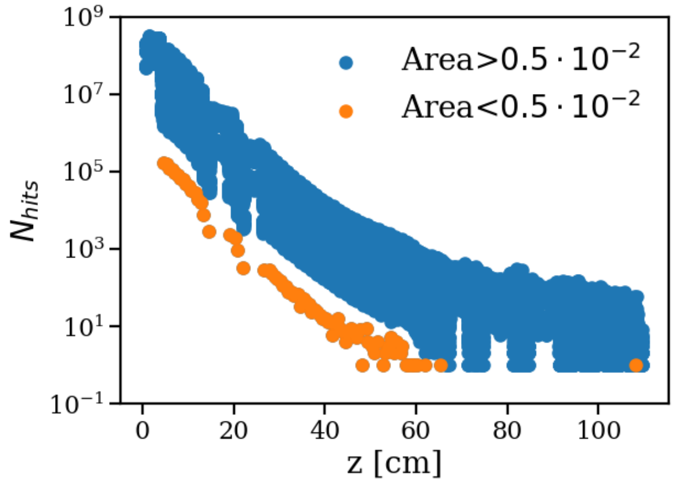

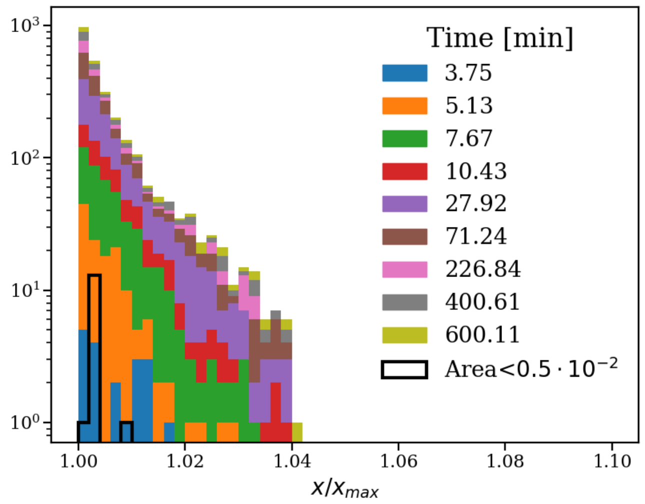

- **Complete geometry is probed** during simulation
- **Oversaturation below 4%**

- Average absorbed virtual particle at saturation around 10^3
- **Statistical uncertainty**:
  28% on x_{conc}, 39% on s_{avg}
  → **Reduced accuracy compare to H_2**

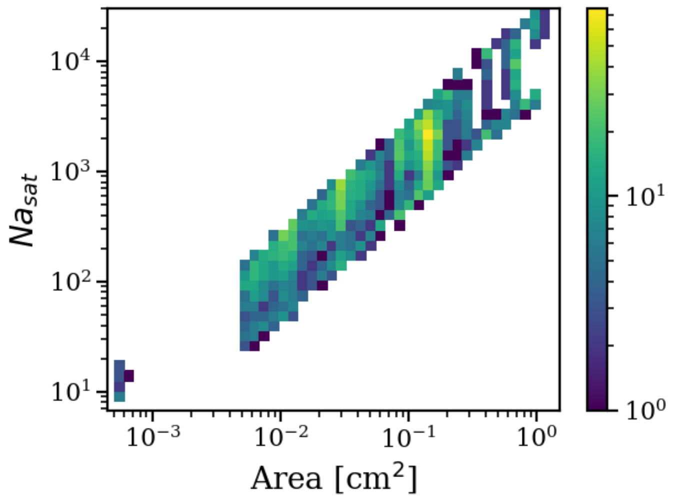

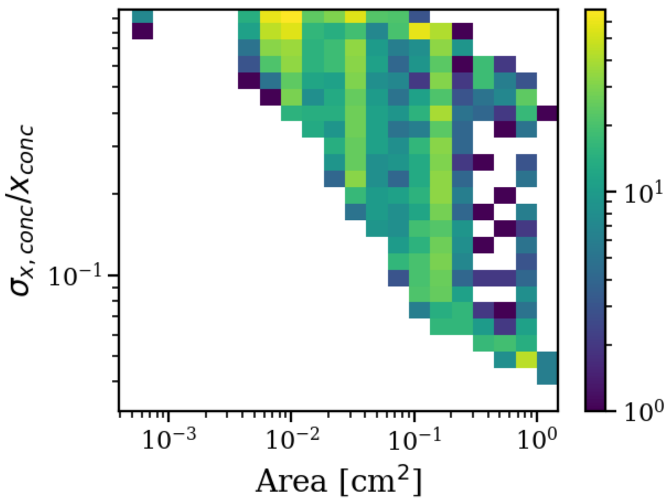

Results: H_2

- **Saturation** starts **after 20h** of injection
- Fraction of saturated area increases linearly but spatial propagation slows down after 48h (~5 cm)
  → **Corrugations hinder gas flow**
- **After 96h** of continuous injection, **saturation up to ~11 cm** (but saturation >10% up to ~7 cm).
  → **2% area saturated, 20% reduction of average s_{avg}**
- Atomic concentration x_H: 3% (z<20 cm)
  → **Well below embrittlement threshold**

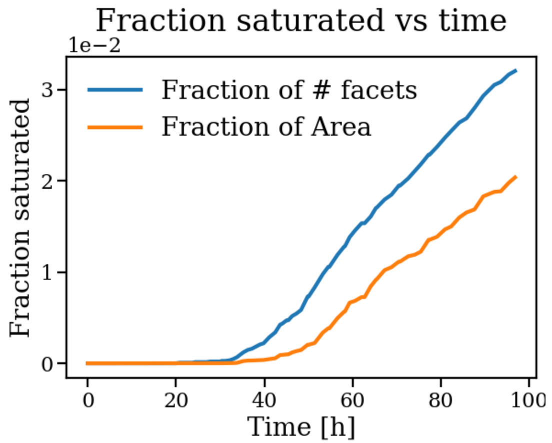

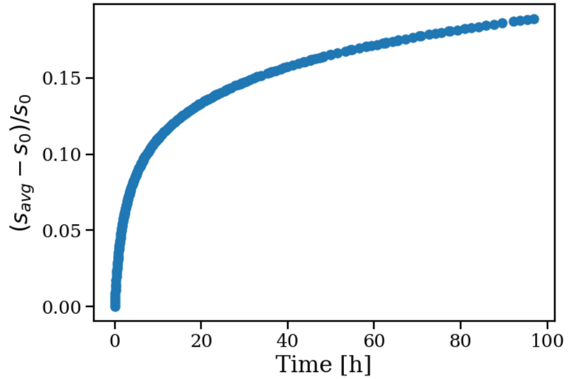

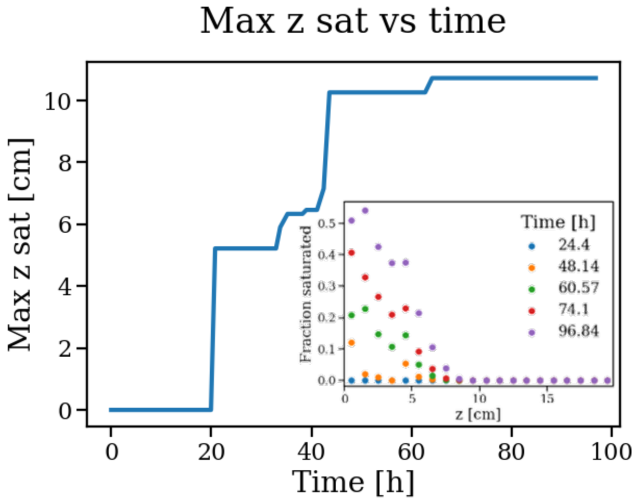

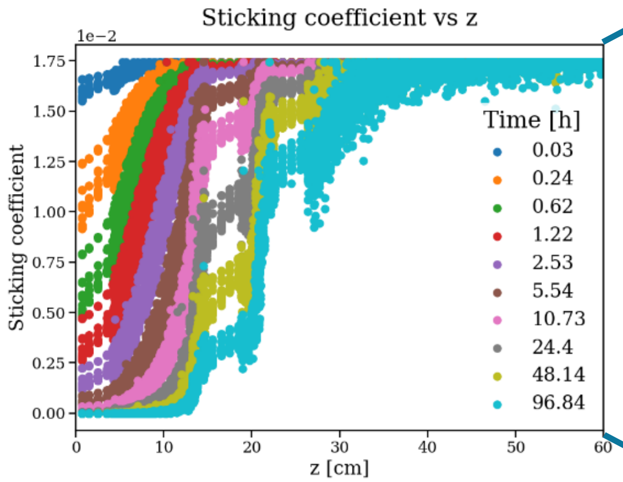

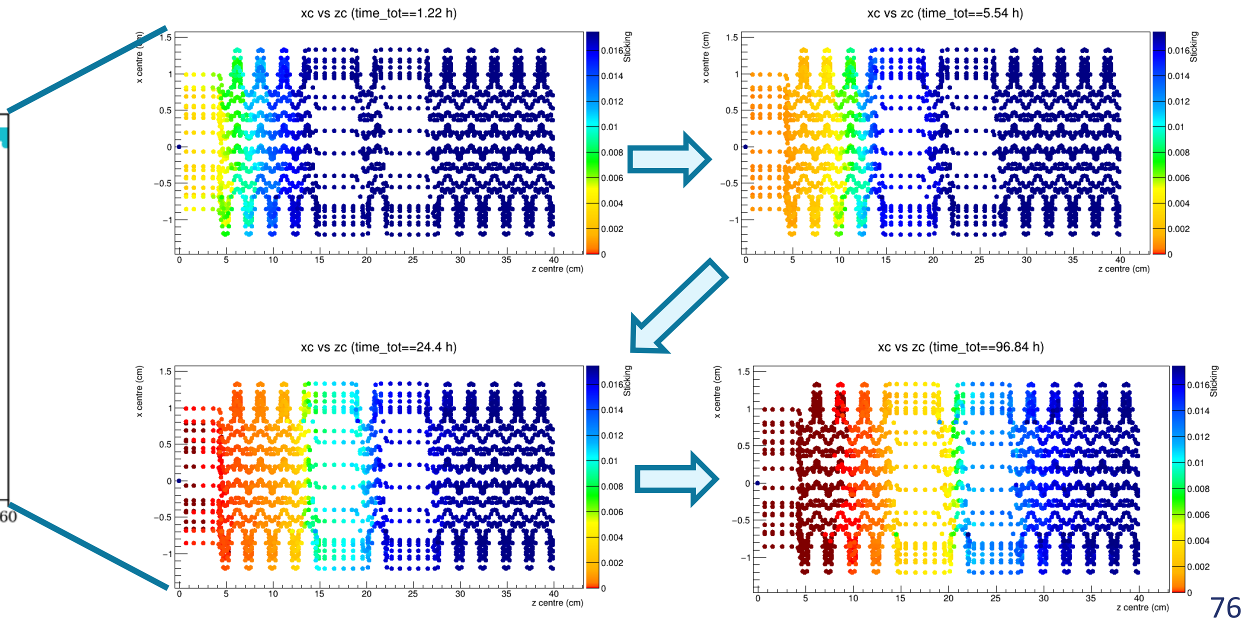

Results accuracy: H_2

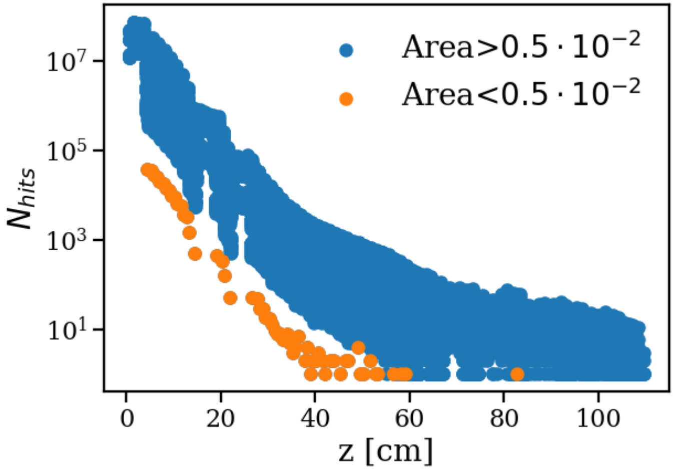

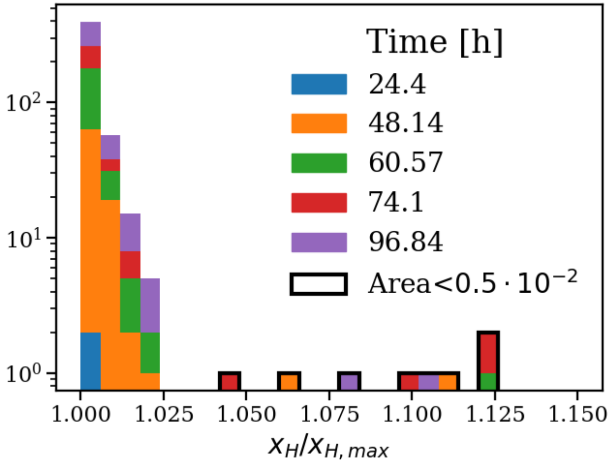

- **Complete geometry is probed** during simulation
- **Oversaturation below 2.5%**

- Absorbed virtual particle at saturation proportional to area facet
  - → **Statistical uncertainty inversely proportional to area**
- **Statistical uncertainty**: **4.7% on x_H, 17.3% on s_{avg}**

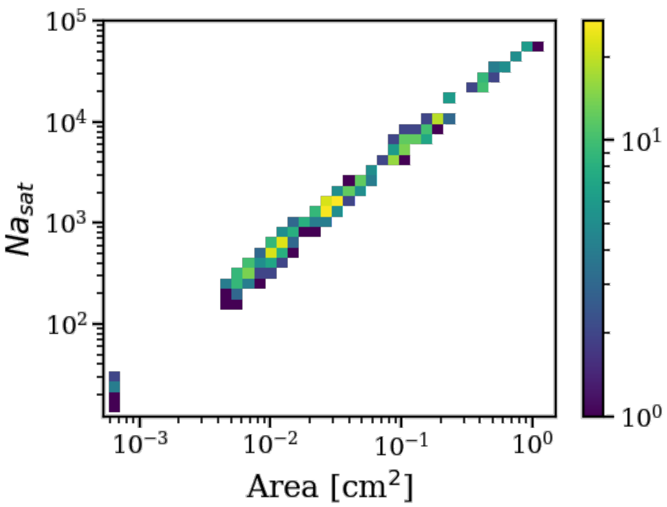

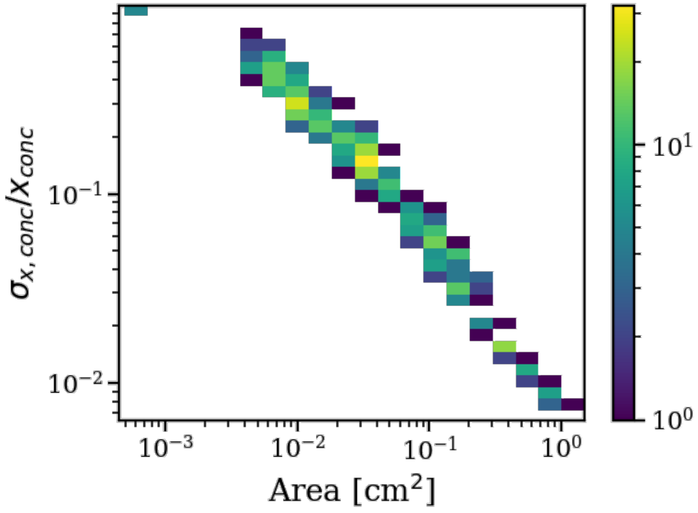

Python script: Molflow+

A brief explanation of Molflow's algorithm:

- Test Particle Monte Carlo method: simulation of virtual test particles (vp). Only collisions with walls (characterized by temperature, opacity, sticking coefficient). Physical quantities derived scaling from virtual to real physical molecules:

$$\frac{df_{real}}{dt} = scale * f_{vp}, \qquad scale = outgassing\ rate / \#\ desorbed\ vp$$

- Steady-state simulation: simulation of system at equilibrium. Continuous influx of gas particles (constant outgassing rate) and pumping speed.
    - **Only rates are simulated!** Impingement rate, absorption rate, …
    - Absolute quantities (i.e. # absorbed particles by a facet) can be obtained multiplying the rate by an arbitrary time (***physical time***).
- Statistical accuracy of simulation roughly connected to # hits per facets and on the scale factor:

Fix # desorbed vp:
higher #desorbed = lower scale factor,
but simulation time can diverge.

Fix simulation time (timeCPU):
longer timeCPU ≈ better statistic,
but no real control on scale factor.

Python script: input and output

Input:

- xml/zip geometry file (from the Molflow GUI).
  → Must already include outgassing.

- Starting sticking coefficient.

Output:

- xml/zip MolflowCLI output file for each step (option: overwrite input file).
- xml summary file with relevant data:
  - simulation parameters: gas mass, total outgassing, input and output file.
  - *facet parameters*: id, temperature, area, centre coordinates.
  - *iteration data*: id, CPU time step, scale factor, total time, pressure, density, # hits and absorbed (for iteration and total), concentration, sticking.
    → *NB: starting conditions memorized with iteration id = -1*

Python script: parameters and controls

Parameters:

- ***CPU Time steps:*** It's possible to define variable CPU time steps that follows a predefined sequence or update CPU time steps so that the scale factor remains (almost) constant.
- ***Physical time (and total time):*** the physical time of each step is chosen in order to move along the sticking coefficient curve evenly for every facet (i.e. no extreme coefficient jump in one step) → Minimum time (for all facets) that produces a decrease in sticking coefficient lower than a fixed value (i.e. decrease of 10% of the sticking coeff.)
- ***Facets*** to be updated (indexes, intervals, selection groups).
- ***Sticking evolution model:*** N_2, CO and H_2.
- ***Stop condition:*** condition that interrupts the simulations loop. Currently available: maximum simulation time, maximum saturation propagation along z, maximum number of iterations and saturation in any of the facets.
- ***Starting point:*** the simulation can start from any intermediated simulation step

Validation strategy

Validation of the script on a simple pipe in order to reproduce Yasunori Tanimoto results (presentation).

- Constant outgassing from one extreme; constant pumping speed from opposite extreme (7 l/s).
  - Starting sticking coefficient: 1.
  - Simple test model: s = 1 – coverage (=x/x_{max}).
  - Stop condition: complete saturation of the pipe.

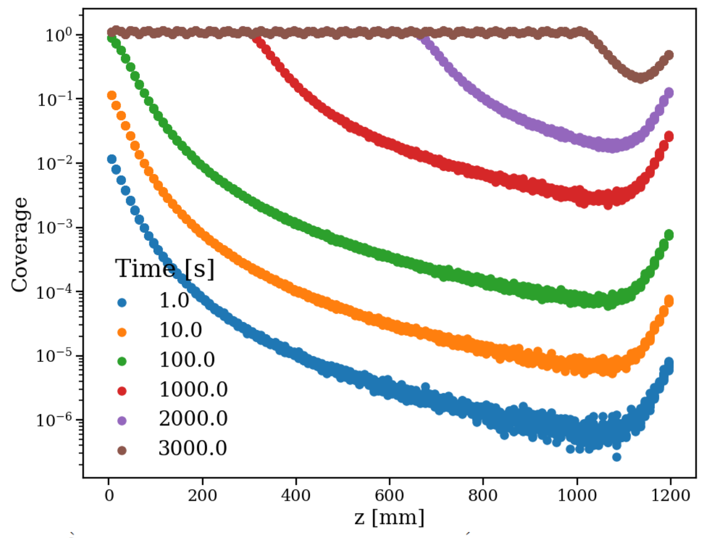

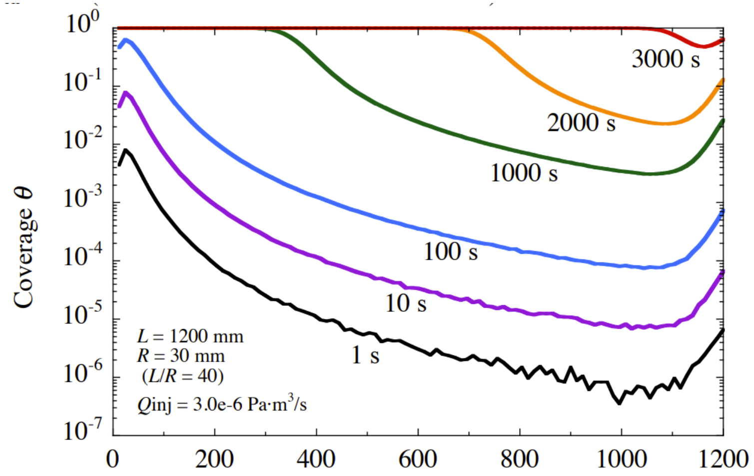

Results:

- **Good reproduction of results with independent simulation strategy.**

BGI: transversal uniformity

Beam-Gas Imaging (BGI): interaction between beam and gas molecules within LHCb interaction region to measure beams properties and luminosity → **SMOG2 gas injection to enhance beam-gas interaction rate.**

Transverse density profile: in principle uniform, but important to evaluate non-uniformity for systematic effects on BGI

<u>Target</u>: evaluate non uniformity $\frac{\rho(r,z)-\langle\rho\rangle_z}{\langle\rho\rangle_z}$ in transverse plane inside the cell

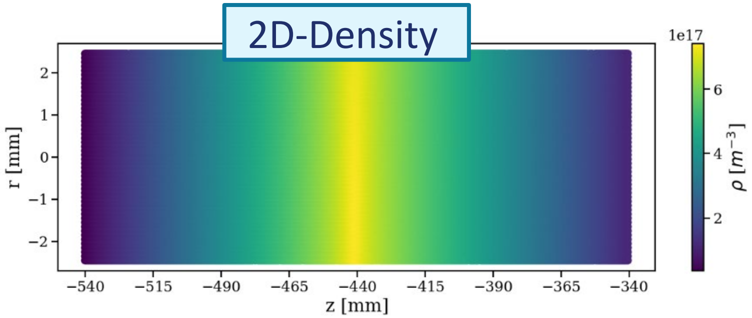

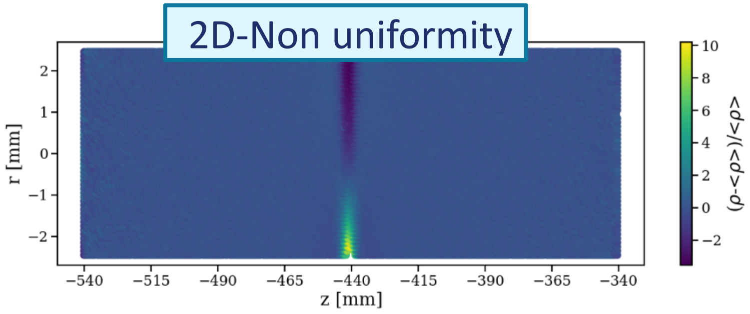

- **Capillary injection produces density cusp** under injection point
  → high non uniformity ±5 mm around injection
- **Outside injection region, uniform density at 0.15%**
  → **within BGI limits**

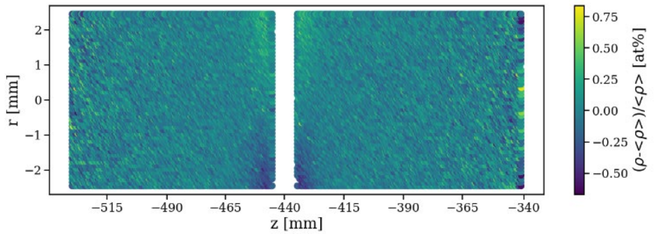

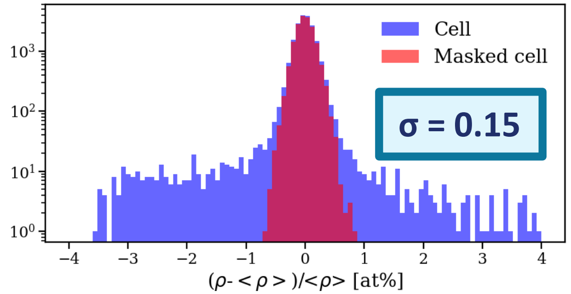

GFS and injection

Gas injected into cell or VELO tank through the Gas Feed System:

- Four gas reservoirs (3 noble gases + 1 non getterable line), used to fill the calibrated volumes V1 and V2, controlled by dosing valve DV601
- Table with calibrated volumes used during injection, pumping group to clean line and dosing valve DV602 to control injected flux.
- Gas feed line to feed either the VELO tank (PV503) or the cell (PV611)
- Turbo pump TP301 connected to VELO tank through GV302 (open during SMOG2 operations) to provide pumping when ion pumps off.

- Multiple gauges to measure pressure along the line and in the VELO tank:
  1. PZ602: pressure at calibration volumes, around 10 mbar when full.
  2. PZ601 and PI601: pressure at the beginning and end of GF line, O(0.01) mbar for SMOG2, O(0.001) mbar a-la-SMOG (PI601 under sensibility).
  3. PE301: pressure at the turbo pump TP301 (SMOG injection point), O(1e-8) mbar for SMOG2, O(1e-6) mbar a-la-SMOG.
  4. PE411 and PE412: pressure in the VELO tank in Ne equivalent, O(1e-8) mbar.

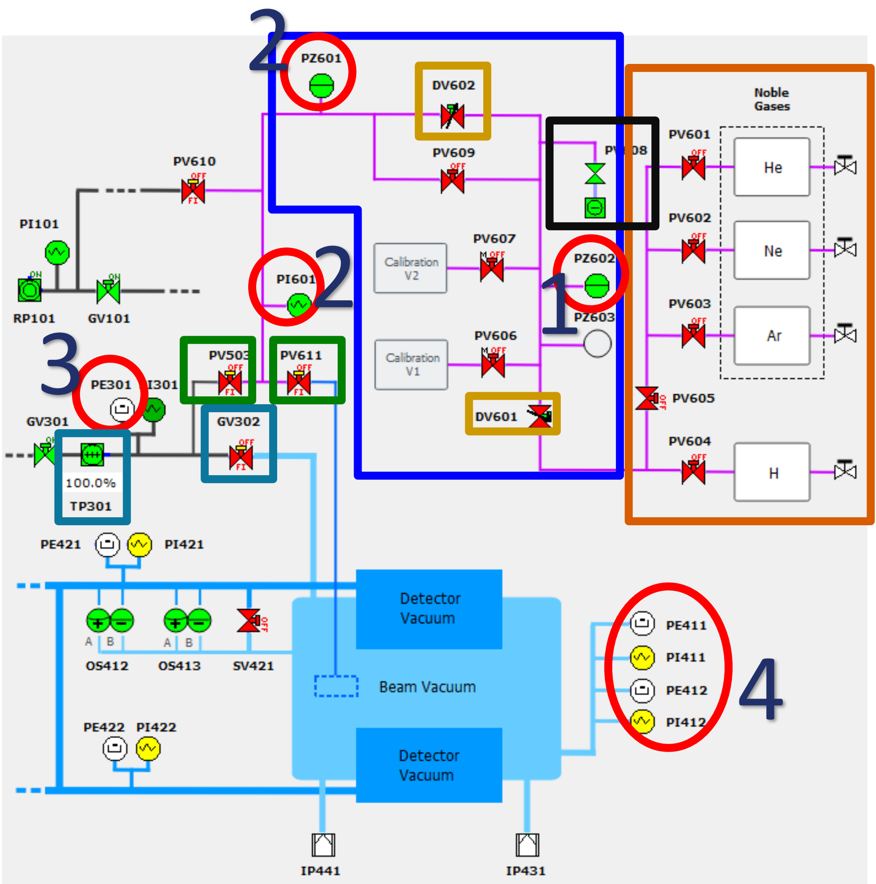

Semi-automatic GFS control

New FSM allows a semi-automatic control of GFS operation:

- Part of VELO vacuum control, accessible via remote desktop (dedicated SMOG piquet account?)
- Two (almost) independent FSM:
  - GFS preparation: gas reservoirs operation and table preparation
  - Gas injection: pumps regime selection and injection control

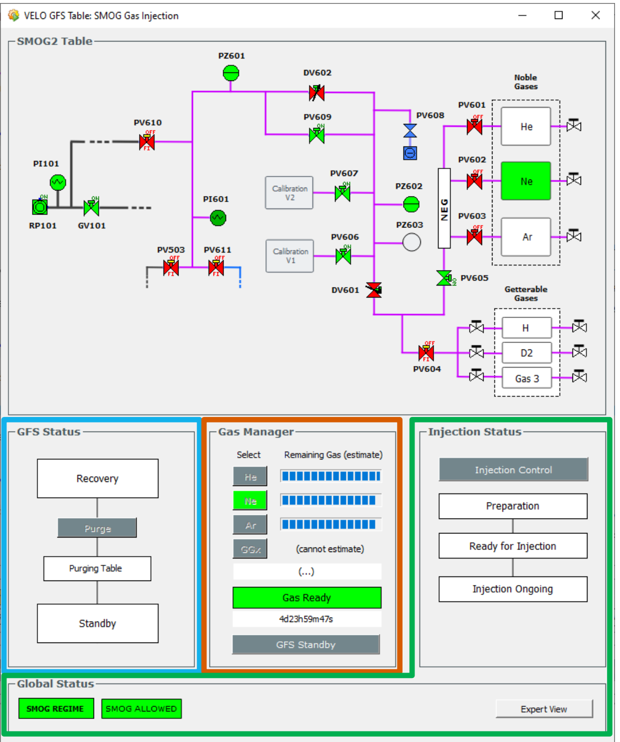

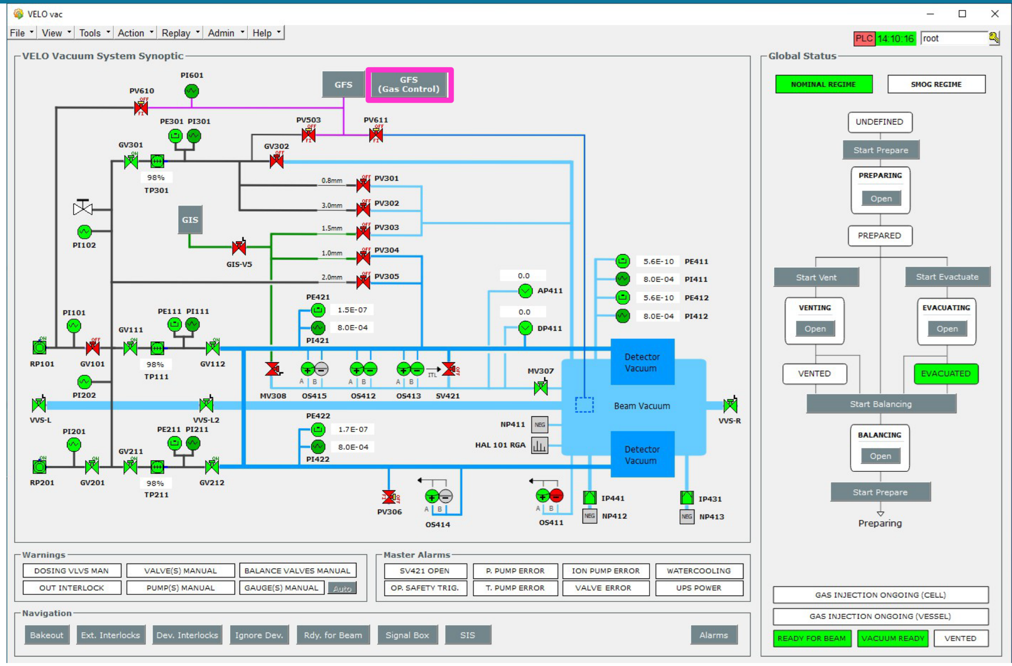

GFS preparation: GFS Gas Control

Preparation of GFS table for desired gas: purging from existing gases, preconditioning for new gas → Independent of injection process.

- It can be performed whenever outside injection procedure.
- Preconditioning guaranteed for 15 days → after expiration, forced purging.
- Swap between two gases requires 30-40 min (purging 20 min + preconditioning 15 min).

Semi-automatic GFS control

New FSM allows a semi-automatic control of GFS operation:

- Part of VELO vacuum control, accessible via remote desktop (dedicated SMOG piquet account)
- Two (almost) independent FSM:
  - GFS preparation: gas reservoirs operation and table preparation
  - Gas injection: pumps regime selection and injection control

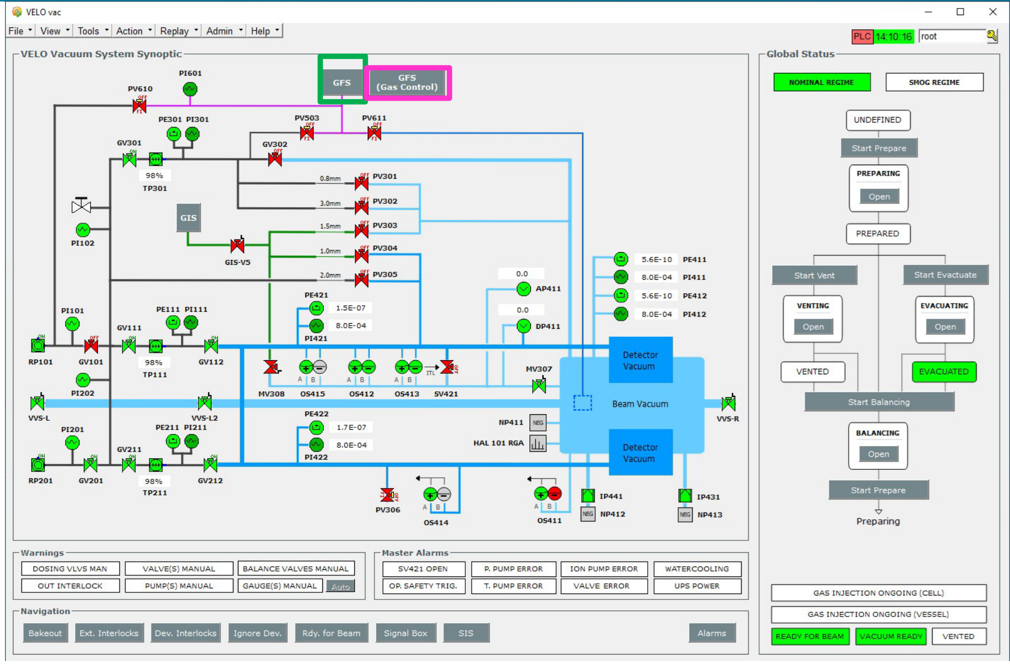

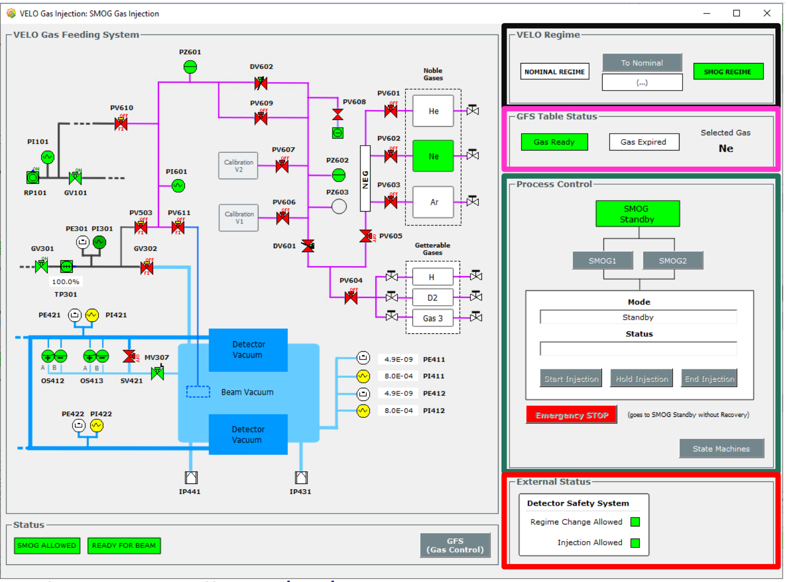

Injection: GFS

- Control swap between Nominal (ion pump on, TurboPump isolated) and SMOG regime (ion pump off, pumping through TurboPump).
  - Possible only when there is no beam, it takes 15 min.
    → Regime Change Allowed interlock, to be tested.
- Prepare line (15 min) for injection and control start/hold/stop of injection.
  - Fixed injection flux (Oct23 calibration) → 2e-5 mbar l/s for Ar.
  - Injection on Hold up to 30/60 min → after timeout, forced recovery (40 min).
  - Interlock (Injection Allowed) when VELO is moving, to be tested.

Automatic run change: implementation

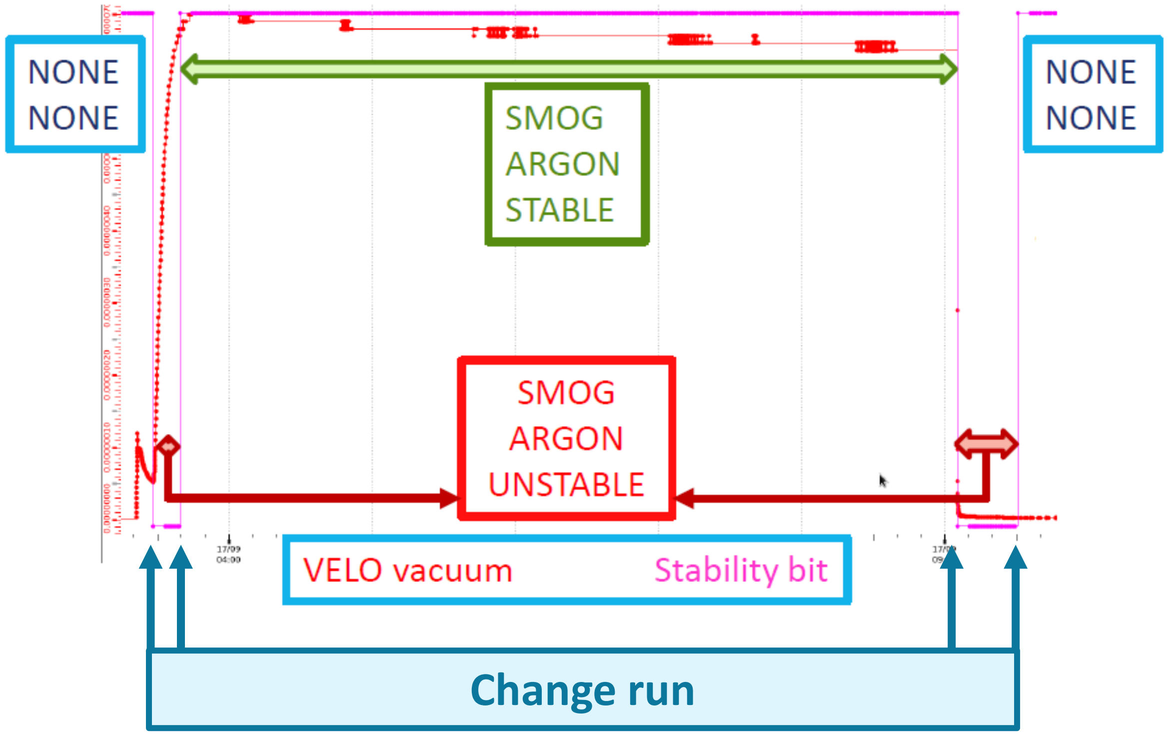

Run change when:

- NONE<->SMOG/SMOG2 transitions.
- STABLE<->UNSTABLE transitions.

  → Expected 4 run changes for each injection cycle

Automatic run change when injection conditions change:

- **Identify start/stop** of injection.
- **Identify stable pressure** plateau (slow decrease of pressure) **and pressure spikes** (unstable).

⇩

- If mode == NONE → No status monitoring.
- When injection valve change status → Mode == INJ, status == UNSTABLE, stability monitoring ON.
- Moving average over 10 readings of pressure: STABLE if change wrt previous reading <0.7%.
- When injection valve is closed and status == STABLE → Mode == NONE, stability monitoring OFF.
- **In order to exclude frequent run changes, status freezed for 2.5 minutes (minimum time for Data Quality in *pp*)**

VELO incident – January 2023

RF foil separates LHC primary vacuum from VELO secondary vacuum

Multiple vacuum equipment failures → **No control over pressure protection systems**

Δpressure ~ 200 mbar but foil designed for Δpressure<10 mbar

⇩

Plastic **deformation up to 14 mm** of RF foil towards beam pipe

→ VELO and SMOG2 cannot be closed

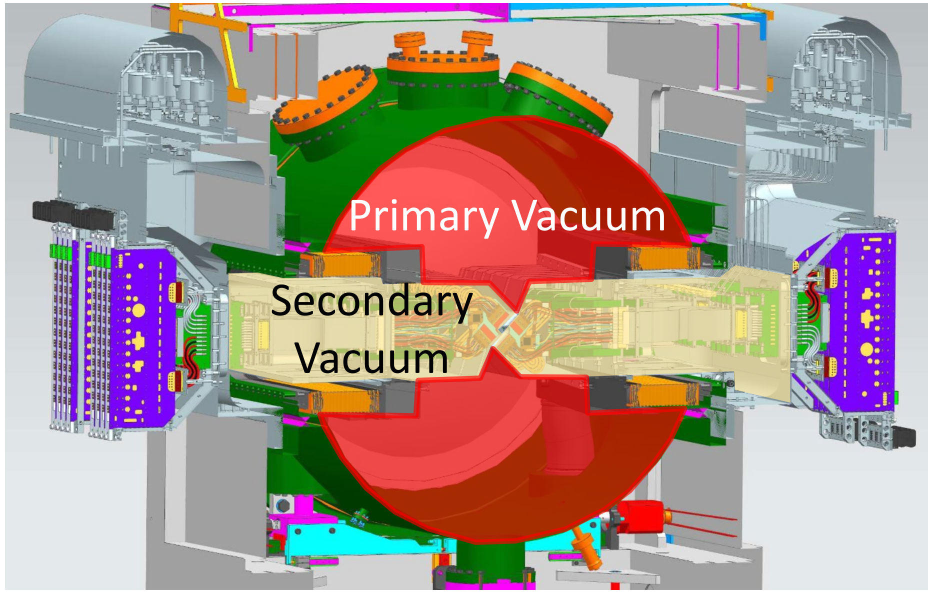

No data acquired with SMOG2 in 2023